Imperial College London

Process Development using Organic Solvent Nanofiltration (OSN) for Oligonucleotide Synthesis

Appendix

A thesis submitted in fulfillment of the requirements for the Doctor of Philosophy degree

Kim

Jeong Kim

March 2014

Department of Chemical Engineering

Imperial College of Science, Technology, and Medicine

Appendix A: Modeling of Diafiltration Process

The single-stage diafiltration system can be modeled by writing a mass balance around the system (Figure A1).

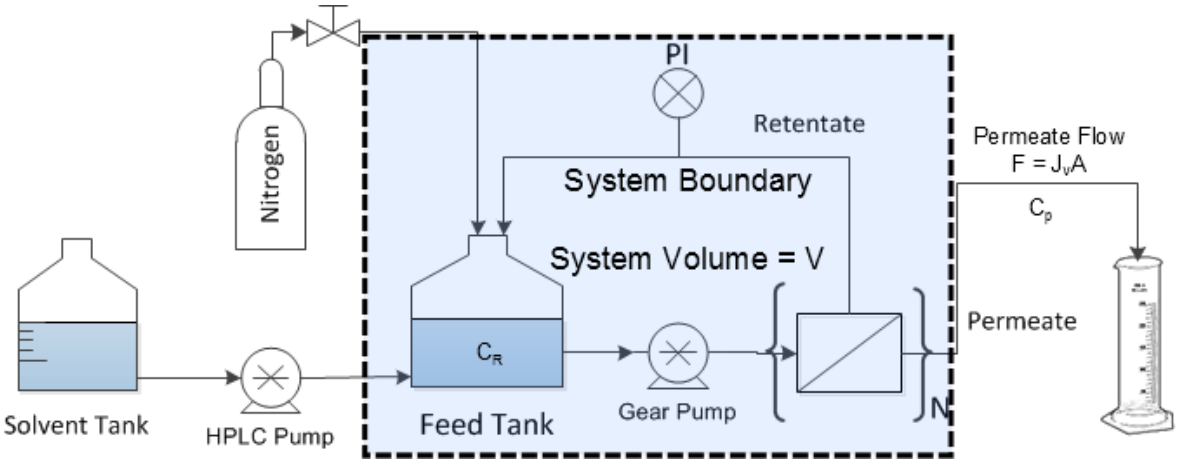


Figure A1. System boundary for a diafiltration process for process model development.

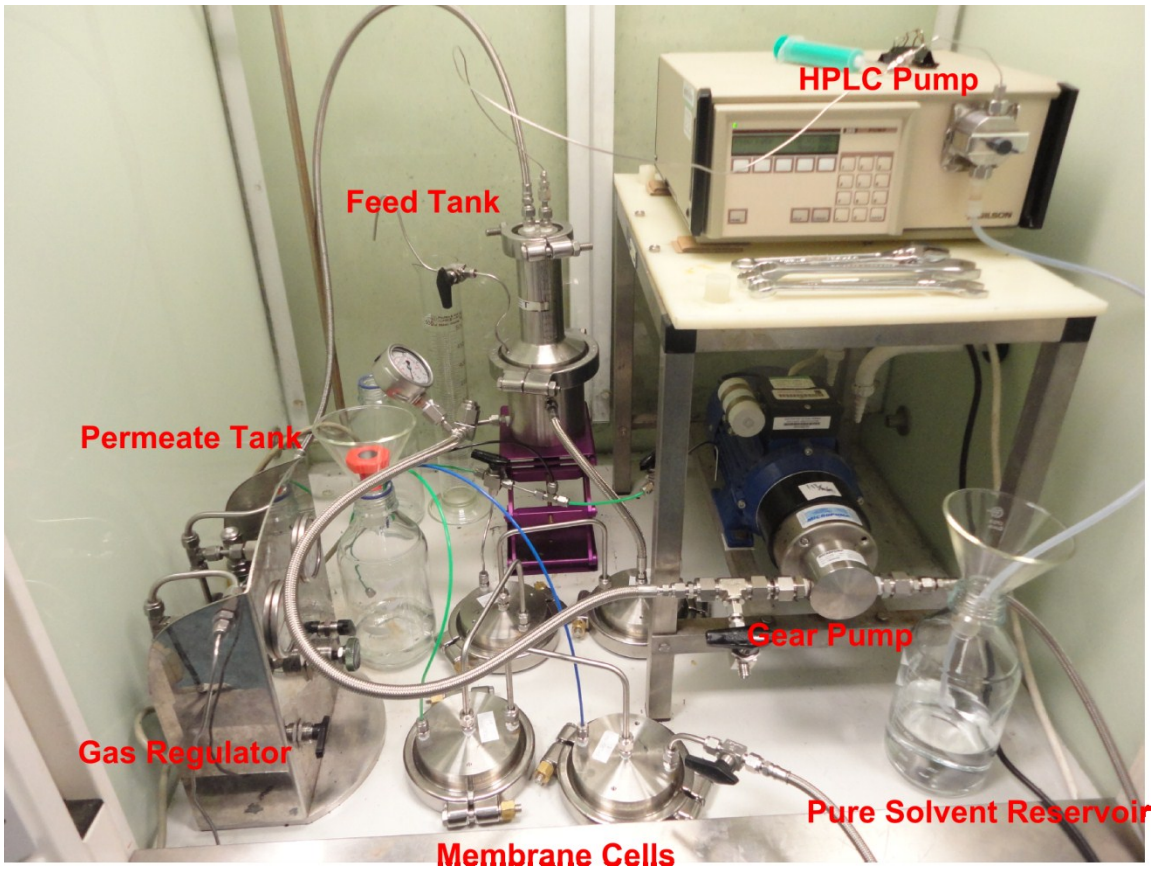


Figure A2. Photo of the membrane diafiltration rig.

Assuming that the system operates at a constant volume and it is perfectly mixed,

$$V\frac{dC_{R,i}}{dt} = -F \cdot C_{p,i} = J_v \cdot A \cdot C_{p,i} \quad \text{(Eq. A1)}$$

where V (L) is the entire system volume, F is the permeate flow-rate ($L.hr^{-1}$), J_v ($L.m^{-2}.hr^{-1}$) is the membrane flux, A (m^2) is the membrane area, and $C_{R,i}$ and $C_{P,i}$ ($g.L^{-1}$) are the concentrations of species i in the retentate and permeate, respectively.

Defining the observed rejection of species *i* as,

$$R_{obs} = 1 - \frac{C_{p,i}}{C_{R,i}} \quad \text{(Eq. A2)}$$

and substituting Eq. (A2) into Eq. (A1) yields,

$$\frac{dC_{R,i}}{dt} = -\left(\frac{1}{V}\right) J_v A\, C_{R,i}(1 - R_{obs}) \quad \text{(Eq. A3)}$$

This equation can be solved either numerically or analytically. When integrated analytically with appropriate boundary conditions, the following equation is obtained:

$$\frac{C_{r,i}}{C_{r,i,o}} = \exp\left[-\frac{J_v A t}{V}\,(1 - R_{obs})\right] = \exp[-diavolume\,(1 - R_{obs})] \quad \text{(Eq. A4)}$$

where *diavolume* represent the total volume of permeate collected relative to the initial system volume. This useful time-like dimensionless parameter allows different diafiltration systems to be compared.

A similar analysis of the two-stage diafiltration can be solved numerically (Diagram shown in Figure 3.2). As the two stages are interconnected, a total of four ordinary differential equations can be written for species *i* and *j* in stages 1 and 2.

$$\frac{dC_{R1,i}}{dt} = \left(\frac{1}{V_1}\right)\left[-F_1 C_{R1,i}(1 - R_{1,i}) + F_3 C_{R2,i}\right] \quad \text{(Eq. A5)}$$

$$\frac{dC_{R2,i}}{dt} = \left(\frac{1}{V_2}\right)\left[F_1 C_{R1,i}(1 - R_{1,i}) - F_2 C_{R2,i}(1 - R_{2,i}) - F_3 C_{R2,i}\right] \quad \text{(Eq. A6)}$$

$$\frac{dC_{R1,j}}{dt} = \left(\frac{1}{V_1}\right)\left[-F_1 C_{R1,j}(1 - R_{1,j}) + F_3 C_{R2,j}\right] \quad \text{(Eq. A7)}$$

$$\frac{dC_{R2,j}}{dt} = \left(\frac{1}{V_2}\right)\left[F_1 C_{R1,j}\left(1 - R_{1,j}\right) - F_2 C_{R2,j}\left(1 - R_{2,j}\right) - F_3 C_{R2,j}\right] \quad \text{(Eq. A8)}$$

where V_1 is the feed tank plus the first-stage volume, V_2 is the second-stage volume, and F_i (equal to $J_v \cdot A$) is the flow as shown in Figure 3.2.

Appendix B: Supporting Information for Chapter 2

B1. Effect of Adding Acid Prior to Purifying the Chain Extension Crude

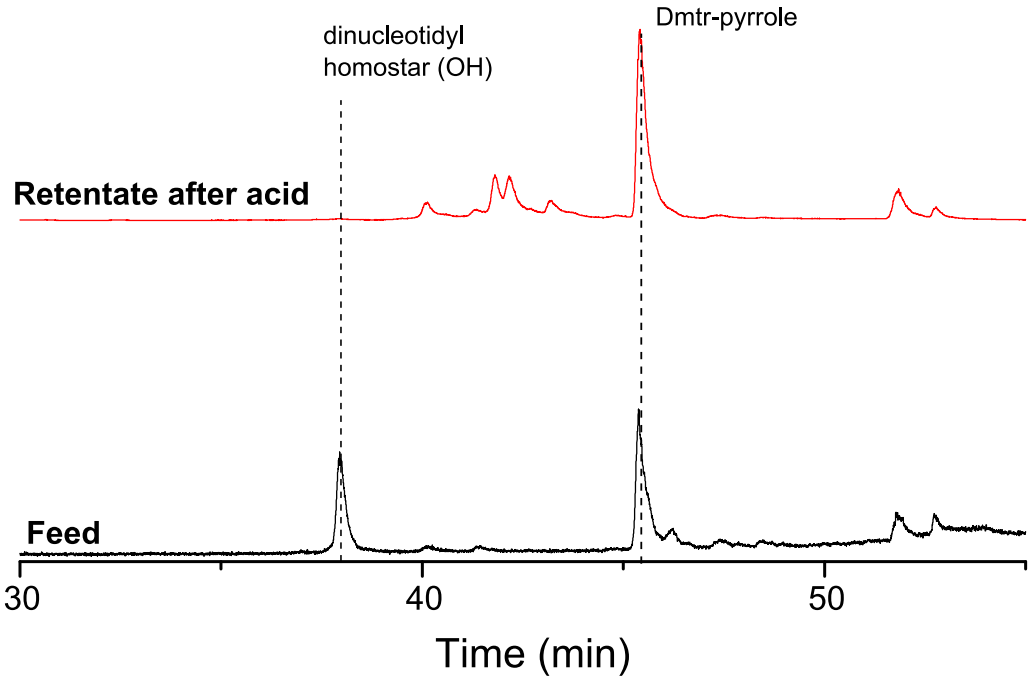


Figure B1.1 – HPLC chromatogram illustrating the product degradation of chain extension crude upon acid (DCA) exposure.

To test the effect of acid, a mock solution containing a detritylated dinucleotidyl Homostar combined with PADS, ETT, and detritylated thioamidate and amidate (R=OH) was charged to the rig which was spiked with 1 *vol*% DCA. It can be in seen in Figure B1 that the addition of acid prior to purification of chain extension crude results in unknown side reactions. Most likely the presence of PADS and ETT under acidic condition degrades the growing oligo products. Hence, it was decided to split one chain extension cycle into two diafiltrations: once after chain extension reaction, and once after detritylation reaction. This modified protocol prevented the product degradation issue.

B2. Peak Broadening in HPLC

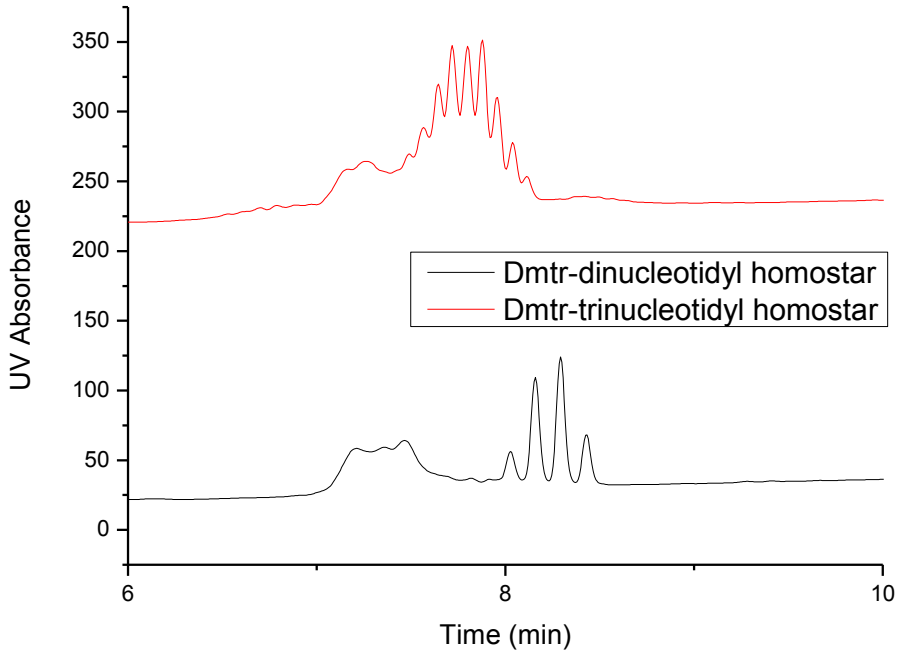


Figure B2.1. The peak broadening effect observed with increasing oligo lengths, due to the exponential increase in number of diastereomers.

B3. Detection of Incomplete Chain Extension using HPLC

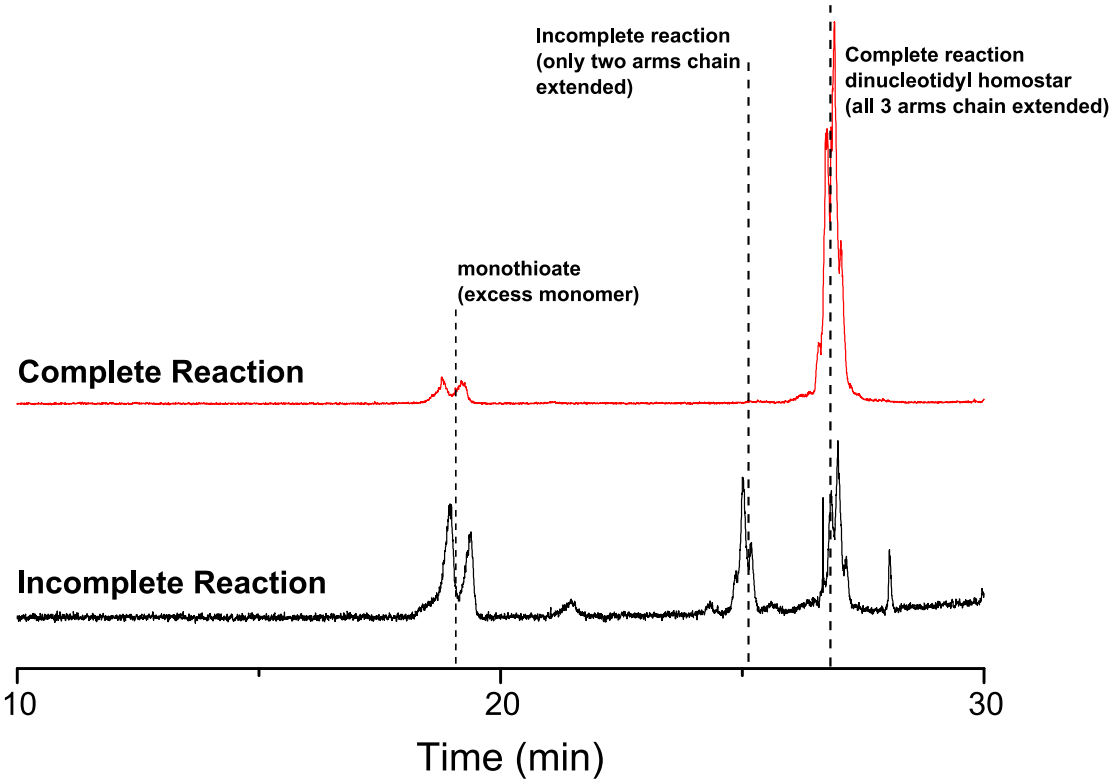


Figure B3.1. Incomplete chain extension to dimer shown by HPLC.

It can be seen in Figure B3.1 that incomplete reaction clearly shows up in the HPLC chromatogram. In such case, the reaction can simply be repeated (after membrane diafiltration to get rid of other reaction debris) to push the reaction to completion. Unfortunately, such clear trend is not possible with longer oligos.

B4. Characterization of Oligos

**These oligo characterization data have been compiled by Dr. Piers Gaffney.*

Crude Dmtr-dimer homostar, **7**, [tris(mUp^{Cne}SmC^{Ac}-ODmtr) homostar] (400 MHz, D_6-acetone).

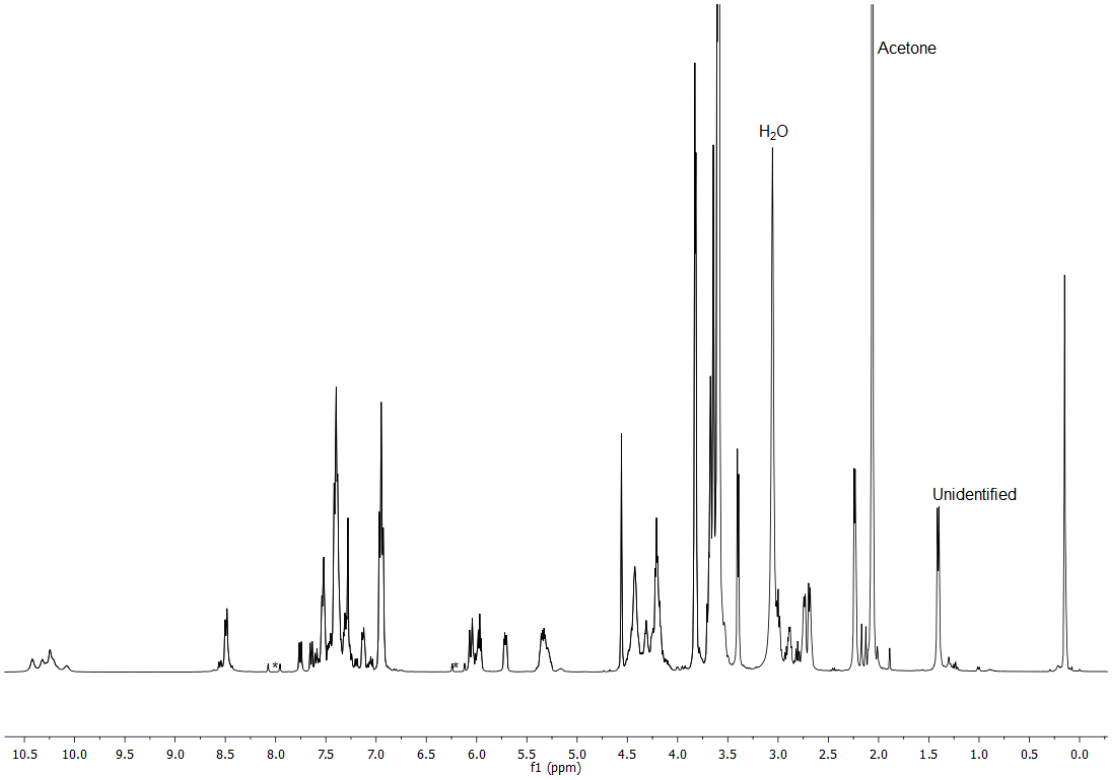


Figure B4.1. ^{1}H-NMR spectrum of tris(mUp^{Cne}SmC^{Ac}-ODmtr) homostar, **7**, after 1st diafiltration.

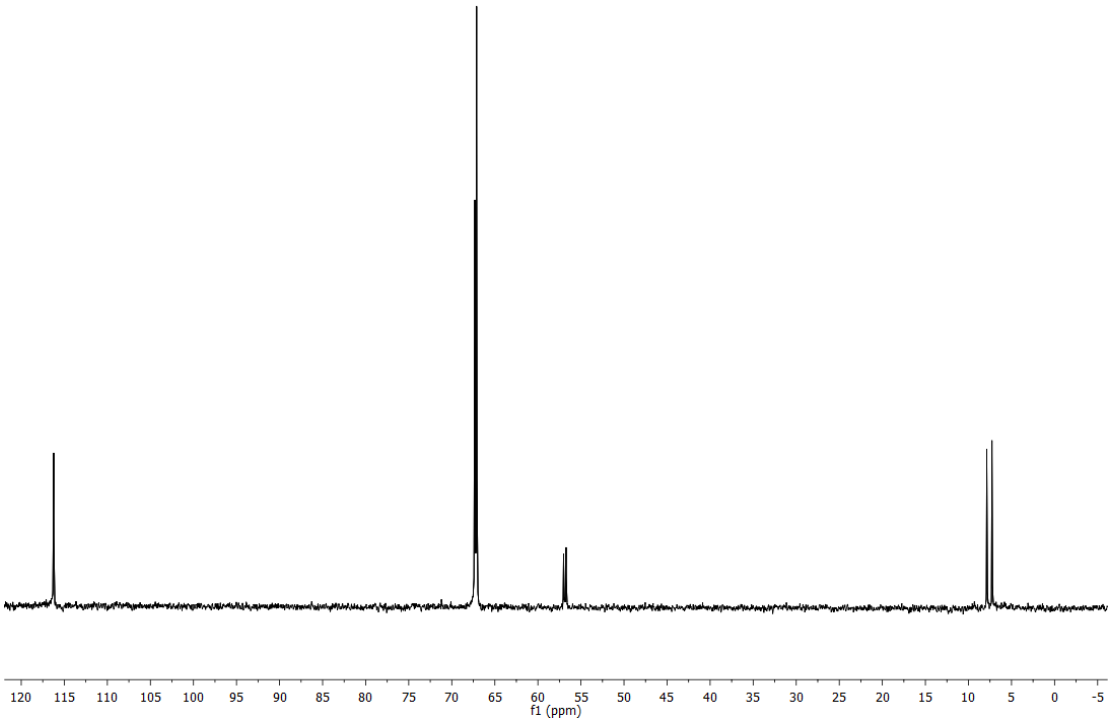


Figure B4.2. ^{31}P-NMR spectrum of tris(mUp^{Cne}SmC^{Ac}-ODmtr) homostar, **7,** after 1st diafiltration.

Tris(mUp^{Cne}SmC^{Ac}-OH) homostar, **8** (500 MHz, $CDCl_3$-CD_3OD 2:1).

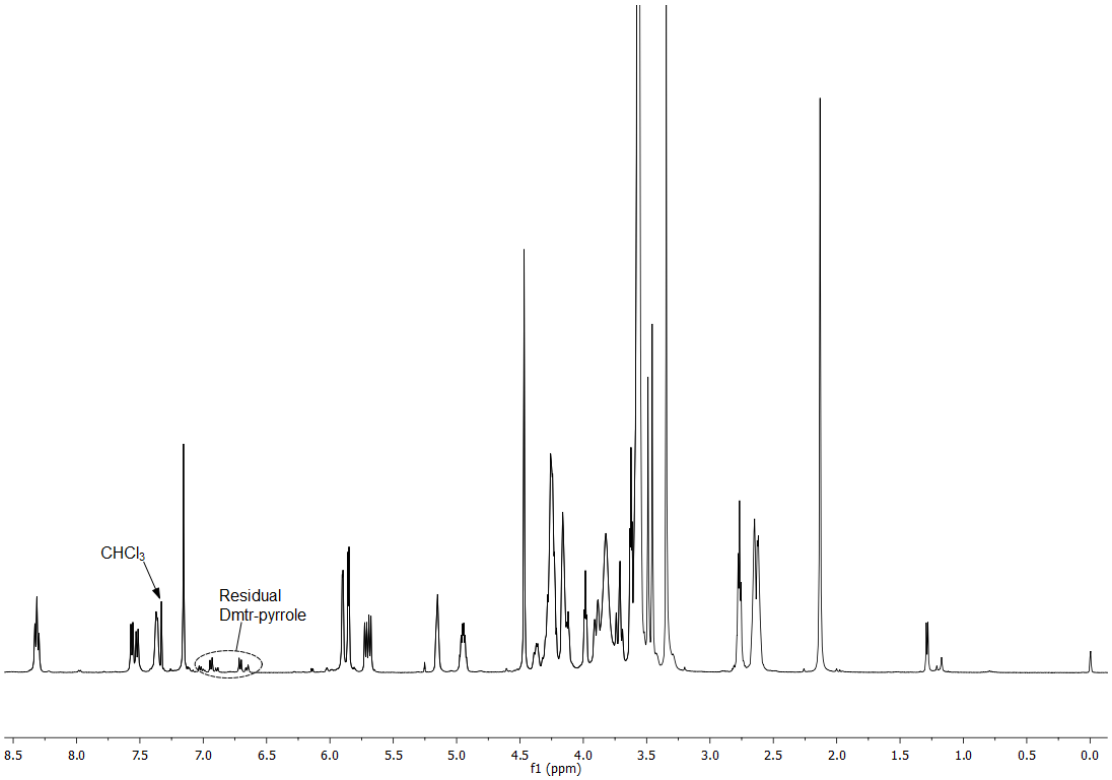


Figure B4.3. ^{1}H-NMR spectrum of Tris(mUp^{Cne}SmC^{Ac}-OH) homostar, **8,** after 2nd diafiltration.

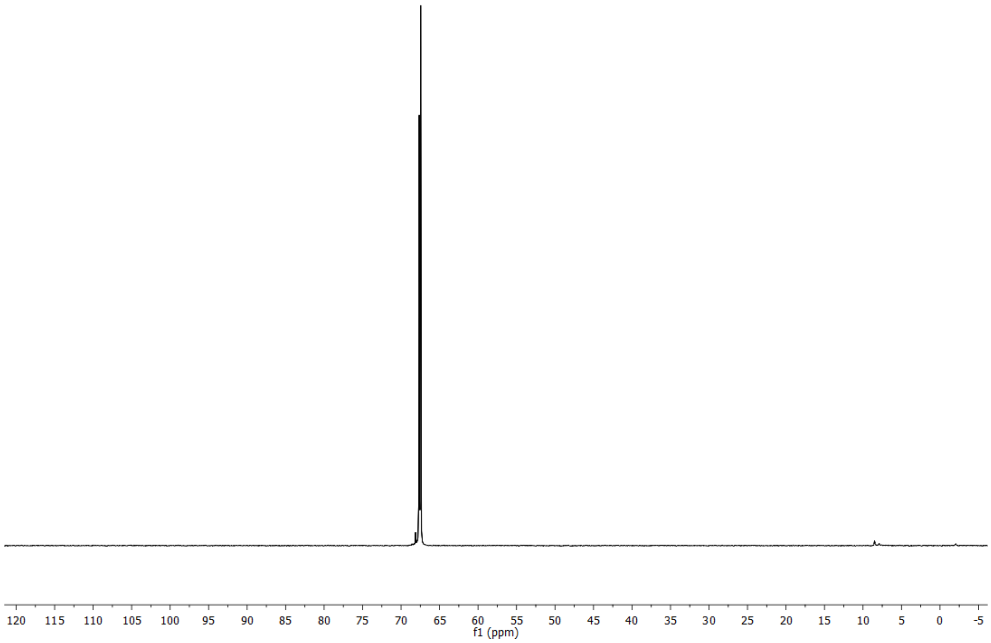


Figure B4.4. ^{31}P-NMR spectrum tris(mUp^{Cne}SmC^{Ac}-OH) homostar, **8,** after 2nd diafiltration.

Crude tris(mUp^{Cne}SmC^{Ac}p^{Cne}SmC^{Ac}-ODmtr) homostar, **9** (400 MHz, D_6-acetone).

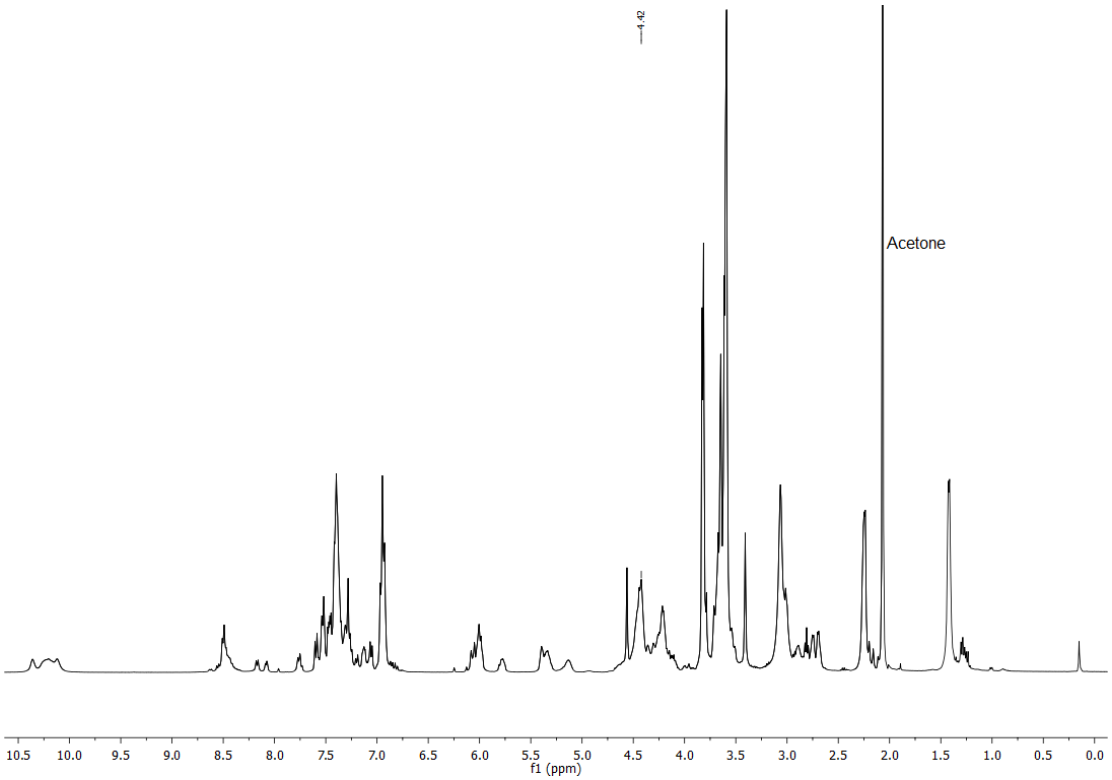


Figure B4.5. ^{1}H-NMR spectrum of crude tris(mUp^{Cne}SmC^{Ac}p^{Cne}SmC^{Ac}-ODmtr) homostar, **9**.

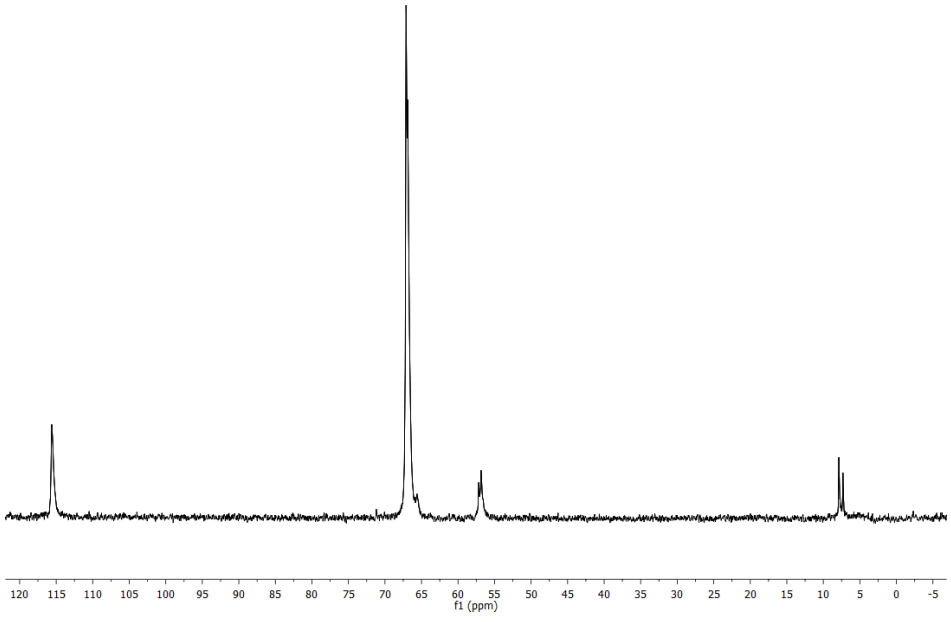


Figure B4.6. ^{31}P-NMR spectrum of crude tris(mUp^{Cne}SmC^{Ac}p^{Cne}SmC^{Ac}-ODmtr) homostar, **9.**

Tris(mUp^{Cne}SmC^{Ac}p^{Cne}SmC^{Ac}-OH) homostar, **10** (500 MHz,$CDCl_3$-CD_3OD 3:1), before trituration**.**

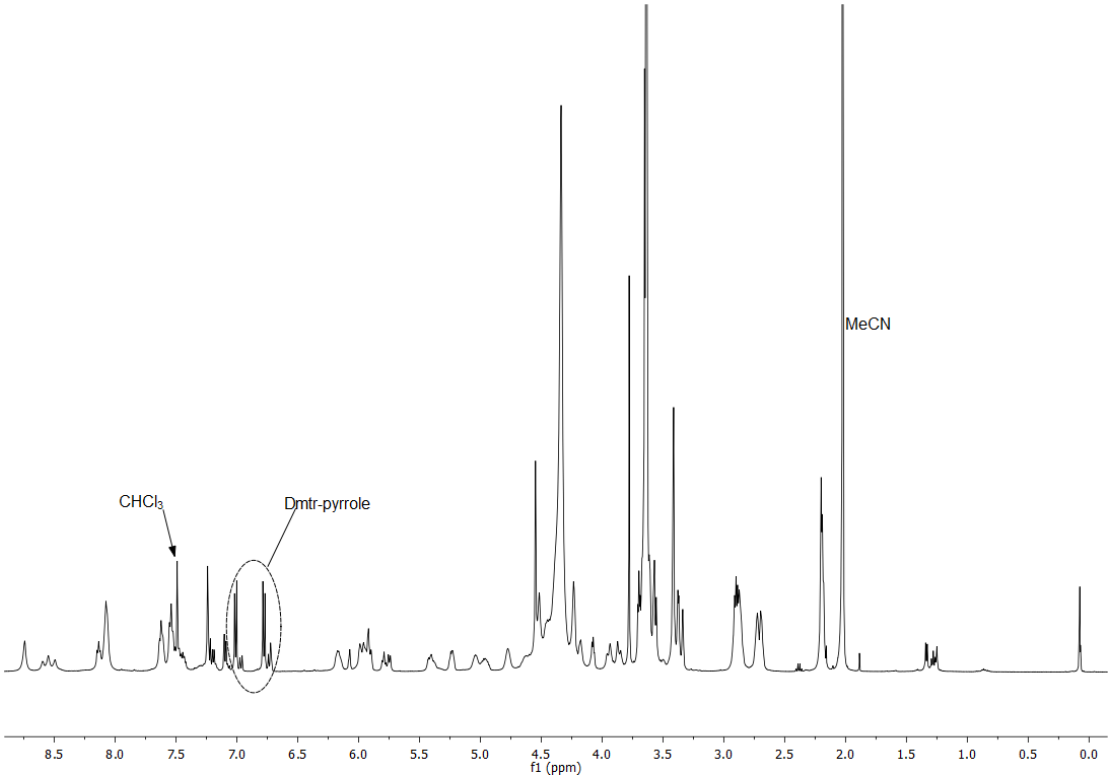


Figure B4.7. ^{1}H-NMR spectrum of Tris(mUp^{Cne}SmC^{Ac}p^{Cne}SmC^{Ac}-OH) homostar, **10**.

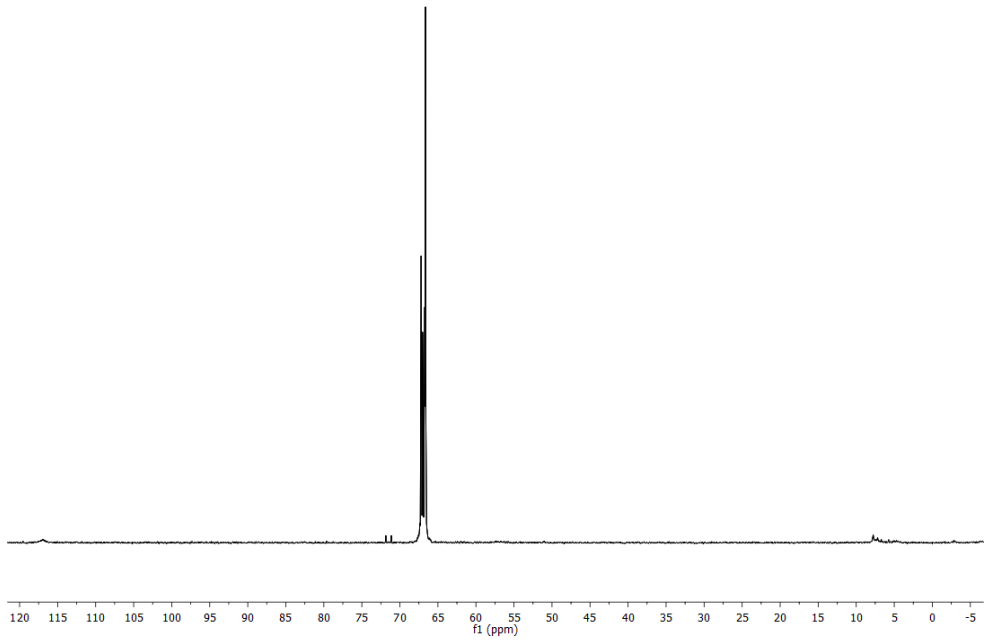


Figure B4.8. ^{31}P-NMR spectrum of Tris(mUp^{Cne}SmC^{Ac}p^{Cne}SmC^{Ac}-OH) homostar, **10.**

Crude tris(mUp^{Cne}SmC^{Ac}p^{Cne}SmC^{Ac}p^{Cne}SmA^{Bz}-ODmtr) homostar, **11** (400 MHz, $CDCl_3$).

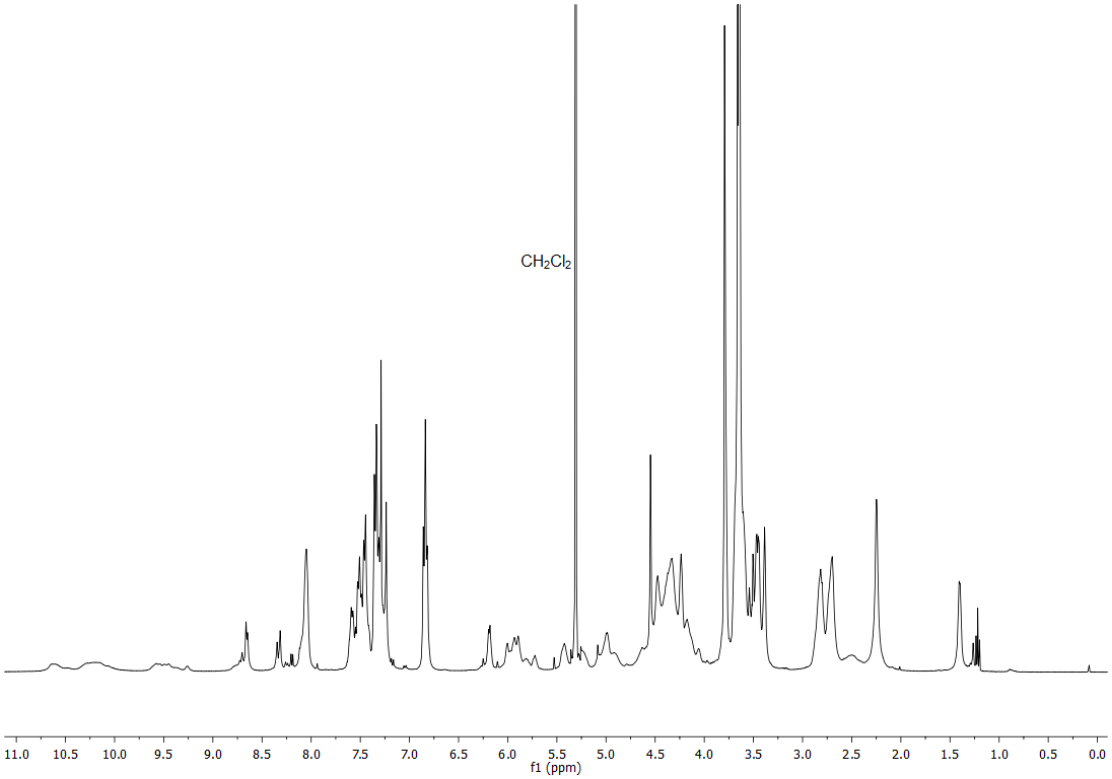


Figure B4.9. ^{1}H-NMR spectrum of crude tris(mUp^{Cne}SmC^{Ac}p^{Cne}SmC^{Ac}p^{Cne}SmA^{Bz}-ODmtr) homostar, **11** .

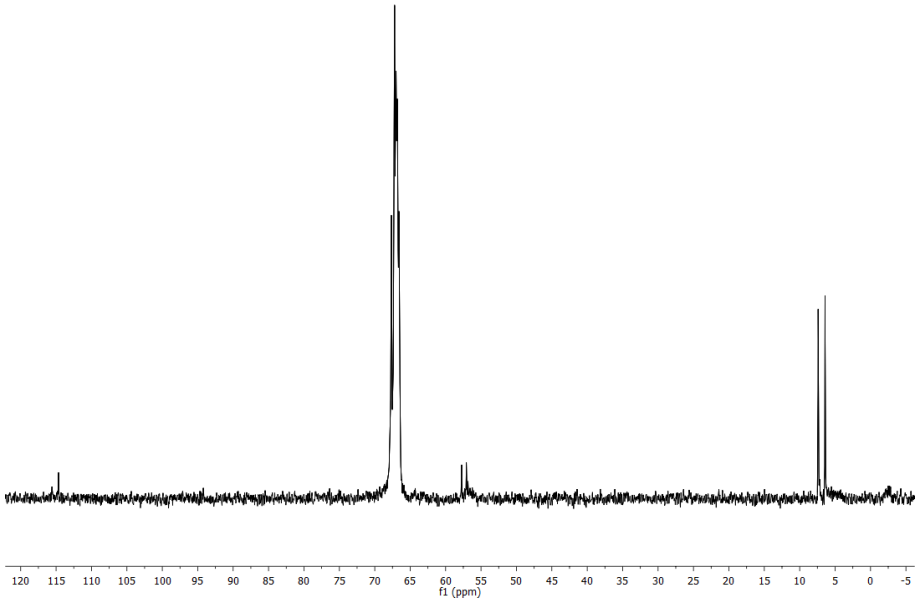


Figure B4.10. ^{31}P-NMR spectrum of Crude tris(mUp^{Cne}SmC^{Ac}p^{Cne}SmC^{Ac}p^{Cne}SmA^{Bz}-ODmtr) homostar, **11.**

Tris(mUp^{Cne}SmC^{Ac}p^{Cne}SmC^{Ac}p^{Cne}SmA^{Bz}-OH) homostar, **12** (500 MHz, $CDCl_3$-CD_3OD 3:1) before trituration**.**

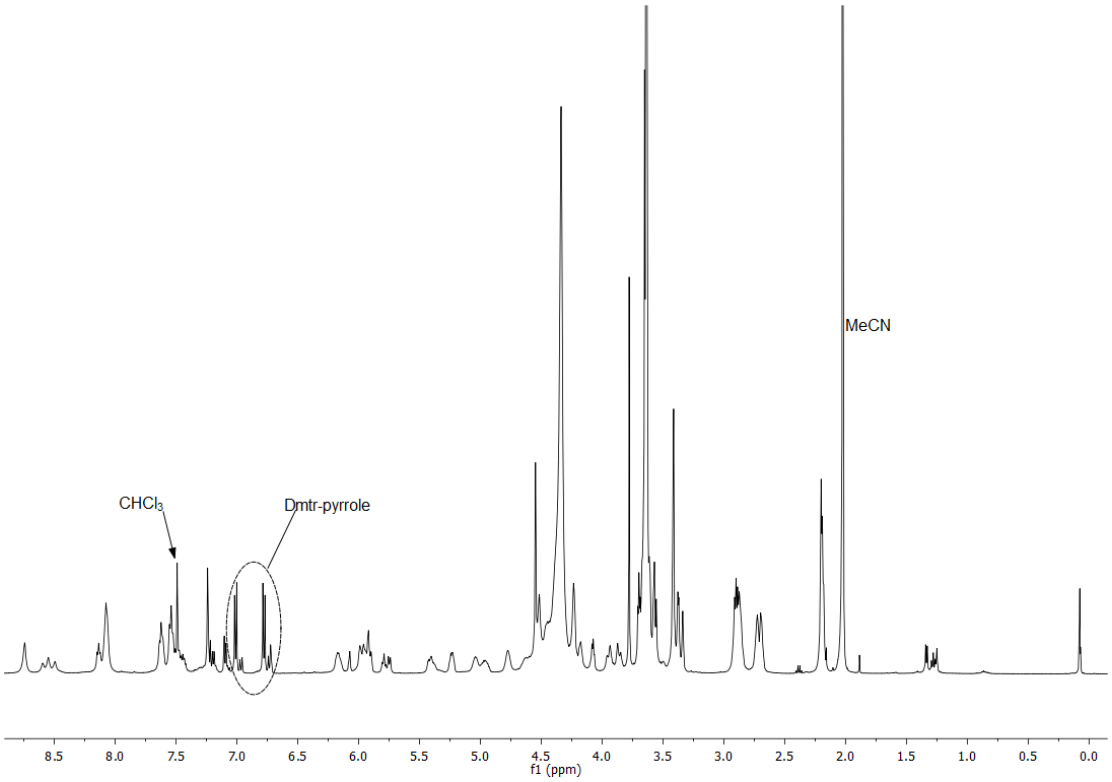


Figure B4.11. ^{1}H-NMR spectrum of Tris(mUp^{Cne}SmC^{Ac}p^{Cne}SmC^{Ac}p^{Cne}SmA^{Bz}-OH) homostar, **12.**

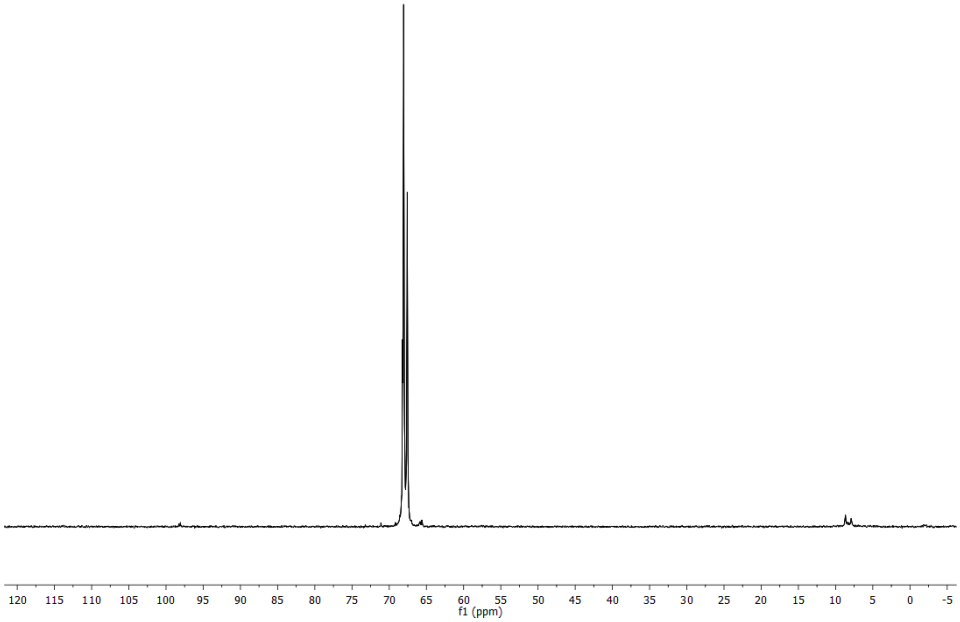


Figure B4.12. ^{31}P-NMR spectrum of Tris(mUp^{Cne}SmC^{Ac}p^{Cne}SmC^{Ac}p^{Cne}SmA^{Bz}-OH) homostar, **12.**

Crude tris(mUp^{Cne}SmC^{Ac}p^{Cne}SmC^{Ac}p^{Cne}SmA^{Bz}p^{Cne}SmU-ODmtr) homostar, **13** (400 MHz, $CDCl_3$).

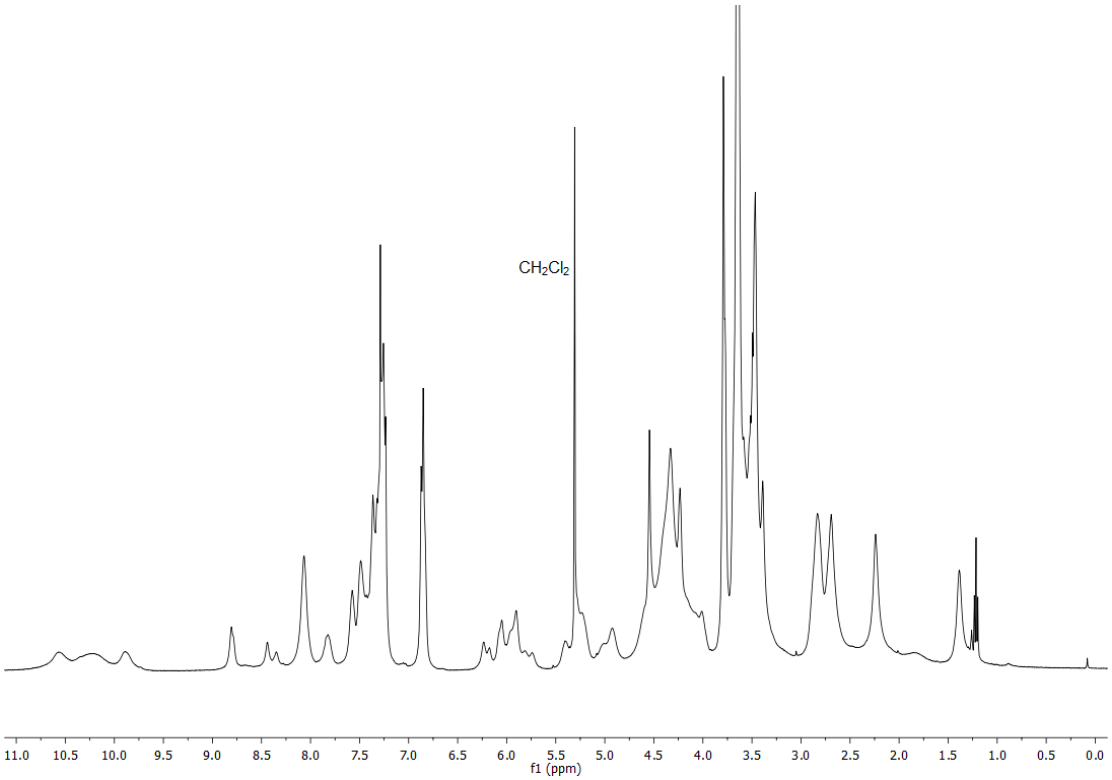


Figure B4.13. ^{1}H-NMR spectrum of Crude tris(mUp^{Cne}SmC^{Ac}p^{Cne}SmC^{Ac}p^{Cne}SmA^{Bz}p^{Cne}SmU-ODmtr) homostar, **13**.

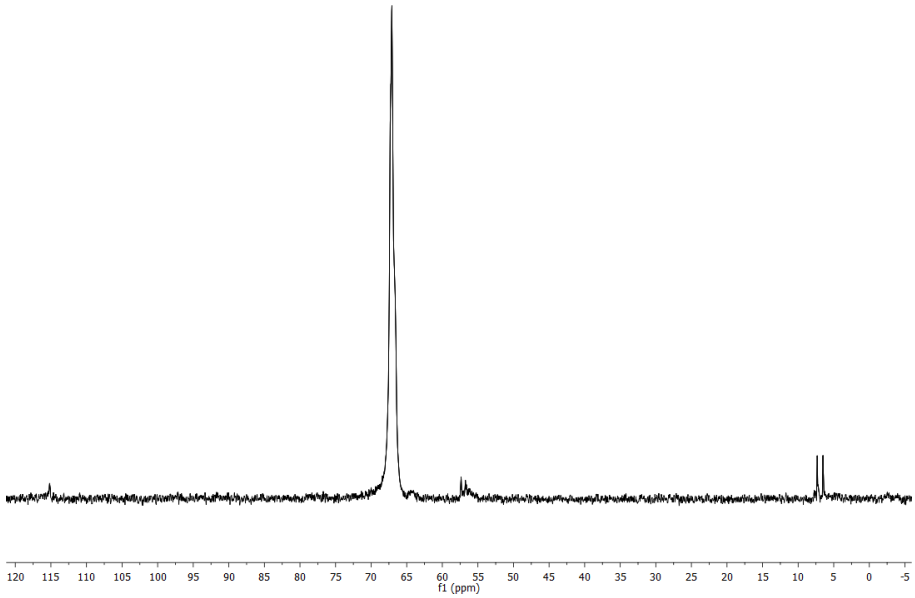


Figure B4.14. ^{31}P-NMR spectrum of Crude tris(mUp^{Cne}SmC^{Ac}p^{Cne}SmC^{Ac}p^{Cne}SmA^{Bz}p^{Cne}SmU-ODmtr) homostar, **13.**

Tris(mUp^{Cne}SmC^{Ac}p^{Cne}SmC^{Ac}p^{Cne}SmA^{Bz}p^{Cne}SmU-OH) homostar, **14** (400 MHz, $CDCl_3$-CD_3OD 3:1).

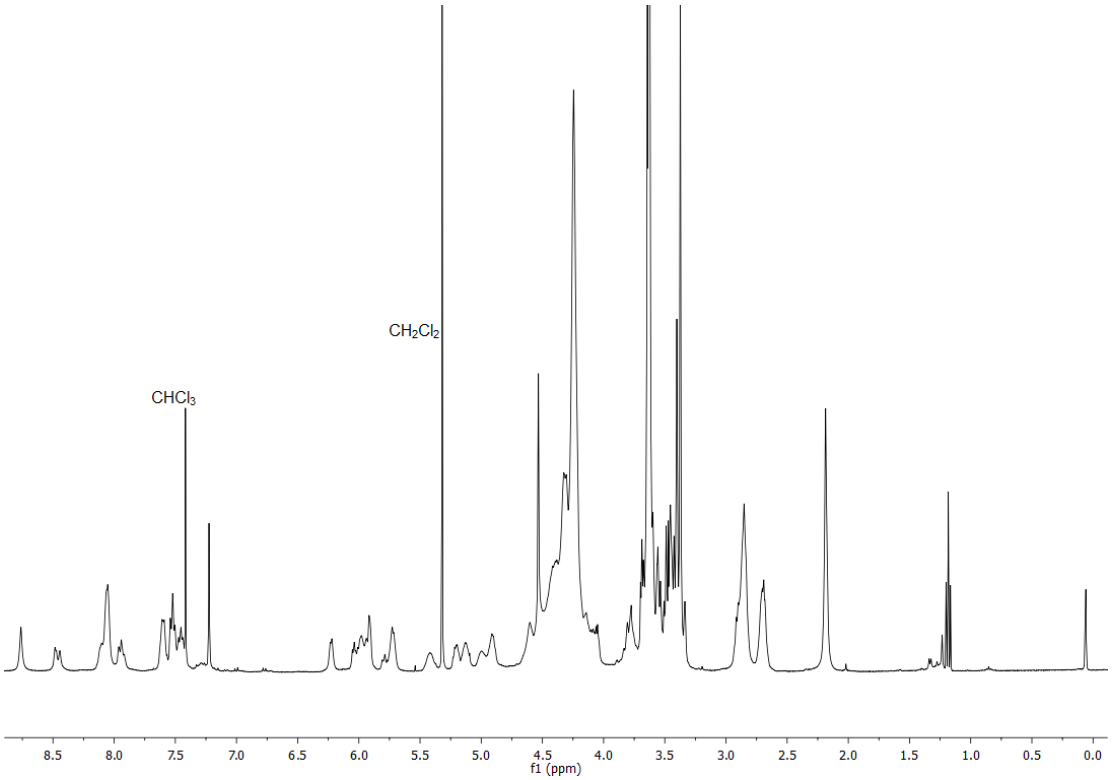


Figure B4.15. ^{1}H-NMR spectrum of Tris(mUp^{Cne}SmC^{Ac}p^{Cne}SmC^{Ac}p^{Cne}SmA^{Bz}p^{Cne}SmU-OH) homostar, **14**.

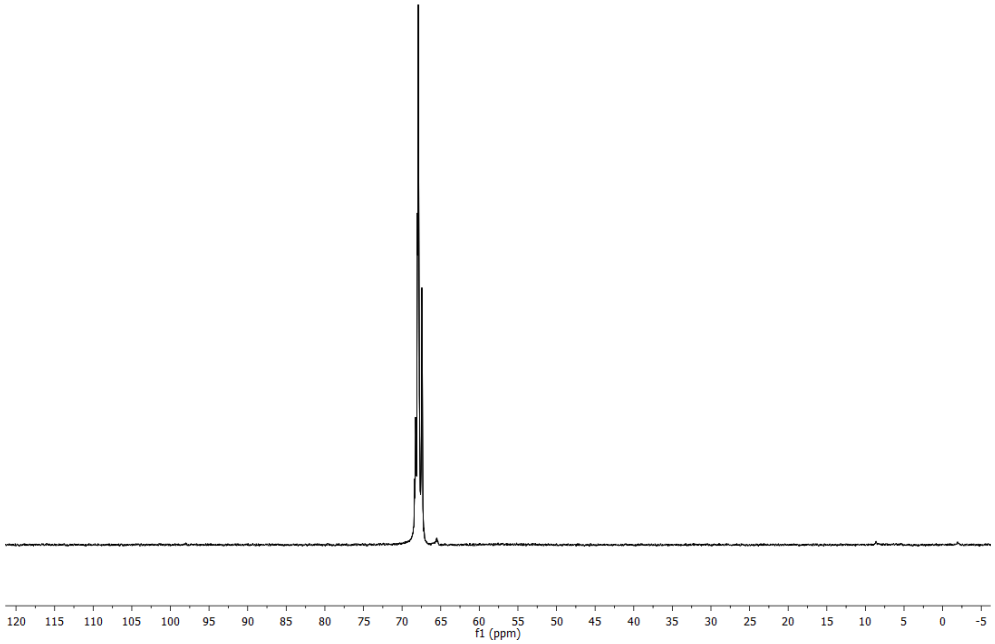


Figure B4.16. ^{31}P-NMR spectrum of Tris(mUp^{Cne}SmC^{Ac}p^{Cne}SmC^{Ac}p^{Cne}SmA^{Bz}p^{Cne}SmU-OH) homostar, **14.**

Crude tris(mUp^{Cne}SmC^{Ac}p^{Cne}SmC^{Ac}p^{Cne}SmA^{Bz}p^{Cne}SmUp^{Cne}SmU-ODmtr) homostar, **15** (500 MHz, D_6-acetone-CD_3OD 3:1).

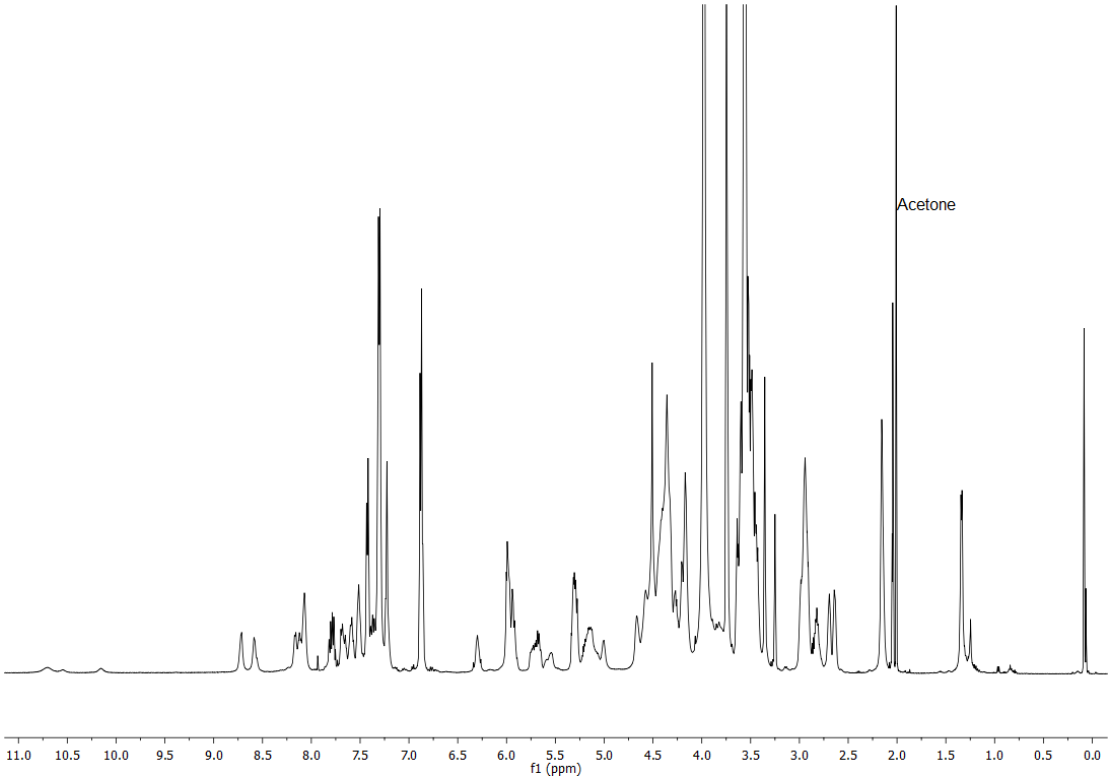


Figure B4.17. ^{1}H-NMR spectrum of Crude tris(mUp^{Cne}SmC^{Ac}p^{Cne}SmC^{Ac}p^{Cne}SmA^{Bz}p^{Cne}SmUp^{Cne}SmU-ODmtr) homostar, **15.**

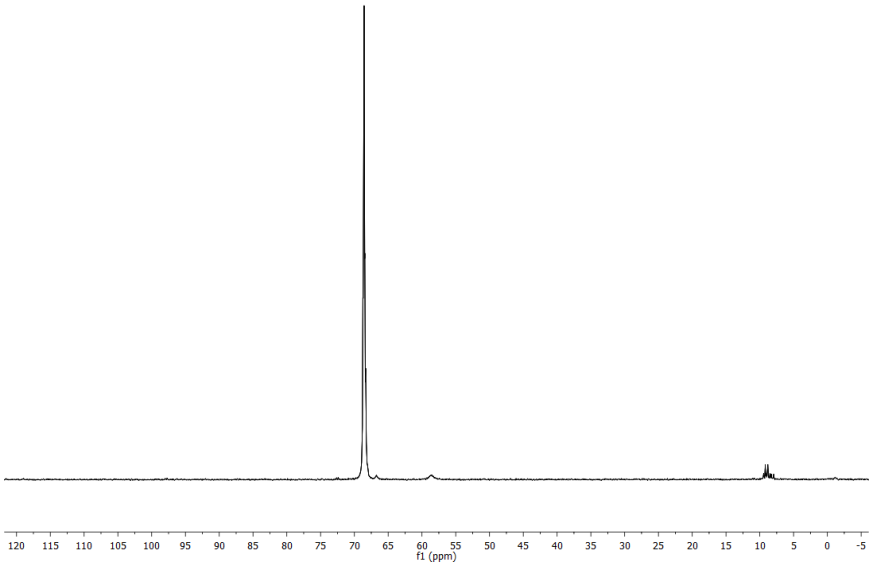


Figure B4.18. ^{31}P-NMR spectrum of Crude tris(mUp^{Cne}SmC^{Ac}p^{Cne}SmC^{Ac}p^{Cne}SmA^{Bz}p^{Cne}SmUp^{Cne}SmU-ODmtr) homostar, **15.**

Tris(mUp^{Cne}SmC^{Ac}p^{Cne}SmC^{Ac}p^{Cne}SmA^{Bz}p^{Cne}SmUp^{Cne}SmU-OH) homostar, **16** (500 MHz, $CDCl_3$-CD_3OD 3:1).

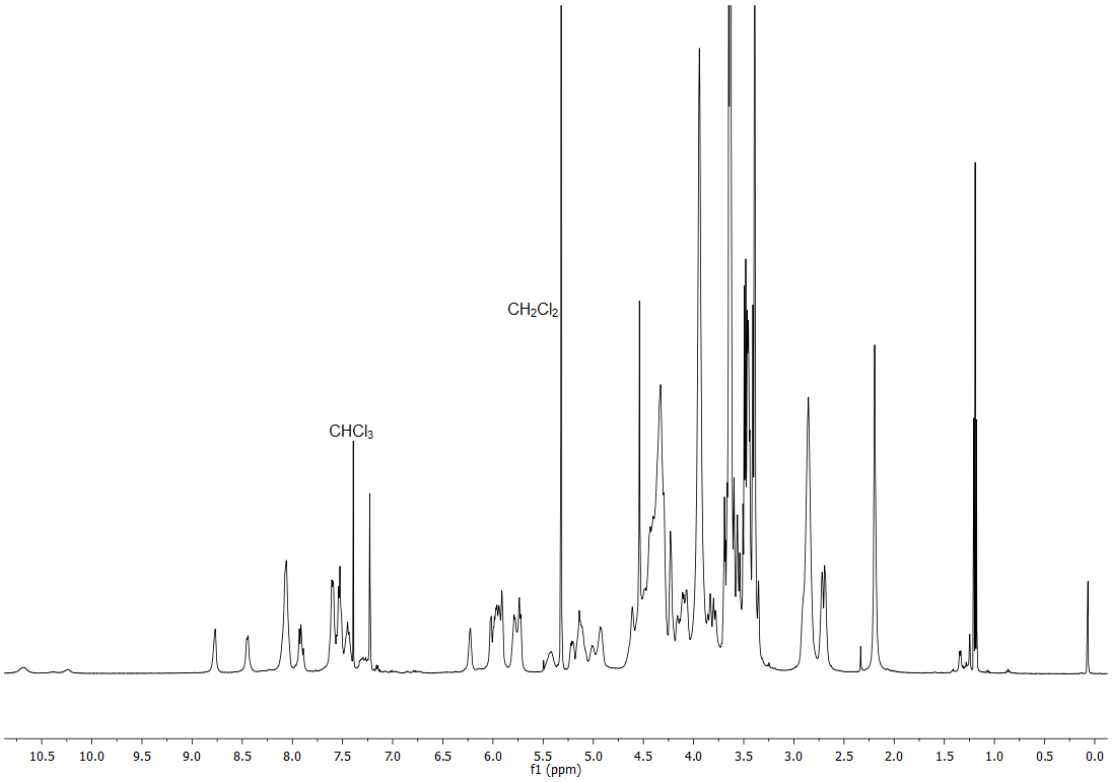


Figure B4.19. ^{1}H-NMR spectrum of Tris(mUp^{Cne}SmC^{Ac}p^{Cne}SmC^{Ac}p^{Cne}SmA^{Bz}p^{Cne}SmUp^{Cne}SmU-OH) homostar, **16.**

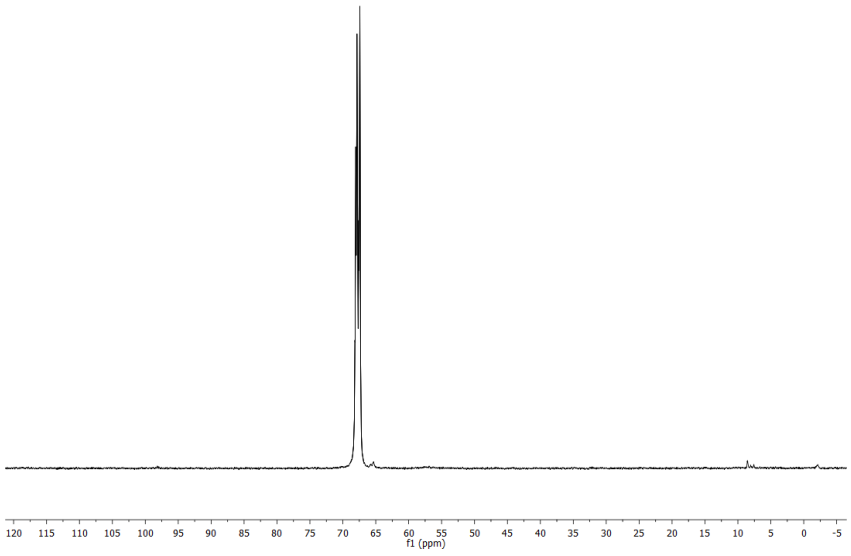


Figure B4.20. ^{31}P-NMR spectrum of Tris(mUp^{Cne}SmC^{Ac}p^{Cne}SmC^{Ac}p^{Cne}SmA^{Bz}p^{Cne}SmUp^{Cne}SmU-OH) homostar, **16**

Crude tris(mUp^{Cne}SmC^{Ac}p^{Cne}SmC^{Ac}p^{Cne}SmA^{Bz}p^{Cne}SmUp^{Cne}SmUp^{Cne}SmC^{Ac}-ODmtr) homostar, **17** (400 MHz, D_6-acetone CD_3OD 3:1).

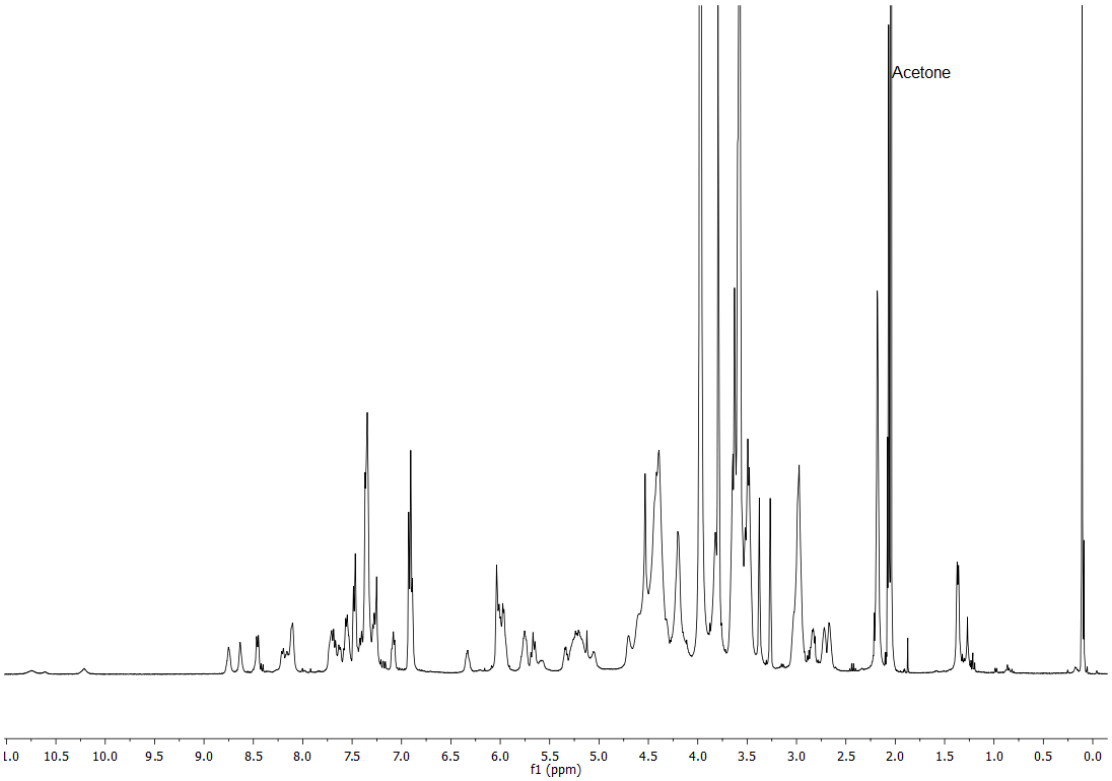


Figure B4.21. ^{1}H-NMR spectrum of crude tris(mUp^{Cne}SmC^{Ac}p^{Cne}SmC^{Ac}p^{Cne}SmA^{Bz}p^{Cne}SmUp^{Cne}SmUp^{Cne}SmC^{Ac}-ODmtr) homostar, **17.**

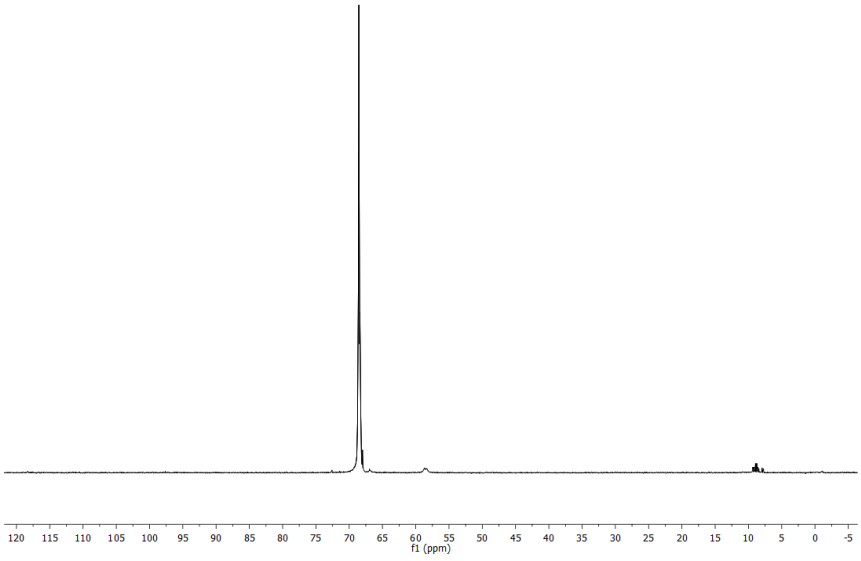


Figure B4.22. ^{31}P-NMR spectrum of Crude tris(mUp^{Cne}SmC^{Ac}p^{Cne}SmC^{Ac}p^{Cne}SmA^{Bz}p^{Cne}SmUp^{Cne}SmUp^{Cne}SmC^{Ac}-ODmtr) homostar, **17.**

Tris(mUp^{Cne}SmC^{Ac}p^{Cne}SmC^{Ac}p^{Cne}SmA^{Bz}p^{Cne}SmUp^{Cne}SmUp^{Cne}SmC^{Ac}-OH) homostar, **18** (500 MHz, $CDCl_3$-CD_3OD 3:1).

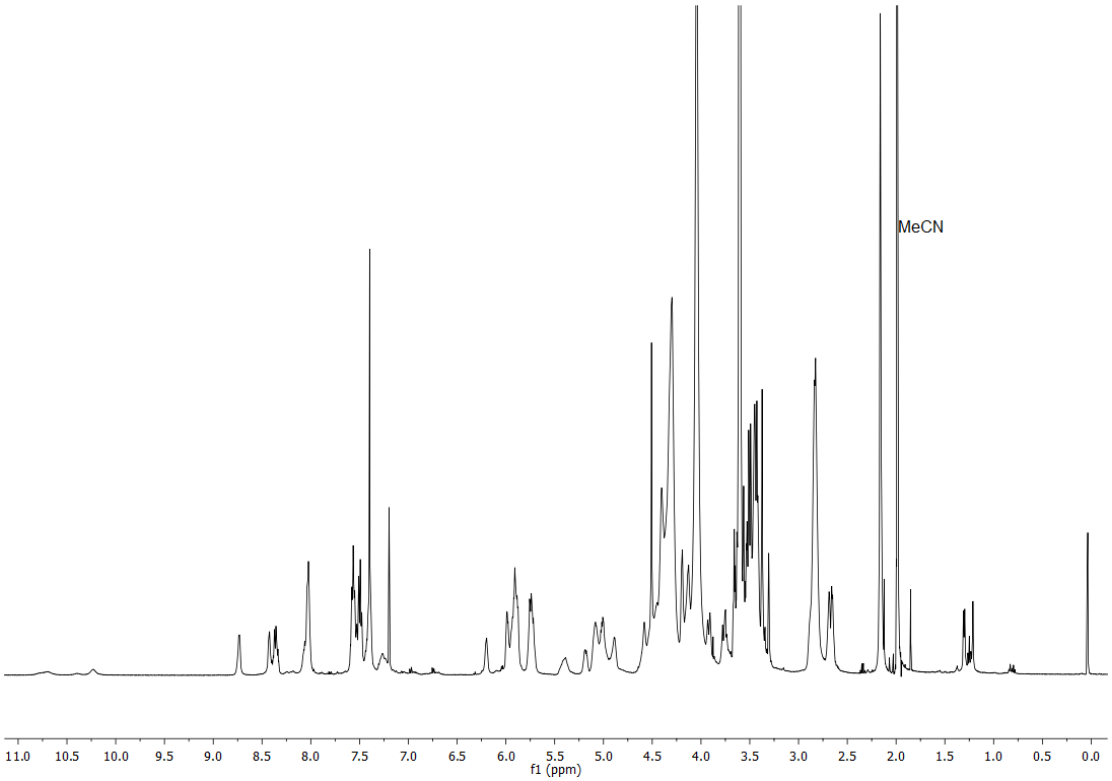


Figure B4.23. ^{1}H-NMR spectrum of Tris(mUp^{Cne}SmC^{Ac}p^{Cne}SmC^{Ac}p^{Cne}SmA^{Bz}p^{Cne}SmUp^{Cne}SmUp^{Cne}SmC^{Ac}-OH) homostar, **18.**

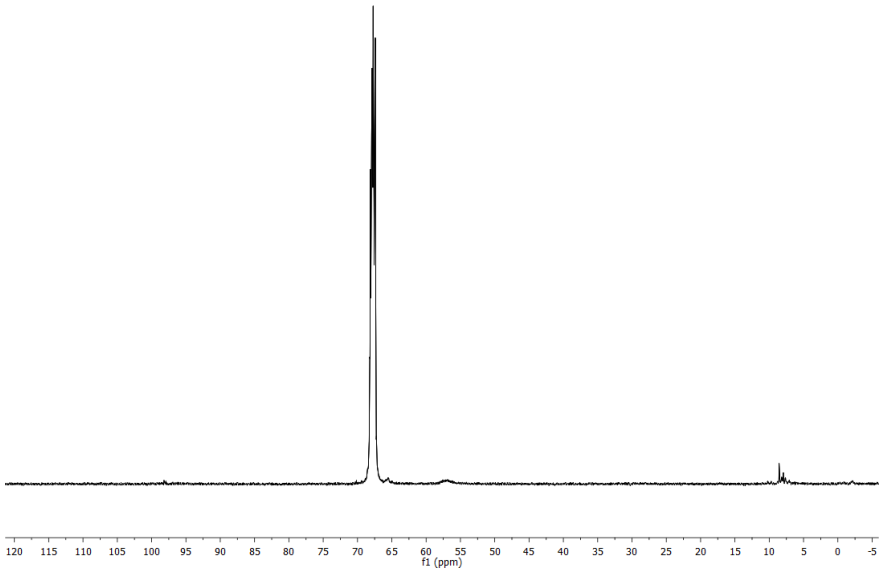


Figure B4.24. ^{31}P-NMR spectrum of Tris(mUp^{Cne}SmC^{Ac}p^{Cne}SmC^{Ac}p^{Cne}SmA^{Bz}p^{Cne}SmUp^{Cne}SmUp^{Cne}SmC^{Ac}-OH) homostar, **18**

Crude tris(mUp^{Cne}SmC^{Ac}p^{Cne}SmC^{Ac}p^{Cne}SmA^{Bz}p^{Cne}SmUp^{Cne}SmUp^{Cne}SmC^{Ac}p^{Cne}SmG^{iBu}-ODmtr) homostar, **19**.

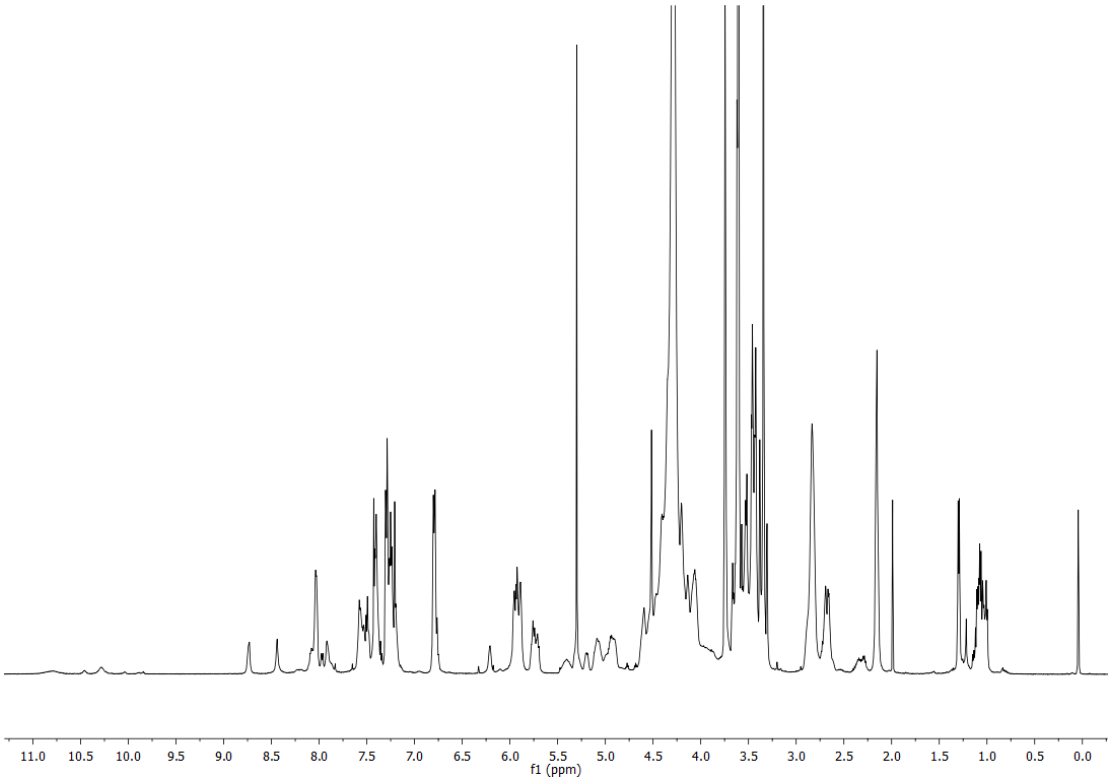


Figure B4.25. ^{1}H-NMR spectrum of crude tris(mUp^{Cne}SmC^{Ac}p^{Cne}SmC^{Ac}p^{Cne}SmA^{Bz}p^{Cne}SmUp^{Cne}SmUp^{Cne}SmC^{Ac}p^{Cne}SmG^{iBu}-ODmtr) homostar, **19**.

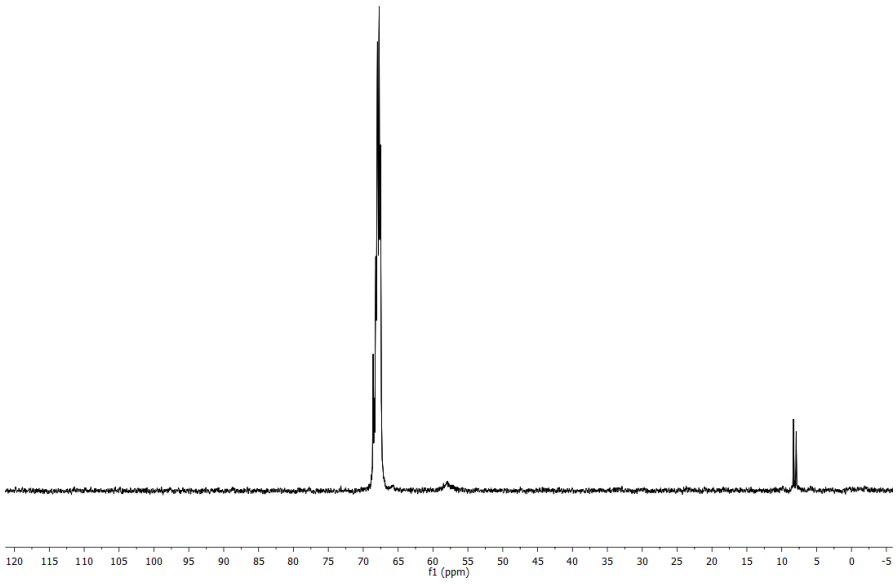


Figure B4.26. ^{31}P-NMR spectrum of Crude tris(mUp^{Cne}SmC^{Ac}p^{Cne}SmC^{Ac}p^{Cne}SmA^{Bz}p^{Cne}SmUp^{Cne}SmUp^{Cne}SmC^{Ac}p^{Cne}SmG^{iBu}-ODmtr) homostar, **19**.

Tris(mUp^{Cne}SmC^{Ac}p^{Cne}SmC^{Ac}p^{Cne}SmA^{Bz}p^{Cne}SmUp^{Cne}SmUp^{Cne}SmC^{Ac}p^{Cne}SmG^{iBu}-OH) homostar, **20**.

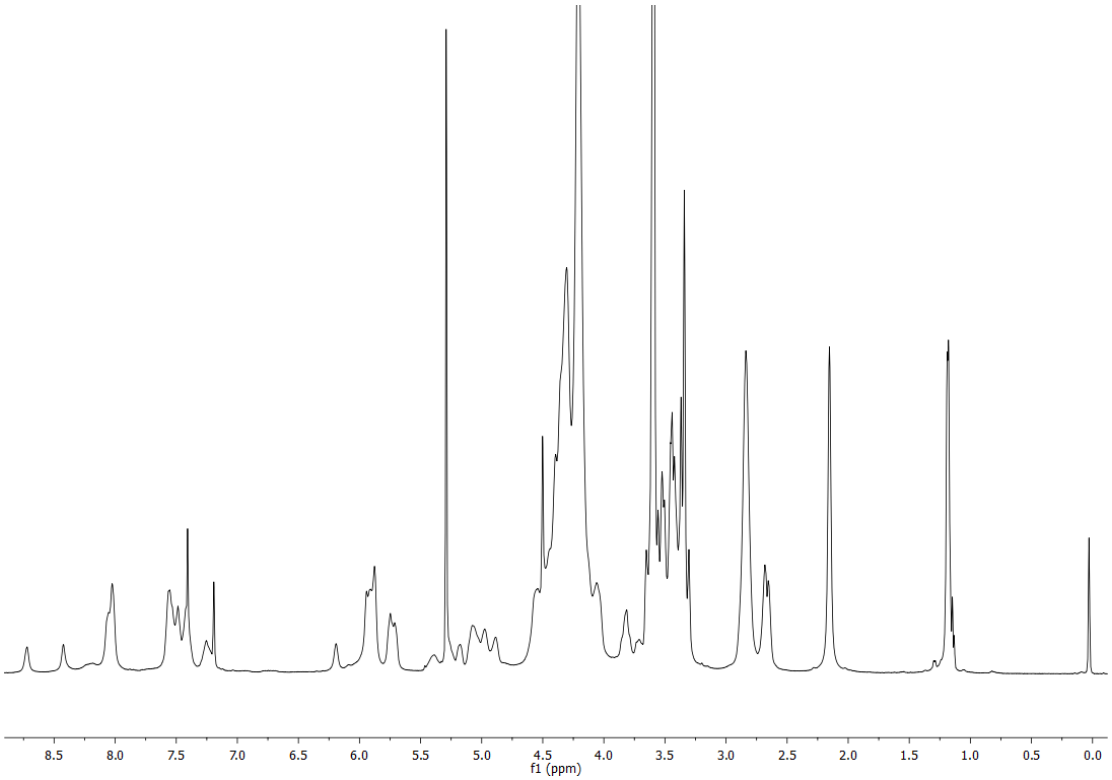


Figure B4.27. ^{1}H-NMR spectrum of Tris(mUp^{Cne}SmC^{Ac}p^{Cne}SmC^{Ac}p^{Cne}SmA^{Bz}p^{Cne}SmUp^{Cne}SmUp^{Cne}SmC^{Ac}p^{Cne}SmG^{iBu}-OH) homostar, **20**.

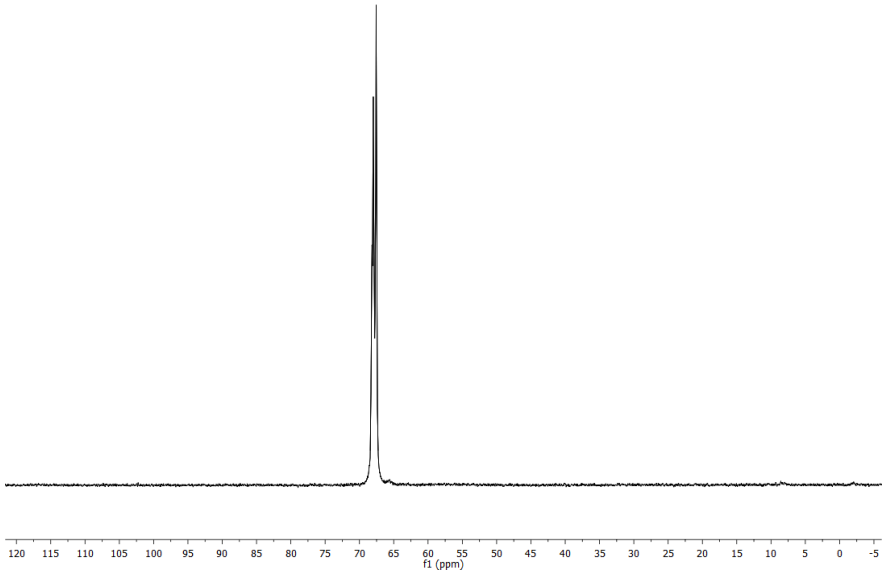


Figure B4.28. ^{31}P-NMR spectrum of Tris(mUp^{Cne}SmC^{Ac}p^{Cne}SmC^{Ac}p^{Cne}SmA^{Bz}p^{Cne}SmUp^{Cne}SmUp^{Cne}SmC^{Ac}p^{Cne}SmG^{iBu}-OH) homostar, **20**.

Crude tris(mUp^{Cne}SmC^{Ac}p^{Cne}SmC^{Ac}p^{Cne}SmA^{Bz}p^{Cne}SmUp^{Cne}SmUp^{Cne}SmC^{Ac}p^{Cne}S-mG^{iBu}p^{Cne}SmG^{iBu}ODmtr) homostar, **21**.

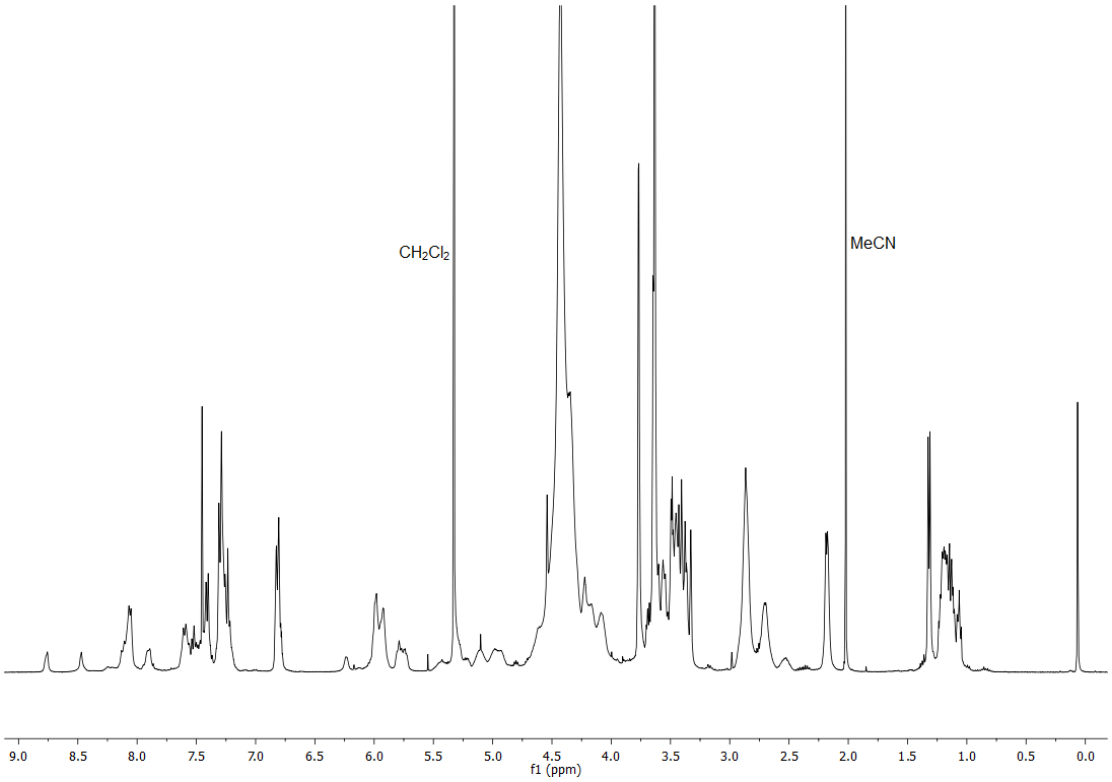


Figure B4.29. ^{1}H-NMR spectrum of crude tris(mUp^{Cne}SmC^{Ac}p^{Cne}SmC^{Ac}p^{Cne}SmA^{Bz}p^{Cne}SmUp^{Cne}SmUp^{Cne}SmC^{Ac}p^{Cne}S-mG^{iBu}p^{Cne}SmG^{iBu}ODmtr) homostar, **21**.

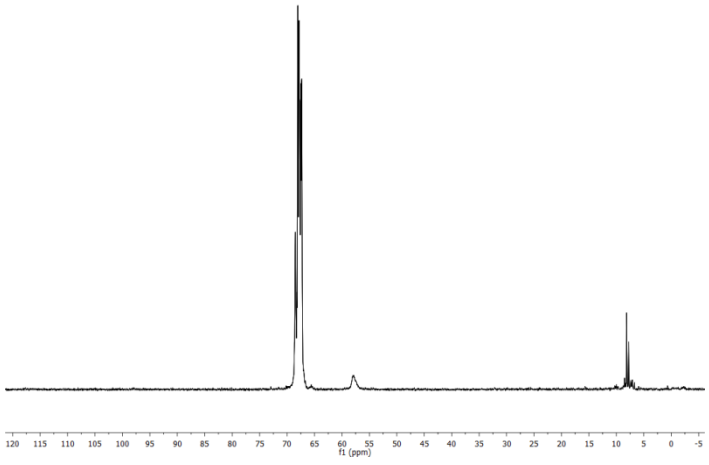


Figure B4.30. ^{31}P-NMR spectrum of crude tris(mUp^{Cne}SmC^{Ac}p^{Cne}SmC^{Ac}p^{Cne}SmA^{Bz}p^{Cne}SmUp^{Cne}SmUp^{Cne}SmC^{Ac}p^{Cne}S-mG^{iBu}p^{Cne}SmG^{iBu}ODmtr) homostar, **21**.

Tris(mUp^{Cne}SmC^{Ac}p^{Cne}SmC^{Ac}p^{Cne}SmA^{Bz}p^{Cne}SmUp^{Cne}SmUp^{Cne}SmC^{Ac}p^{Cne}SmG^{iBu}p^{Cne}SmG^{iBu}-OH) homostar, 22.

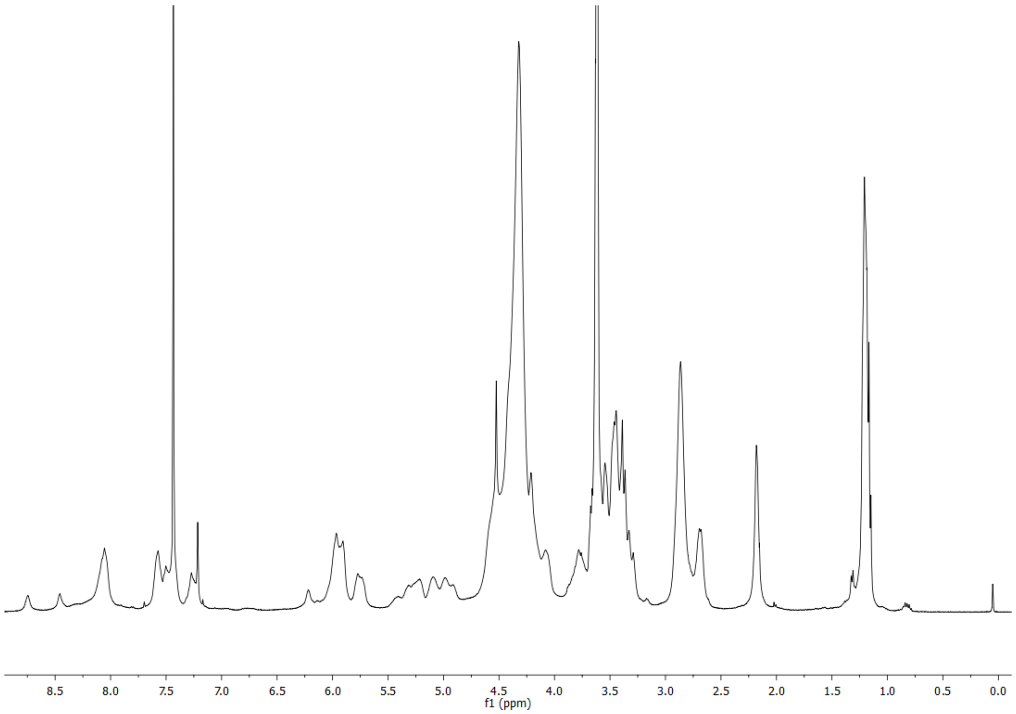


Figure B4.31. ^{1}H-NMR spectrum of Tris(mUp^{Cne}SmC^{Ac}p^{Cne}SmC^{Ac}p^{Cne}SmA^{Bz}p^{Cne}SmUp^{Cne}SmUp^{Cne}SmC^{Ac}p^{Cne}SmG^{iBu}p^{Cne}SmG^{iBu}-OH) homostar, 22.

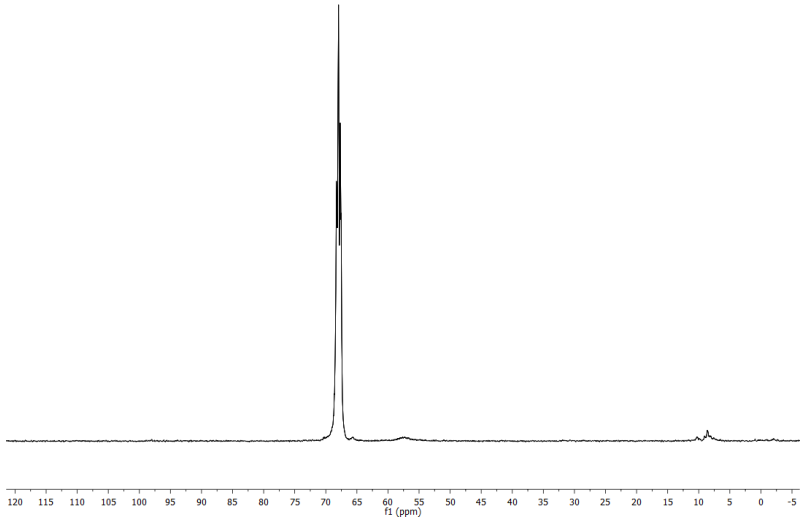


Figure B4.32. ^{31}P-NMR spectrum of Tris(mUp^{Cne}SmC^{Ac}p^{Cne}SmC^{Ac}p^{Cne}SmA^{Bz}p^{Cne}SmUp^{Cne}SmUp^{Cne}SmC^{Ac}p^{Cne}SmG^{iBu}p^{Cne}SmG^{iBu}-OH) homostar, **22**.

Tris(mU-ODmtr) homostar, 3.

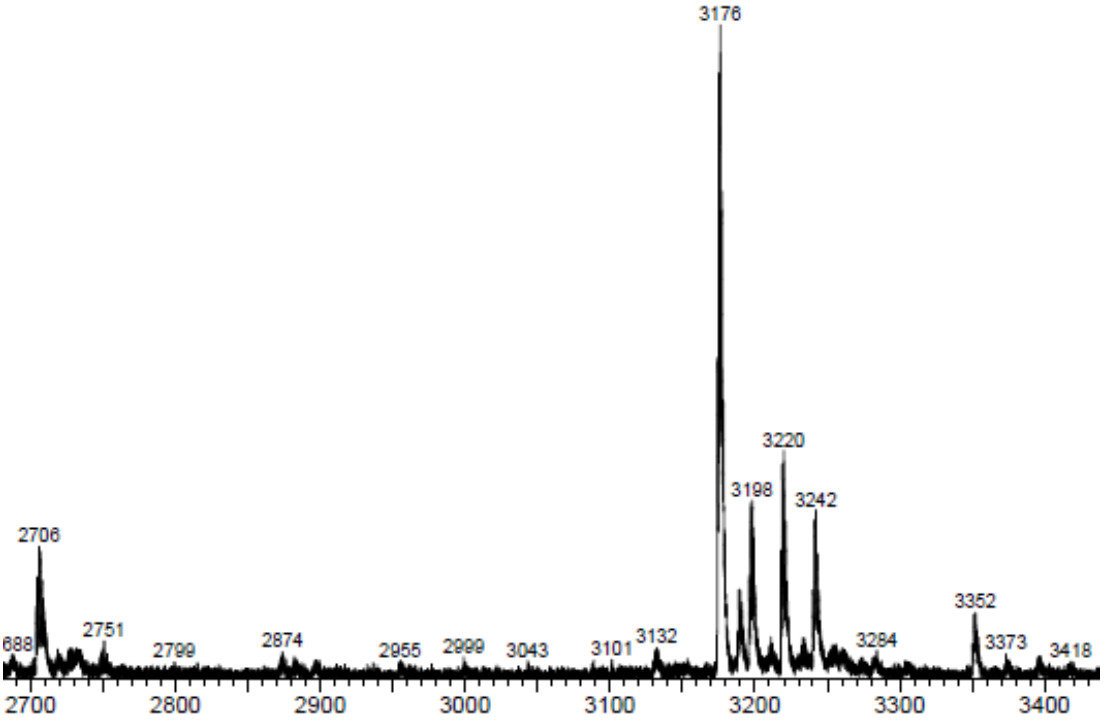


Figure B4.33. *m/z* (MALDI-ToF+) [**3**+Na]$^+$ = 3176, calc. $C_{162}H_{210}N_6NaO_{57}^+$ = 3175.4. [**3**−H+2Na]$^+$ = 3198, [**3**−2H+3Na]$^+$ = 3220, and [**3**−3H+4Na]$^+$ = 3242. Peak at *m/z* = 2706 corresponds to Dcb ester on one arm of the homostar which is not separated until after detritylation. Peak at *m/z* = 3352 may corresponds Dcb acylation of uracil, but is not observed after detritylation.

Tris(mU-OH) homostar, 4.

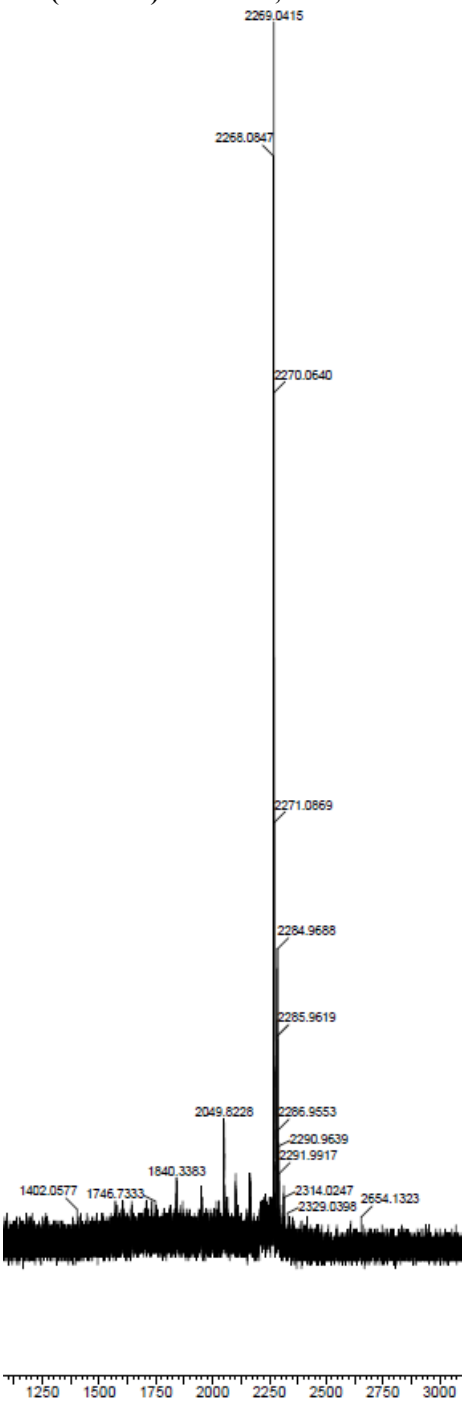


Figure B4.34. *m/z* (MALDI-ToF+) $[\mathbf{4}+Na]^+$ = 2269.0, calc. $C_{99}H_{156}N_6NaO_{51}^+$ = 2268.97. Peak at *m/z* = 2049.8 corresponds to hydrolysis of succinyl mU ester sodium salt, probably during ionisation, calc. $C_{89}H_{143}N_4Na_2O_{46}^+$ = 2049.88.

Tris(mUp^{Cne}SmC^{Ac}-ODmtr) homostar, 7.

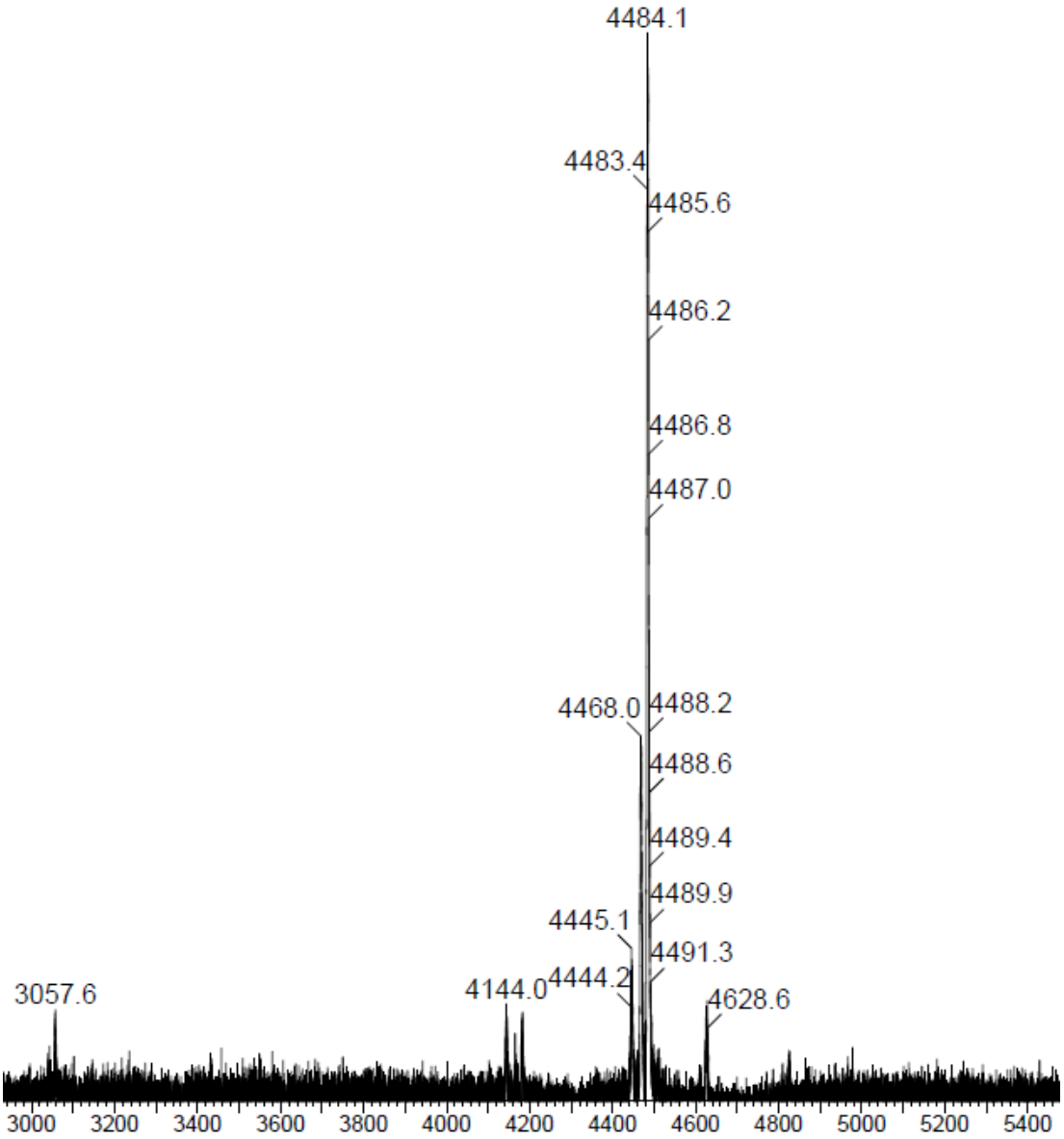


Figure B4.36. *m/z* (MALDI-ToF+) $[\mathbf{7}+Na+H_2O]^+$ = 4484.1, calc. $C_{207}H_{269}N_{18}NaO_{79}P_3S_3^+$ = 4484.59; $[\mathbf{7}+Na]^+$ = 4468.0, and $[\mathbf{7}+H]^+$ = 4445.1. Peak at *m/z* = 4144.0 corresponds to detritylation during ionisation, calc. $C_{188}H_{250}N_{18}O_{76}P_3S_3^+$ = 4142.47, and peak at *m/z* = 3057.6 corresponds to a trace of benzyl ether hydrolysis, probably during ionisation, calc. $C_{141}H_{182}KN_{12}O_{53}P_2S_2^+$ = 3057.05.

Tris(mUp^{Cne}SmC^{Ac}-OH) homostar, 8.

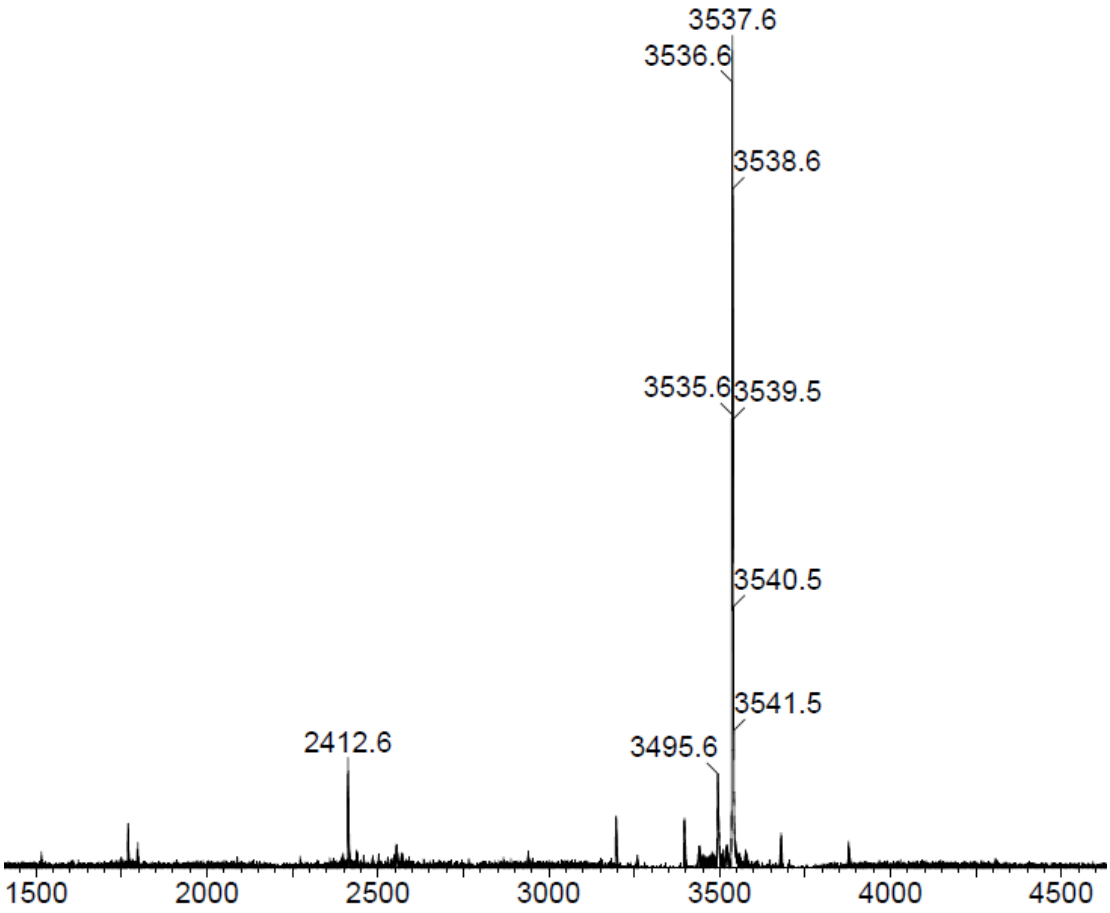


Figure B4.37. *m/z* (MALDI-ToF+) [**8**+H]$^+$ = 3538.3, calc. $C_{144}H_{214}N_{18}NaO_{72}P_3S_3^+$ = 3537.20; [**10**−Ac+2H]$^+$ = 3495.6, calc. $C_{142}H_{212}N_{18}O_{71}P_3S_3^+$ = 3495.19. Peak at *m/z* = 2412.6 corresponds to a trace of benzyl ether hydrolysis, probably during ionisation, calc. $C_{99}H_{147}N_{12}O_{49}P_2S_2^+$ = 2414.83.

LC-MS of tris(mUp^{Cne}SmC^{Ac}-OH) homostar, 8

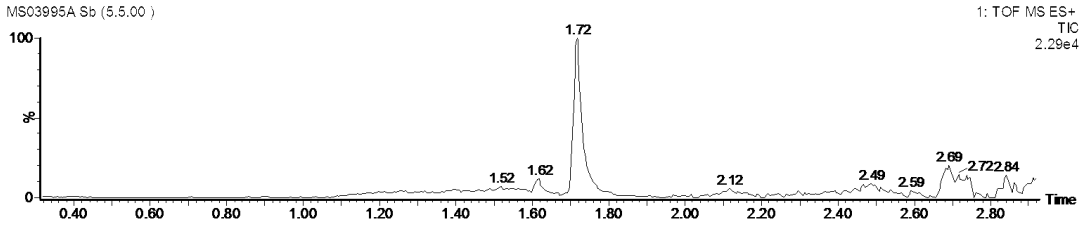


Figure B4.38. Ion chromatogram.



Figure B4.39. MS (ESI+) of peak at 1.62 min. Peak at *m/z* = 1166.1 corresponds to deacetylation of homostar **8**, $[\mathbf{8}-\text{Ac}+\text{K}+2\text{H}]^{2+}$, calc = $C_{142}H_{212}KN_{18}O_{71}P_3S_3^{2+}$ = 1167.08.

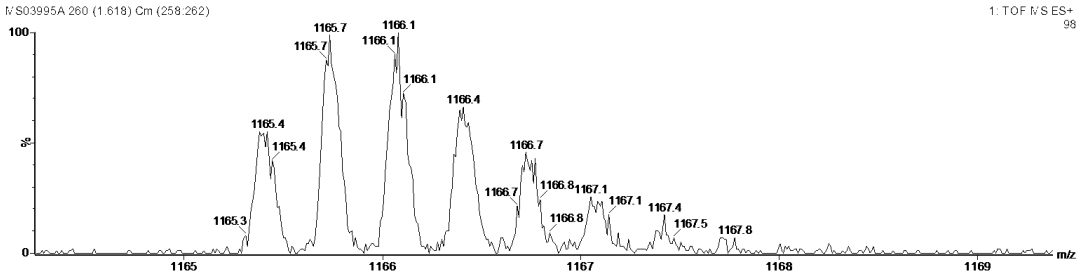


Figure B4.40. Expansion of impurity peak at 1.62 min, $[\mathbf{8}-\text{Ac}+\text{K}+\text{H}]^{2+}$.

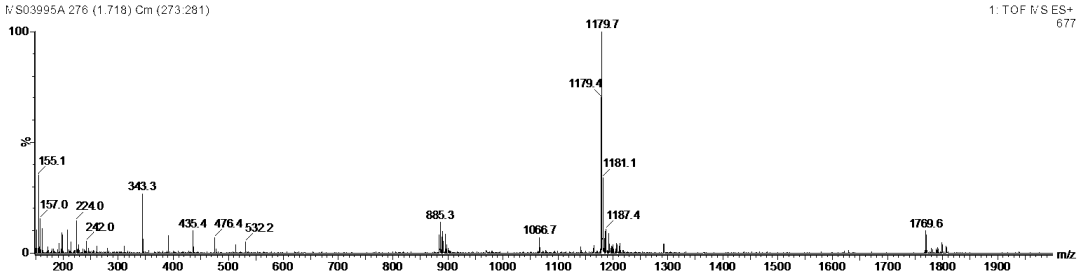


Figure B4.41. MS (ESI+) of main peak at 1.72 min, *m/z* = 1179.7 corresponds to tris(2-mer-OH) homostar $[\mathbf{8}+\text{Na}+\text{H}]^{2+}$, calc. $C_{144}H_{214}N_{18}NaO_{72}P_3S_3^{2+}$ = 1780.09.



Figure B4.42. Expansion of molecular ion at 1.72 min, [**8**+Na+H]$^{2+}$.

Tris(mUp^{Cne}SmC^{Ac}p^{Cne}SmC^{Ac}-ODmtr) homostar, 9.

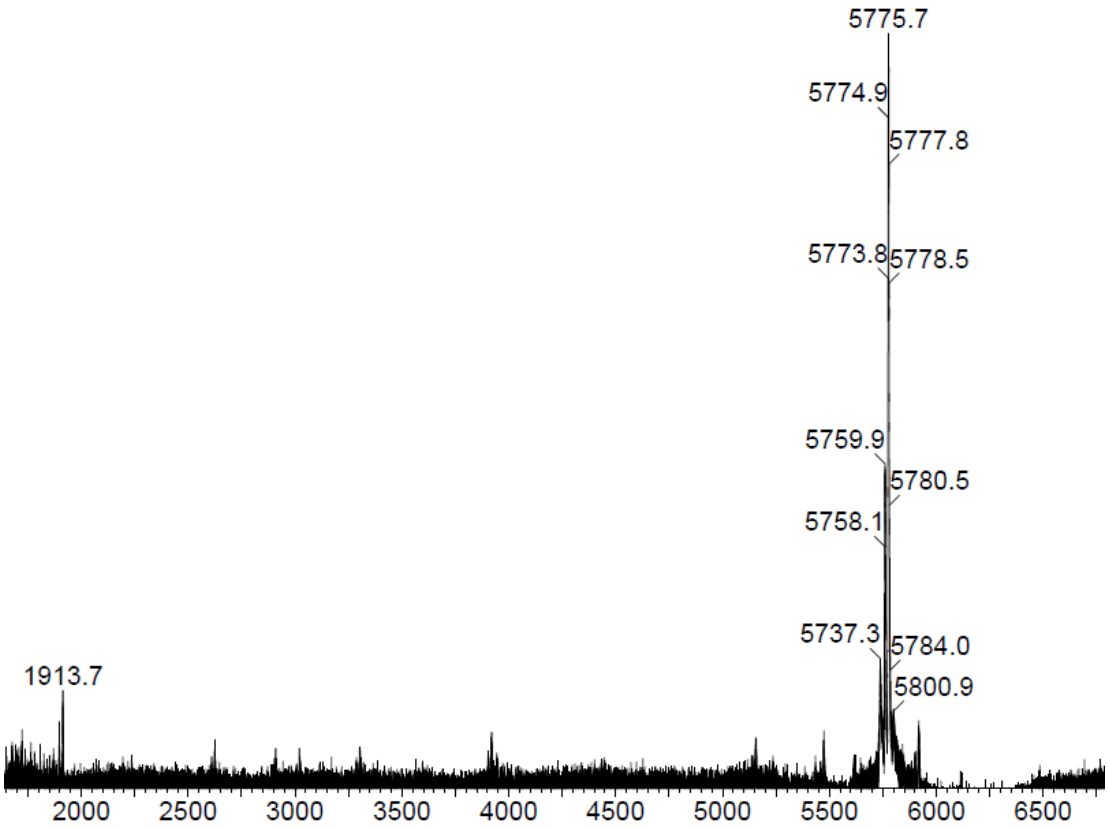


Figure B4.43. *m/z* (MALDI-ToF+) [**9**+Na+H_2O]$^+$ = 5775.7, calc. $C_{252}H_{326}N_{30}NaO_{100}P_6S_6^+$ = 5775.81; [**9**+Na]$^+$ = 5759.9. Peak at *m/z* = 3918.9 corresponds to a trace of benzyl ether hydrolysis, probably during ionisation, calc. $C_{171}H_{220}KN_{20}O_{67}P_4S_4^+$ = 3917.19, and *m/z* = 1913.7 is the corresponding trinucleotidyl Eg_8 species, calc. $C_{81}H_{106}N_{10}KO_{33}P_2S_2^+$ = 1911.55.

Tris(mUp^{Cne}SmC^{Ac}p^{Cne}SmC^{Ac}-OH) homostar, 10.

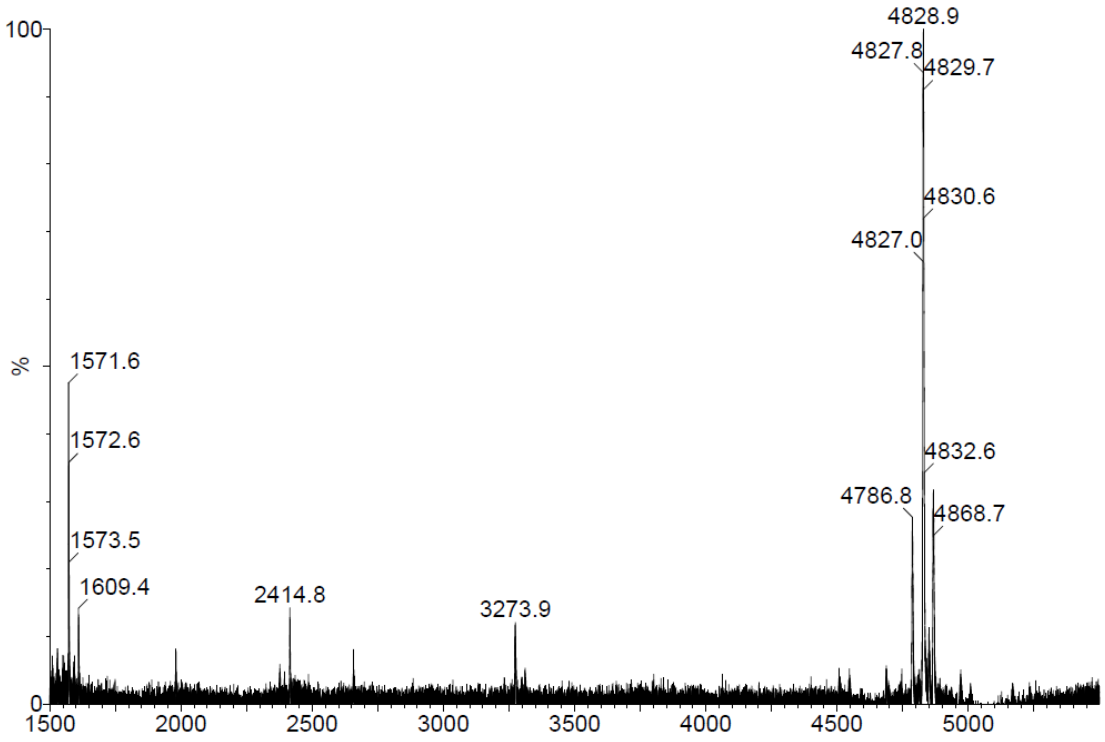


Figure B4.44. *m/z* (MALDI-ToF+) [**10**+H]$^+$ = 4828.9, calc. $C_{189}H_{271}N_{30}O_{93}P_6S_6^+$ = 4828.42; [**10**+Na+H_2O]$^+$ = 4868.7; [**10**+Na+H_3O]$^{2+}$ = 2414.8. [**10**−Ac+2H]$^+$ = 4886.8, calc. $C_{187}H_{269}N_{30}O_{92}P_6S_6^+$ = 4786.4. Peak at *m/z* = 3273.9 corresponds to a trace of benzyl ether hydrolysis, probably during ionisation, calc. $C_{129}H_{185}N_{20}O_{63}P_4S_4^+$ = 3274.98, and *m/z* = 1571.6 is the corresponding trinucleotidyl Eg_8 species, calc. $C_{60}H_{89}N_{10}O_{31}P_2S_2^+$ = 1571.46. NB: There are no peaks around *m/z* = 5216 which would indicate branching on cytosine unprotected 6-NH_2.

Tris(mUp^{Cne}SmC^{Ac}p^{Cne}SmC^{Ac}p^{Cne}SmA^{Bz}-ODmtr) homostar, 11.

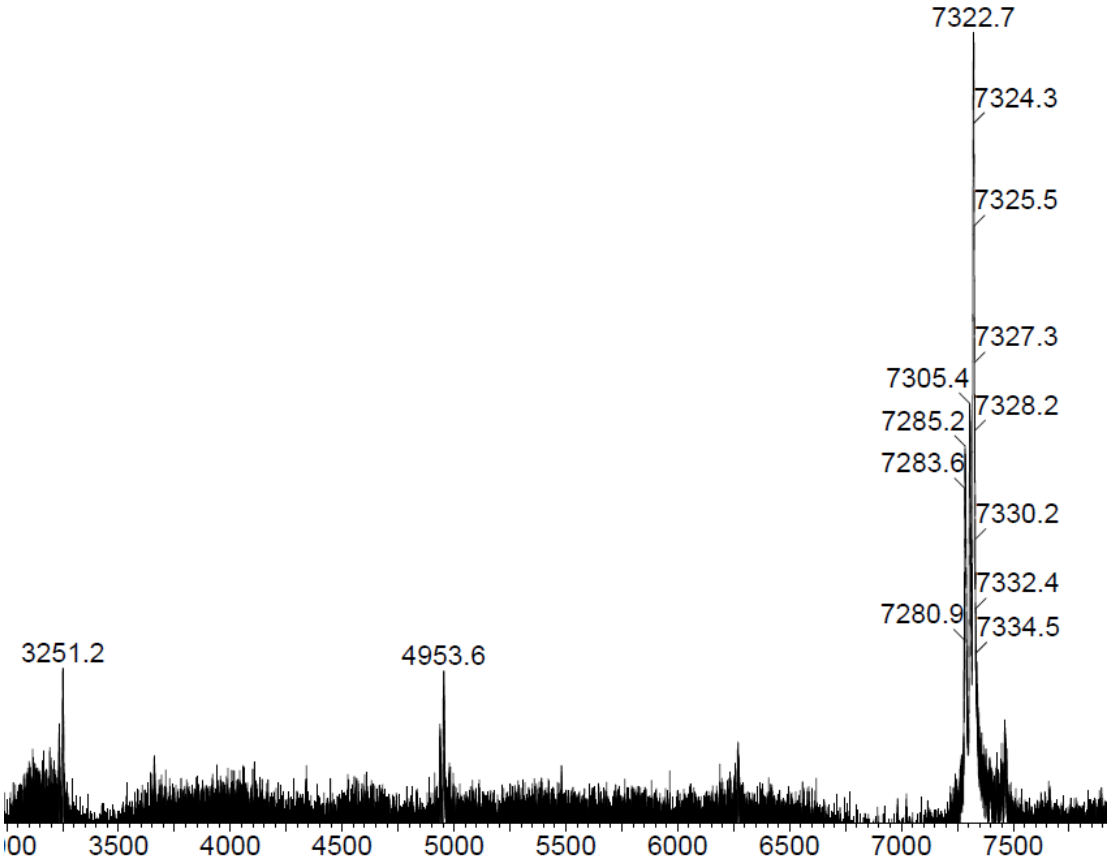


Figure B4.45. *m/z* (MALDI-ToF+) [**11**+K]$^+$ = 7322.7, calc. $C_{315}H_{387}N_{48}KO_{117}P_9S_9^+$ = 7323.07; [**11**+Na]$^+$ = 7305.4; [**11**+H]$^+$ = 7285.2. Peak at *m/z* = 4953.6 corresponds to a trace of benzyl ether hydrolysis, probably during ionisation, calc. $C_{213}H_{264}N_{32}NaO_{80}P_6S_6^+$ = 4953.43.

Tris(mUp^{Cne}SmC^{Ac}p^{Cne}SmC^{Ac}p^{Cne}SmA^{Bz}-OH) homostar, 12.

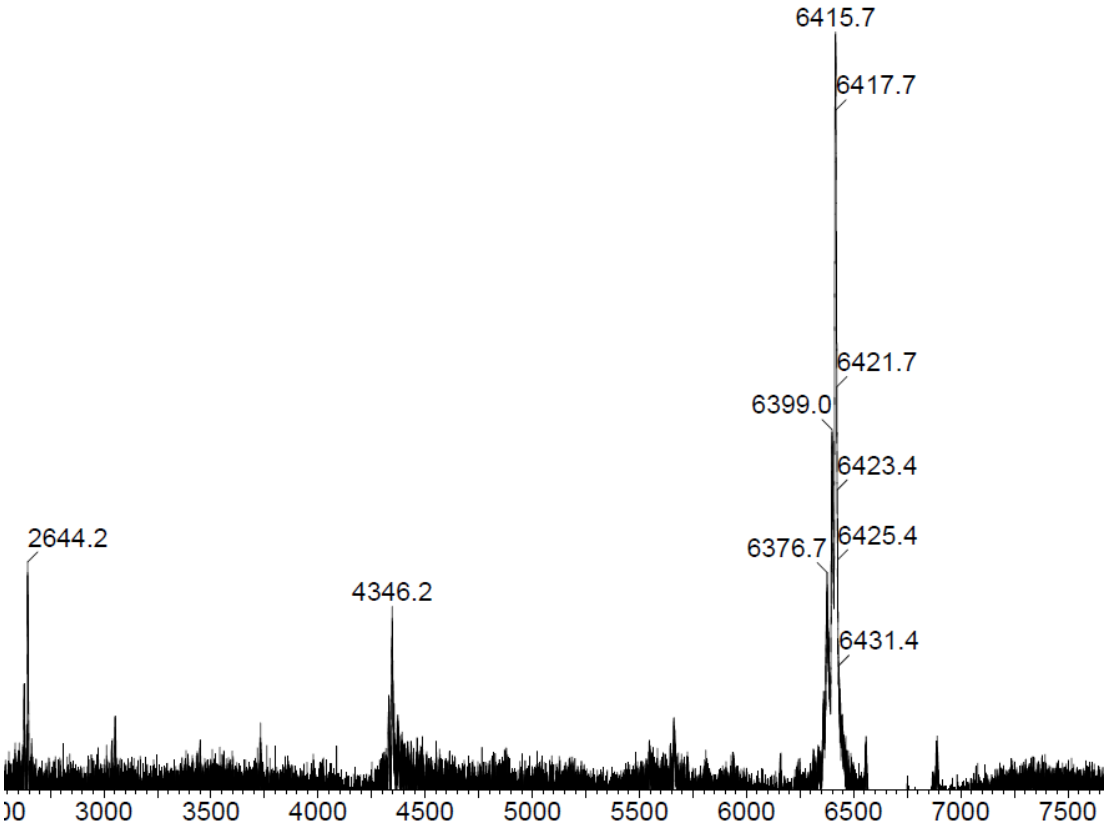


Figure B4.46. *m/z* (MALDI-ToF+) [**12**+K]$^+$ = 6416.7, calc. $C_{252}H_{333}KN_{48}O_{111}P_9S_9^+$ = 6414.67. Peak at *m/z* = 4346.2 corresponds to a trace of benzyl ether hydrolysis, probably during ionisation, calc. $C_{171}H_{225}N_{32}KO_{75}P_6S_6^+$ = 4346.13.

Tris(mUp^{Cne}SmC^{Ac}p^{Cne}SmC^{Ac}p^{Cne}SmA^{Bz}p^{Cne}SmU-ODmtr) homostar, 13.

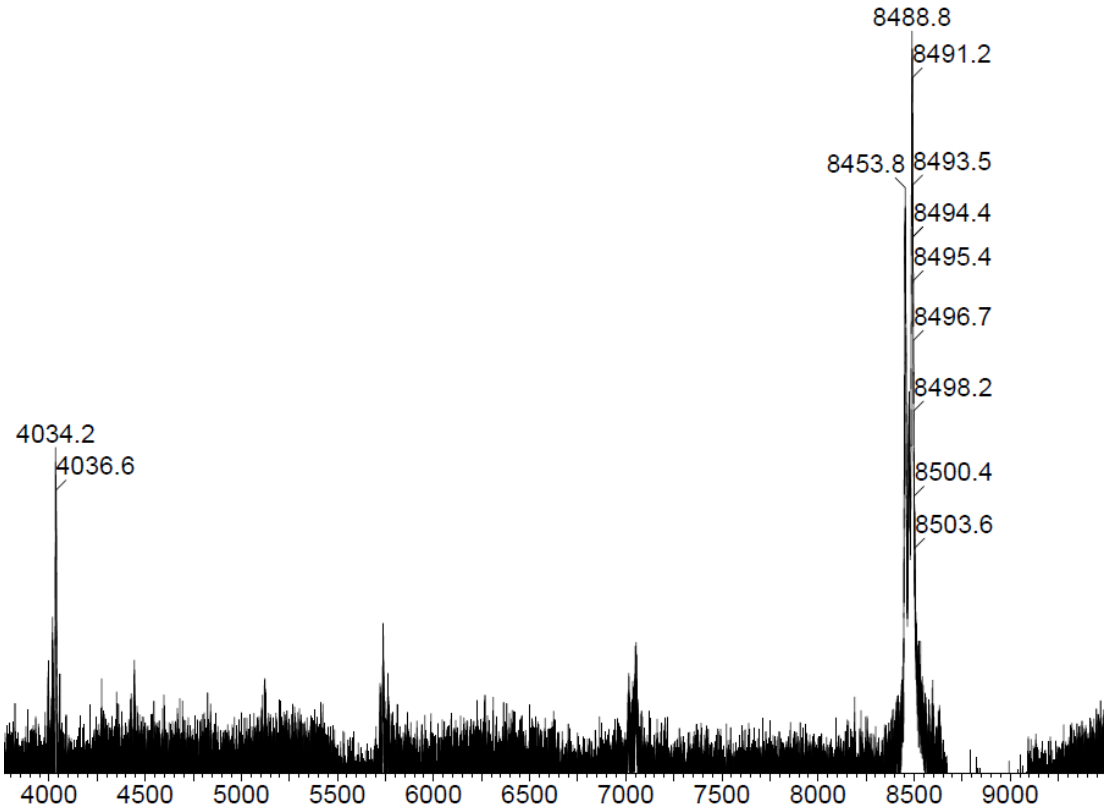


Figure B4.47. *m/z* (MALDI-ToF+) [**13**+K]$^+$ = 8488.8, calc. $C_{354}H_{435}KN_{57}O_{138}P_{12}S_{12}^+$ = 8489.20; [**13**+H]$^+$ = 8453.8.

Tris(mUp^{Cne}SmC^{Ac}p^{Cne}SmC^{Ac}p^{Cne}SmA^{Bz}p^{Cne}SmU-OH) homostar, 14.

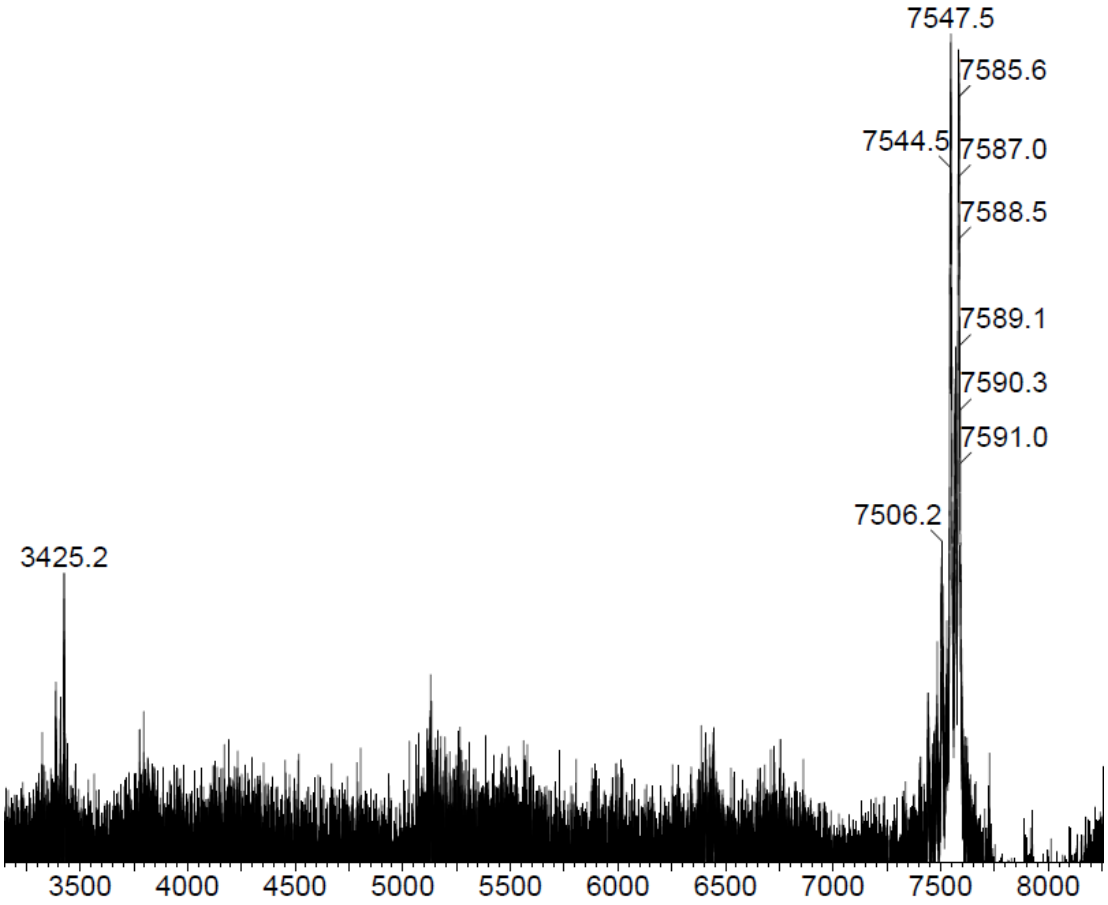


Figure B4.48. *m/z* (MALDI-ToF+) [**14**+H]$^+$ = 7547.5, calc. $C_{291}H_{382}N_{57}O_{132}P_{12}S_{12}^+$ = 7544.85; [**14**+K]$^+$ = 7585.6.

LC-MS of crude HO-mUpSmCpSmCpSmApSmUp-OH, 23.

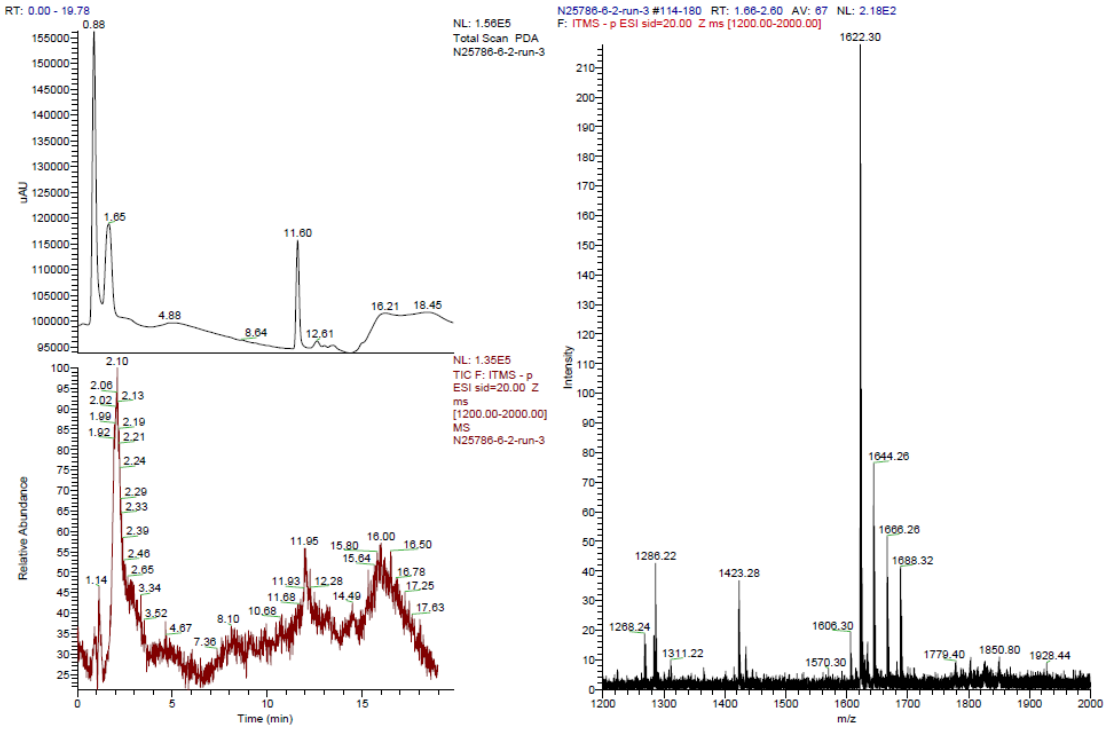


Figure B4.49. Top left) HPLC trace; bottom left) ion chromatogram; right) wide range total MS (ESI+) of peak from 1.66 to 2.60 min, *m/z* [**23**+H]$^+$ = 1622.30, calc. $C_{51}H_{70}N_{15}O_{30}P_4S_4^+$ = 1624.22.

Tris(mUp^{Cne}SmC^{Ac}p^{Cne}SmC^{Ac}p^{Cne}SmA^{Bz}p^{Cne}SmUp^{Cne}SmU-ODmtr) homostar, 15.

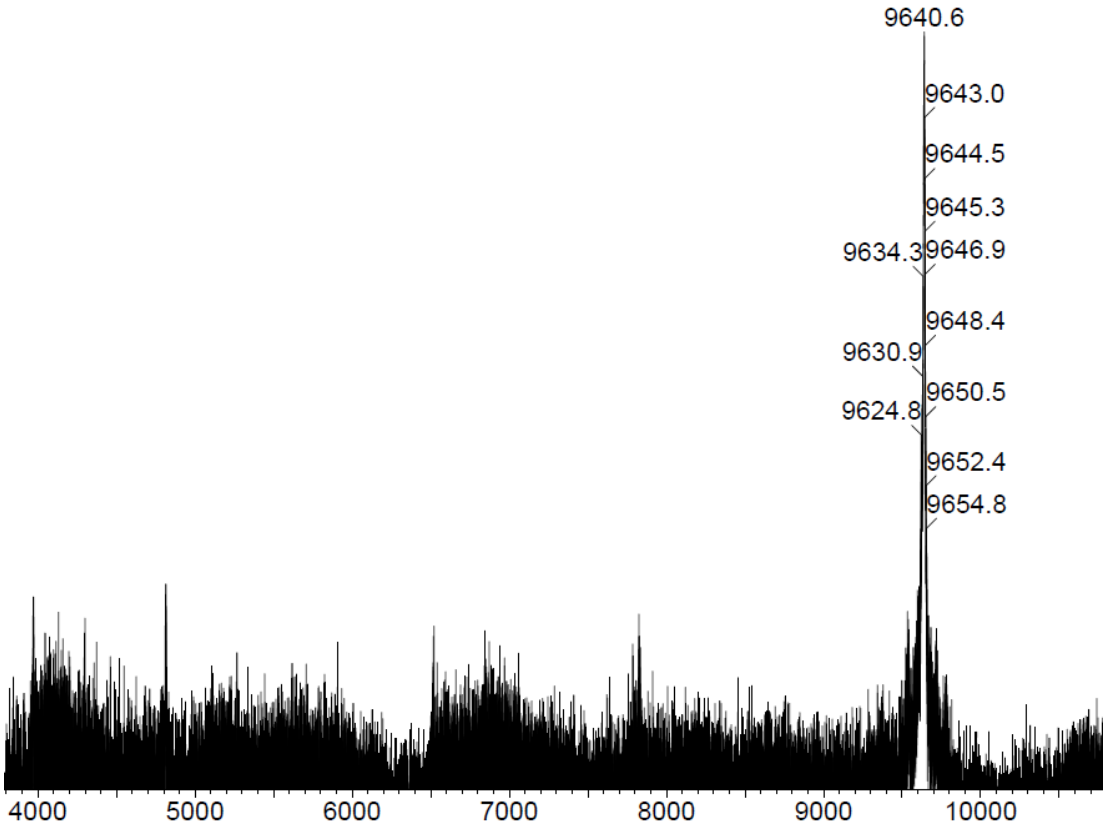


Figure B4.50. *m/z* (MALDI-ToF+) [**15**+Na]$^+$ = 9644, calc. $C_{393}H_{483}N_{66}NaO_{159}P_{15}S_{15}^+$ = 9641.4.

Tris(mUp^{Cne}SmC^{Ac}p^{Cne}SmC^{Ac}p^{Cne}SmA^{Bz}p^{Cne}SmUp^{Cne}SmU-OH) homostar, 16.

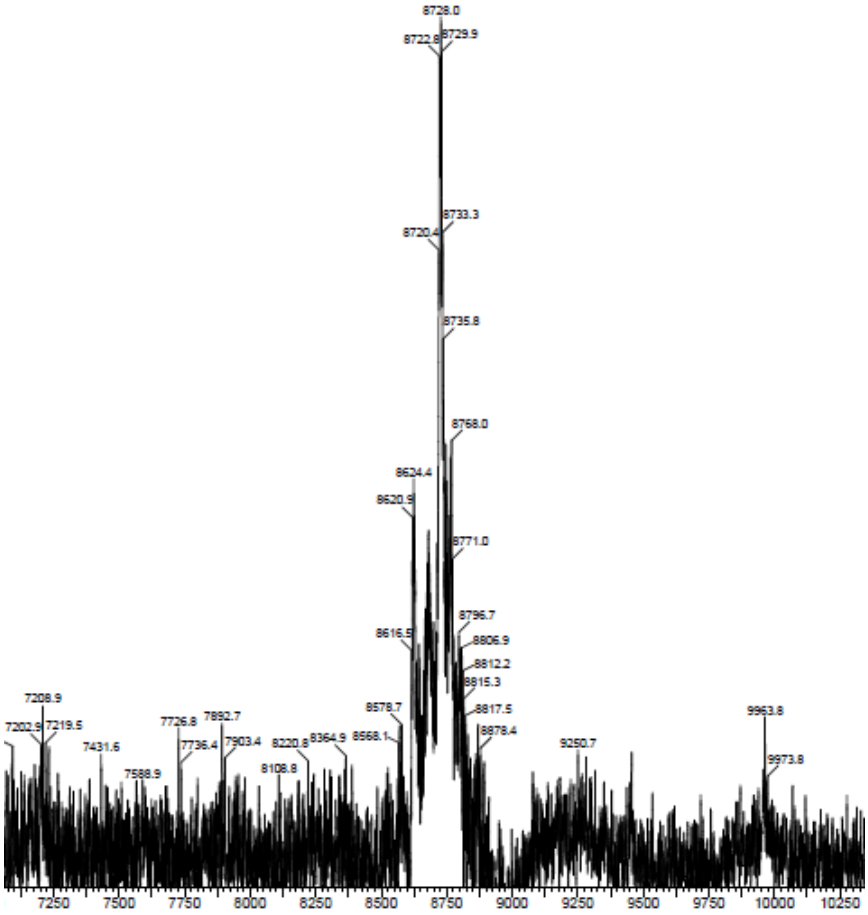


Figure B4.51. *m/z* (MALDI-ToF+) [**16**+Na]$^+$ = 8728, calc. $C_{330}H_{429}N_{66}NaO_{153}P_{15}S_{15}^+$ = 8734.0.

Tris(mUp^{Cne}SmC^{Ac}p^{Cne}SmC^{Ac}p^{Cne}SmA^{Bz}p^{Cne}SmUp^{Cne}SmUp^{Cne}SmC^{Ac}-ODmtr) homostar, 17.

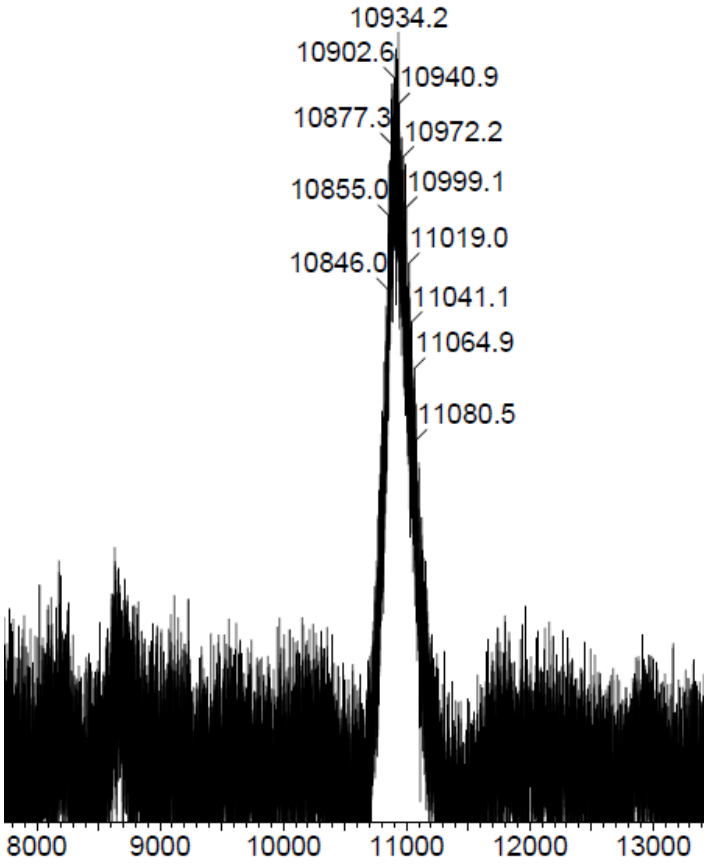


Figure B4.52. *m/z* (MALDI-ToF+) [**17**+Na]$^+$ = 10934, calc. $C_{438}H_{540}N_{78}NaO_{180}P_{18}S_{18}^+$ = 10932.6.

Tris(mUp^{Cne}SmC^{Ac}p^{Cne}SmC^{Ac}p^{Cne}SmA^{Bz}p^{Cne}SmUp^{Cne}SmUp^{Cne}SmC^{Ac}-OH) homostar, 18.

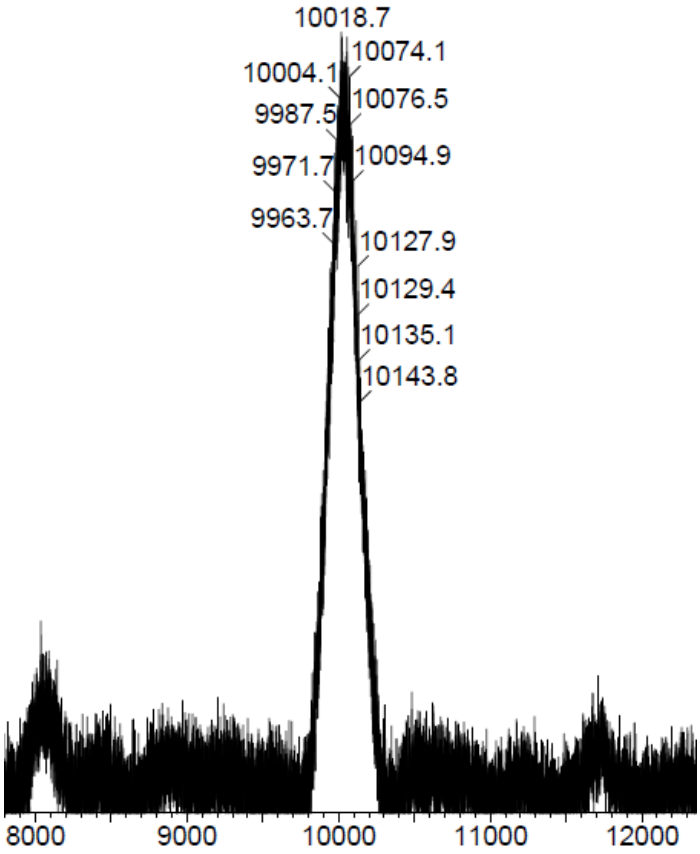


Figure B4.53. *m/z* (MALDI-ToF+) [**18**+Na]$^+$ = 10019, calc. $C_{375}H_{486}N_{78}NaO_{174}P_{18}S_{18}^+$ = 10024.2

Tris(mUp^{Cne}SmC^{Ac}p^{Cne}SmC^{Ac}p^{Cne}SmA^{Bz}p^{Cne}SmUp^{Cne}SmUp^{Cne}SmC^{Ac}p^{Cne}SmG^{iBu}-ODmtr) homostar, 19.

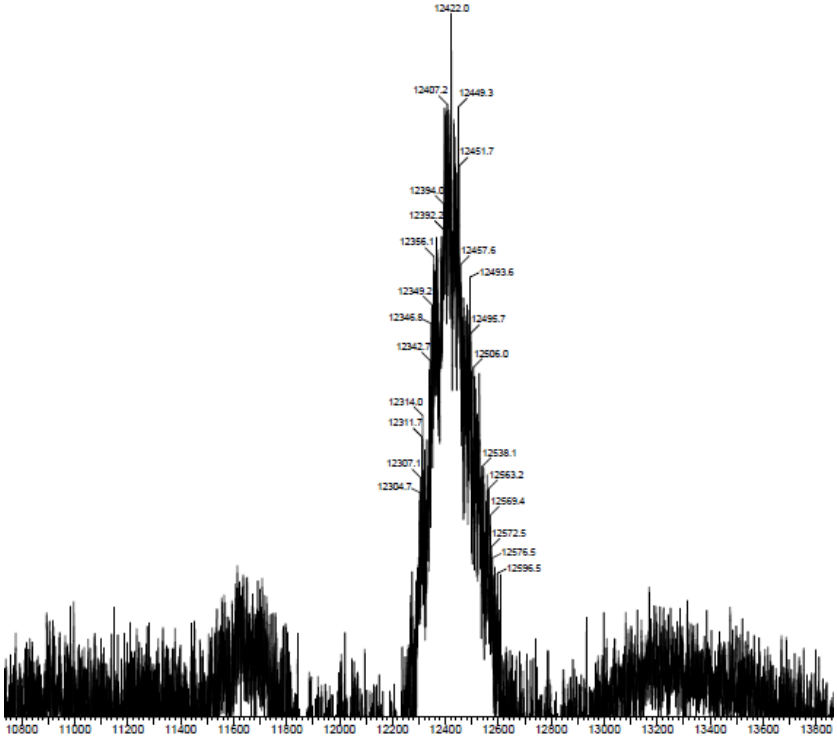


Figure B4.54. *m/z* (MALDI-ToF+) [**19**+Na]$^+$ = 12422, calc. $C_{492}H_{609}N_{96}NaO_{201}P_{21}S_{21}^+$ = 12426.9.

Tris(mUp^{Cne}SmC^{Ac}p^{Cne}SmC^{Ac}p^{Cne}SmA^{Bz}p^{Cne}SmUp^{Cne}SmUp^{Cne}SmC^{Ac}p^{Cne}SmG^{iBu}-OH) homostar, 20.

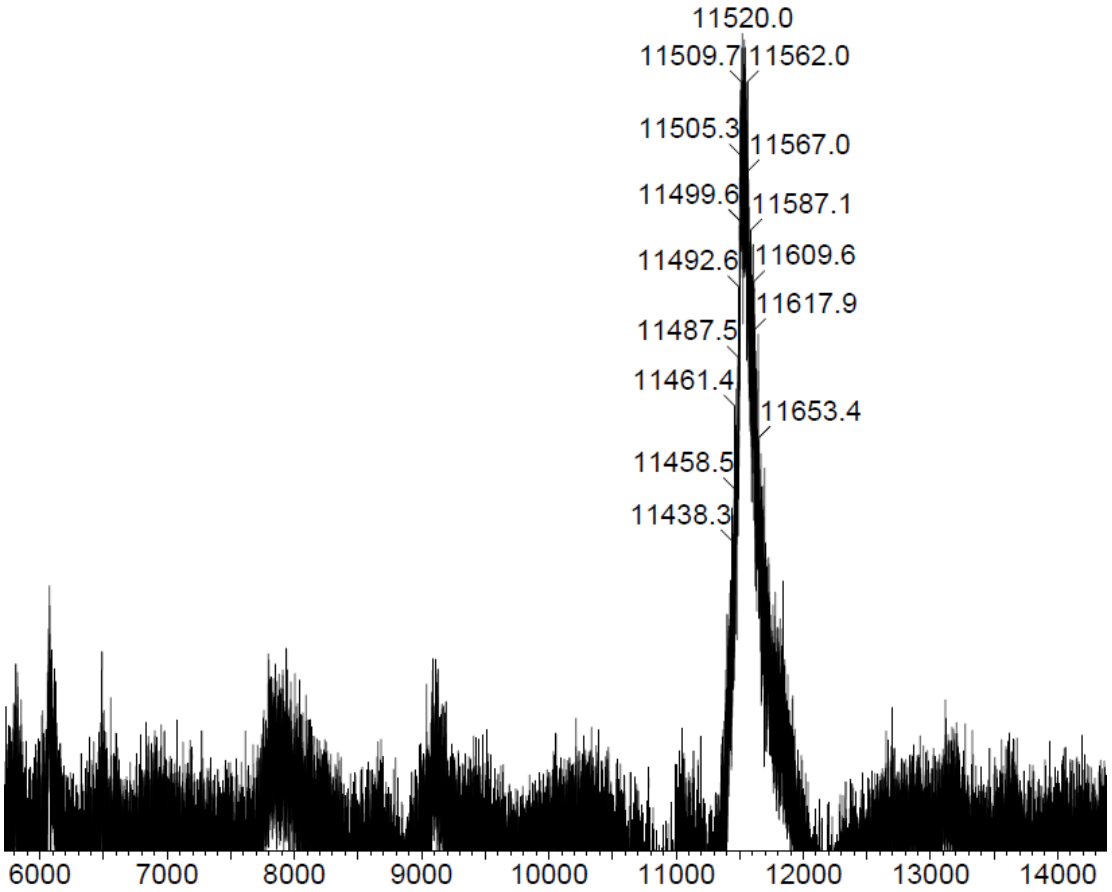


Figure B4.55. *m/z* (MALDI-ToF+) [**20**+Na]$^+$ = 11520.0, calc. $C_{429}H_{555}N_{96}NaO_{195}P_{21}S_{21}^+$ = 11520.52.

Tris(mUp^{Cne}SmC^{Ac}p^{Cne}SmC^{Ac}p^{Cne}SmA^{Bz}p^{Cne}SmUp^{Cne}SmUp^{Cne}SmC^{Ac}p^{Cne}SmG^{iBu}p^{Cne}SmG^{iBu}-ODmtr) homostar, 21.

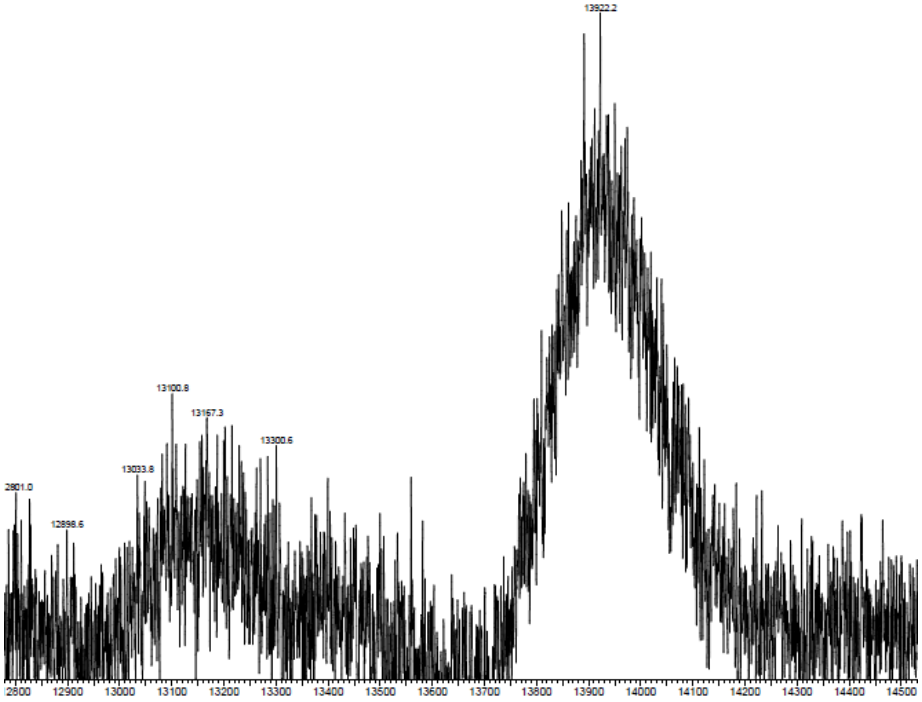


Figure B4.56. *m/z* (MALDI-ToF+) [**21**+Na]$^+$ = 13922, calc. $C_{546}H_{678}N_{114}NaO_{222}P_{24}S_{24}^+$ = 13921.2. Peak at *m/z* = 13101 corresponds to incomplete coupling on one arm of the homostar, $C_{507}H_{637}N_{108}NaO_{213}P_{23}S_{23}^+$ = 13121.

Tris(mUp^{Cne}SmC^{Ac}p^{Cne}SmC^{Ac}p^{Cne}SmA^{Bz}p^{Cne}SmUp^{Cne}SmUp^{Cne}SmC^{Ac}p^{Cne}SmG^{iBu}p^{Cne}SmG^{iBu}-OH) homostar, 22.

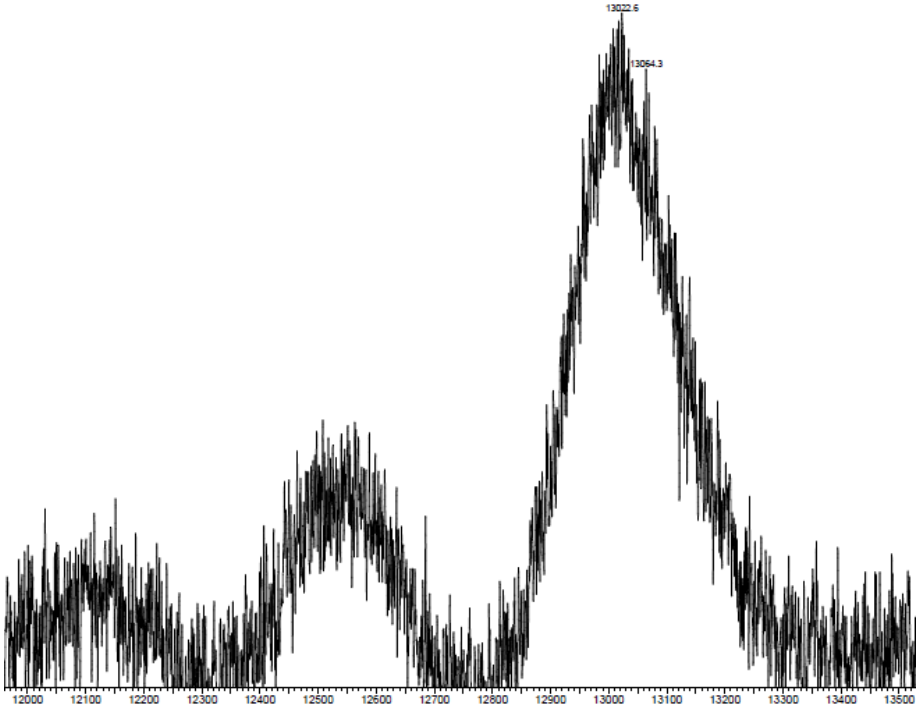


Figure B4.57. *m/z* (MALDI-ToF+) [**22**+Na]$^+$ = 13023, calc. $C_{483}H_{624}N_{114}NaO_{216}P_{24}S_{24}^+$ = 13014.8. Peak at *m/z* = 12505 corresponds to incomplete coupling on one arm of the homostar, $C_{465}H_{601}N_{108}NaO_{209}P_{23}S_{23}^+$ = 12516.7.

LC-MS of purified HO-mUpSmCpSmCpSmApSmUpSmUpSmCpSmGpSmG-OH, 24.

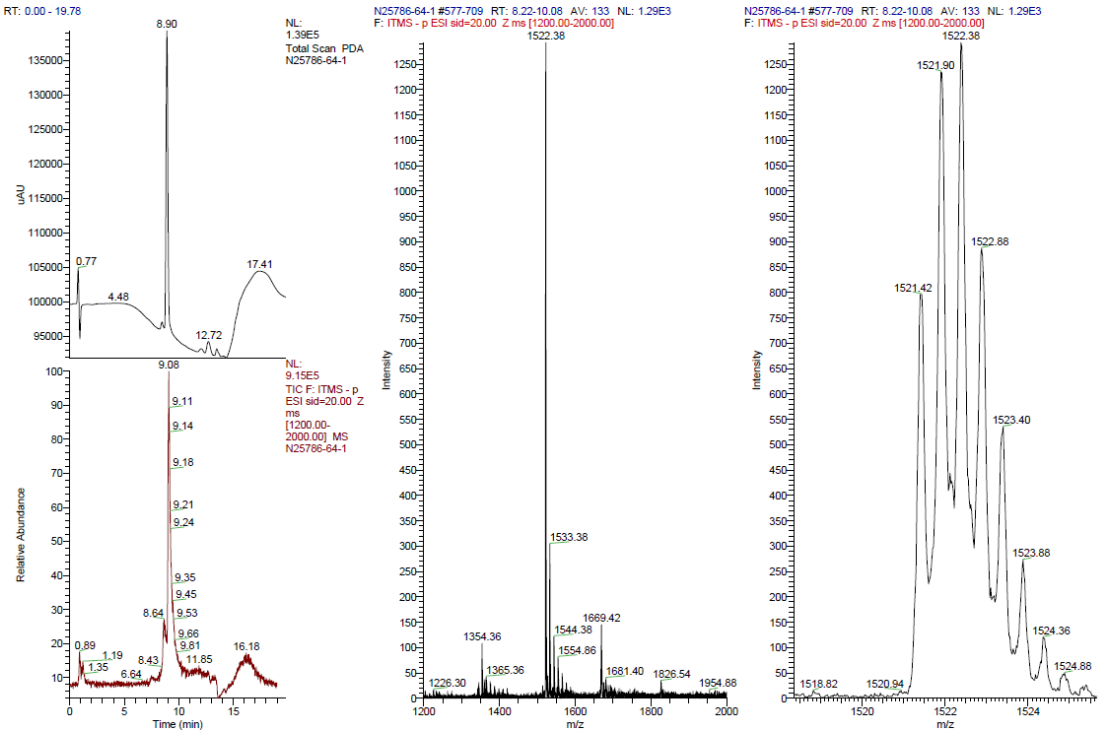


Figure B4.58. Top left) HPLC trace; bottom left) ion chromatogram; middle) wide range total MS (ESI+) of peak from 8.22 to 10.08 min – *m/z* = 1354.36 corresponds to 8-mer impurity $[X+2H]^{2+}$, calc. $C_{82}H_{112}N_{25}O_{49}P_7S_7^{2+}$ = 1335.66, but the peak centred on 1669 is broad and not assignable to a single charge state, or single species; right) expansion of molecular ion, [**24**+2H]$^{2+}$, calc. $C_{93}H_{126}N_{30}O_{55}P_8S_8^{2+}$ = 1523.68.

Appendix C: Supporting Information for Chapter 3

C1. Single- and Two-stage Diafiltration Data using M4-A Membranes

Table C-I. Single-Stage Diafiltration Performance Data for M4-A(2) at 10 bar

Vols (V/Vo)	PEG-400 (M/M_o)	PEG-2000 (M/M_o)	Flux ($L.m^2.hr^{-1}$)	Temp. (^oC)
Neat MeCN	0.0	0.0	25.9	22.1
0	1.00	1.00	21.2	22.4
1.2	0.61	0.93	21.2	22.4
2.4	0.37	0.90	21.2	21.9
3.0	0.30	0.89	21.2	22.3
4.0	0.21	0.84	21.2	22.3
5.1	0.16	0.85	23.5	21.0
6.8	0.07	0.73	23.5	21.2
10.0	0.04	0.64	24.7	22.4
12.6	0.03	0.59	24.7	22.7

The sudden drop of the flux at the beginning of the experiment followed by the slow recovery (Table C-I, column 4) was due to the osmotic pressure effect. Upon addition of the test solution, the osmotic pressure of PEG compounds decreased the flux but, as mainly PEG-400 was washed away, the flux slowly picked back up.

Table C-II. Two-Stage Diafiltration Data with M4-A*

vols (V/V_o)	PEG-400 M/M_o	PEG-2000 M/M_o	Flux [$L.m^2.hr^{-1}$]	r_C
0	1.0	1	--	--
0.1	1.0	1.06	25.9	0.49
0.3	0.98	1.06	24.7	0.51
0.7	0.85	1.06	25.9	0.50
1.1	0.71	1.07	24.7	0.52
2.4	0.43	1.05	25.9	0.48
3.1	0.34	1.07	24.7	0.53
4.6	0.20	1.03	24.7	0.53
6.3	0.13	1.03	25.9	0.53
8.4	0.07	1.01	27.1	0.53
11.0	0.05	0.94	23.5	0.57
12.1	0.05	0.94	--	--

**The temperature of the system remained near constant at 22 ^oC. The first cell was charged with M4-A(1), the second with M4-B(2).*

The recycle ratio was maintained at approximately at 0.5 throughout the experiment. The temperature stayed near constant.

C2. Repeat Experiments with M4-B Membranes Varying r_C

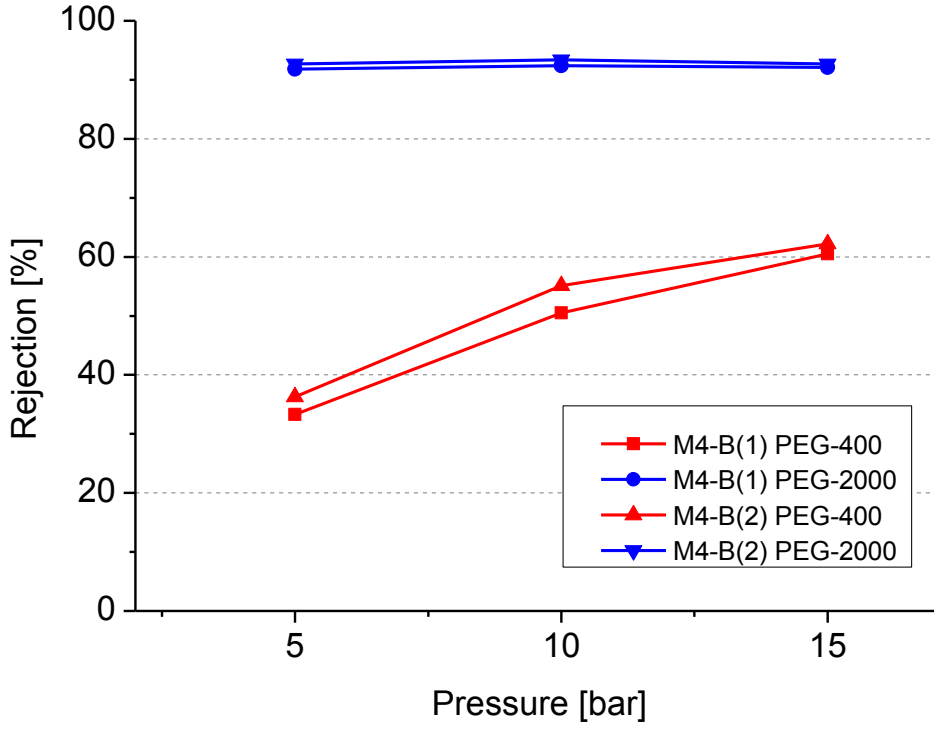


Figure C1. The change of PEG rejection with pressure in M4-B(1) and M4-B(2) membranes.

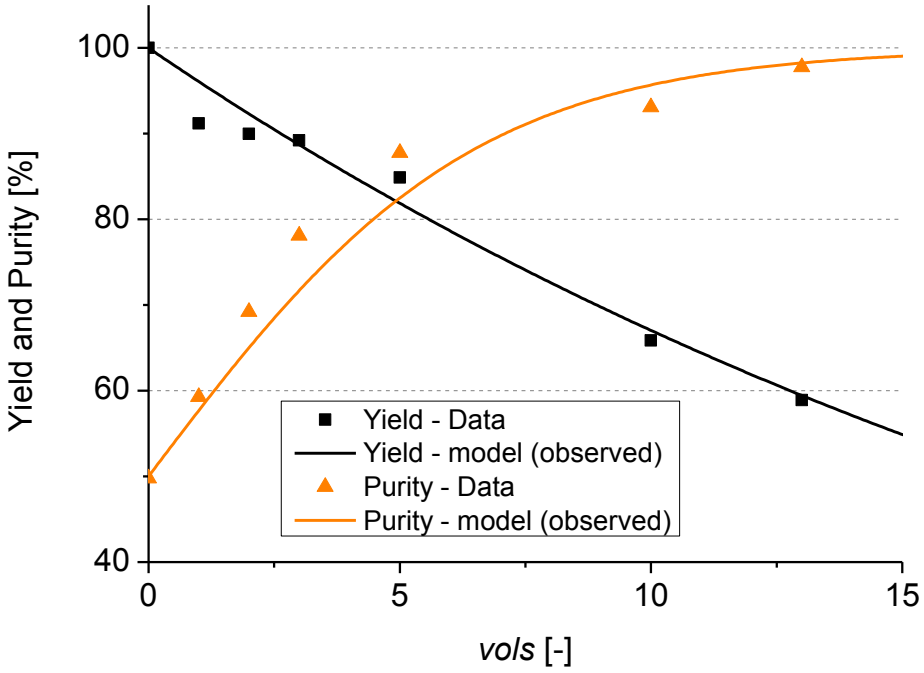


Figure C2. Yield and purity of PEG-2000 during single-stage diafiltration using M4-B(1). The rejections of PEG-400 and PEG-2000 were calculated from the best fit of the model as 60% and 96%, respectively. The final yield of PEG-2000 was 59% after 13 *diavolumes* with 98% purity. The data obtained were very similar to M4-A.

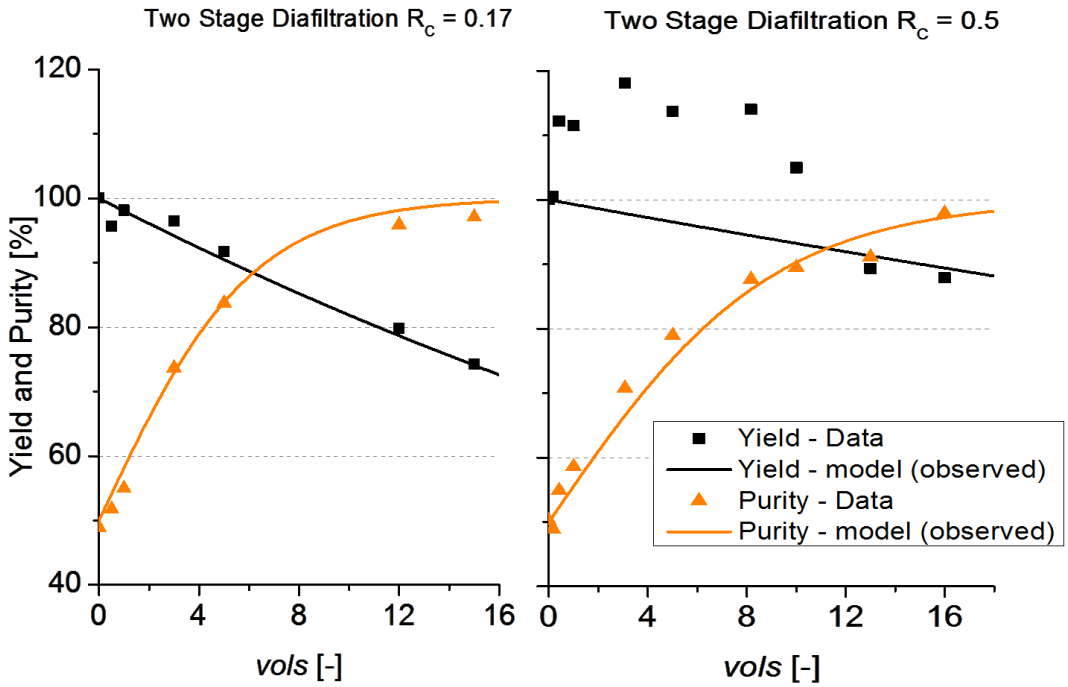


Figure C3. Two-stage cascade diafiltration using M4-B membranes at two different recycle ratios. When $r_C = 0.17$ the yield is much lower at 74% compared to $r_C = 0.5$ when yield is 88% for the same purity of 98% after 16 *diavolumes*.

Appendix D: Supporting Information for Chapter 5

D1. Effect of Different Excess of Water Addition (and BDT)

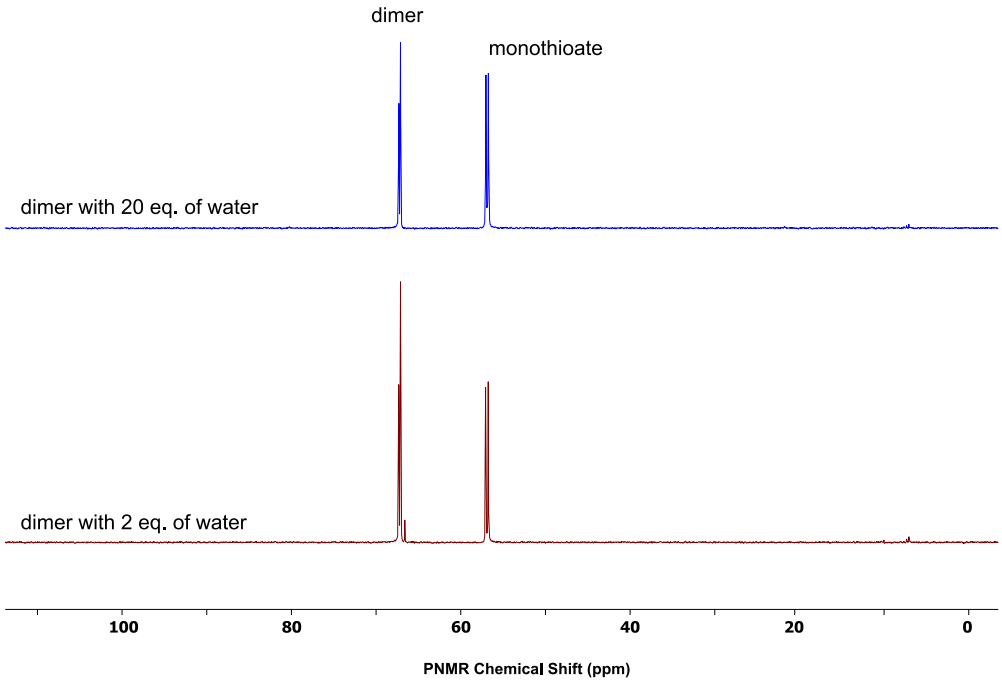


Figure D1.1. Compiled ^{31}P-NMR data for dinucleotidyl homostar (dimer) synthesis with different eq. of water addition. It can be seen that 2 eq. of water are just as effective in hydrolyzing all excess phosphoramidite monomers, subsequently converted to monothioates using BDT.

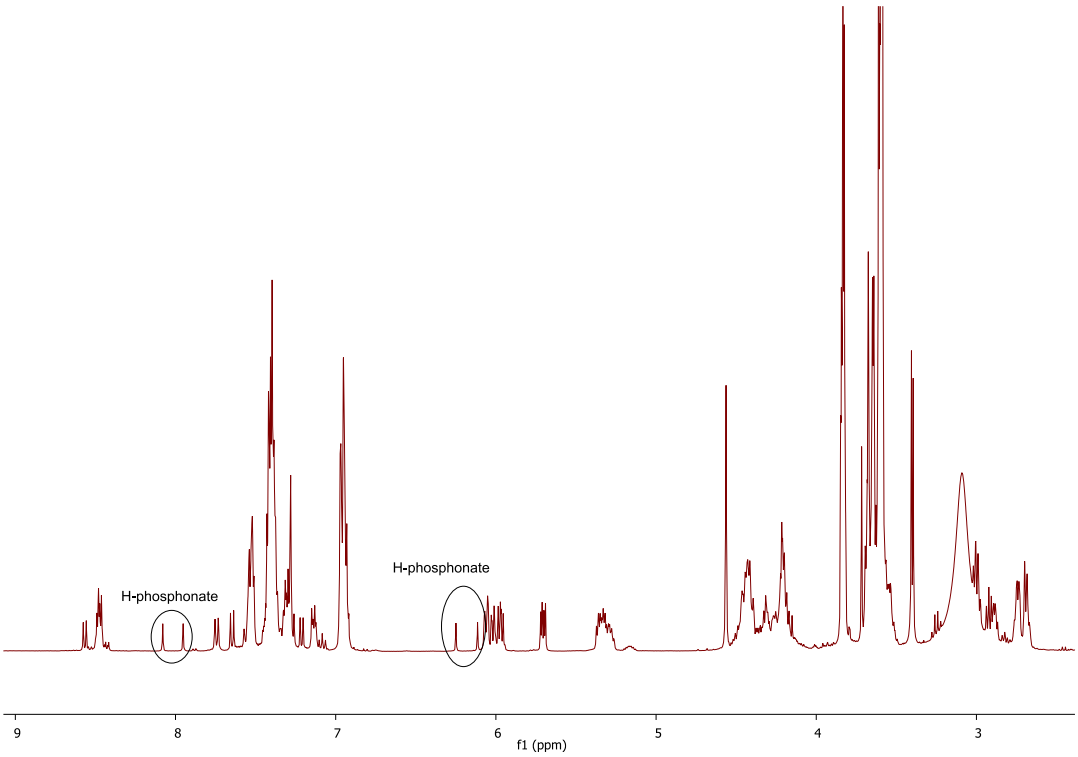


Figure D1.2. ^{1}H-NMR showing the presence of H-Phosphonate (to augment Figure 5.7b)

D2. Detailed 5'-O-MIP PA Synthesis (Show MS analysis, only available in prints)

The reaction scheme is shown in Figure 5.5. This work was carried out at University of Turku, Finland, together with Alejandro Gimenez Molina. Each reaction procedure is described in detail below.

Reaction 1: Protection of 3'-O with TBDMS-Cl

Starting material **12a** (4.5g, 7.5 mmoles) was first dissolved in DMF (100ml) and then imidazole (1.03g, 2 equiv) was added. Then, TBDMS-Cl (2.3g, 2 equiv) was added slowly, and the solution was stirred overnight. The reaction was followed by TLC (5% MeOH/DCM) and showed complete reaction after 40 hrs (the reaction must have finished within 24 hrs though). Without evaporating DMF, the crude was extracted using ethyl acetate/water (20% sodium bicarbonate). Some precipitation was observed in the aqueous layer and suspected it was the product; however, upon addition of more water, the precipitate redissolved in water, suggesting it was salt debris. DMF mainly partitioned into water and the entire product was in ethyl acetate layer. MS confirmed the presence of product **12b**. The final mass (5.92g), yield was above 100% probably due to excess TBDMS-OH remaining in the crude.

Reaction 2: Detritylation of 5'-O-Dmtr

Starting material **12b** (5.92g, 8.3 mmoles) was dissolved in DCM (50ml) in a RB flask to which DCA (1ml, 2% v/v) and pyrrole (2ml, 4% v/v) was added. The reaction was followed by TLC; however, it was not reaching completion after 2 hrs. Total of 2ml DCA and 3.5ml of pyrrole was added to drive the reaction to completion. Without any evaporation, the crude was extracted using 50% sodium bicarbonate twice to remove acids (noticed the change in color from dark brown to faint yellow). A normal phase chromatography: initial loading with DCM and washing with DCM until no Dmtr-pyrrole is detected. A gradient was given with MeOH/DCM 2% step size up to 8% MeOH (200ml each). The product eluted at 6% MeOH. The product fractions were collected then evaporated to dryness. MS confirmed the presence of product **12c**. The final mass was 2.86g, and the overall yield was 92.6%.

Reaction 3: Protection of 5'-O with 2-methoxypropene

Staring material **12c** (2.76g) was dissolved in THF in a RB flask to which 2-methoxypropene (10 eq.) was added. Then, *p*-touenesulfonic acid (<0.01 eq.) was dissolved in 1 ml of THF and

added to the reaction flask. *Caution:* 2-methoxypropene can polymerize under the presence of acid. The reaction was followed by TLC (5% MeOH-DCM), and was complete after 3 hrs. THF was not evaporated prior to extraction. For extraction, do not add DCM yet, add bicarb to neutralize the acid to avoid acetal deprotection (acid/DCM). Then, extract using DCM. Several extraction necessary using DCM to extract all the product into the organic layer. Dry, filter, vac down. The final mass yield (3.13g) gave overall yield of 86.2%. The presence of product **12d** was confirmed by MS.

Reaction 4: Deprotection of 3'-O-TBDMS

Starting material **12d** was split into two fractions. First fraction of the starting material 4 (450mg) was dissolved in THF in a RB flask. Then, tetrabutylamino fluoride trihydrate (TBAF, 2 equiv) was first dissolved in THF then transferred to the reaction flask slowly. The reaction was followed by TLC and it was complete after 0.5 hrs (There was a low R_f compound below the product). Without evaporating THF, the crude was extracted using DCM and 70% bicarb (emulsion observed). The crude was extracted 3x until the product was not detected in the aqueous layers. The organic layer was dried, filtered, and evaporated. Then the solutes were re-dissolved in a small amount of DCM and loaded onto a normal phase column in DCM. Washed with 200 ml DCM, gave a gradient with MeOH/DCM gradient (1% step size up to 8%, 150ml each with few drops of pyridine). The product eluted at 6~8%, and some yellow impurity stayed at the top of the column. The product fraction was collected and evaporated to dryness. The final mass yield (320mg) gave the step-wise yield of 93%, and the presence of product **12e** confirmed by MS.

Second fraction starting material 4 (2.6g, 5.36mmoles) was dissolved in THF (50ml), to which TBAF (1.7 equiv, 3.01g, 9.1 mmoles) dissolved in THF (15ml) was added slowly. The reaction was followed by TLC (5% MeOH/DCM). The crude was extracted with DCM and 100% bicarb 3x to get all the product into the organic layer which was then dried, filtered, then evaporated. The crude was re-dissolved in a small amount of DCM and loaded onto normal phase column, washed with 200ml of DCM, and gave a gradient with MeOH/DCM (1% step size up to 6%, 200ml each with few drops of triethylamine. The product eulted at 5-6%. Before the product, yellow-colored higher Rf (presumably starting material) eluted first. The product

fraction was collected and evaporated to dryness. The presence of 12e confirmed by MS. The final mass yield (1.92g) gave the step-wise yield of 97%.

Reaction 5: Phosphitylation of 3'-OH

Starting material 5 (186mg, 0.5 mmoles) was co-evaporated from dry MeCN 3x and then dissolved in dry DCM in a RB flask to which dry triethylamine (5 equiv, 0.15ml) was added. The RB flask was purged with argon in advance and was kept under inert atmosphere. Then, phosphitylation reagent (1.2 equiv, 0.061 ml) was added and the solution was stirred. After 2 hrs, the solution was transferred directly to a normal phase column (dry silica). Washed with 200 ml DCM, gave a gradient using acetone/hexane (50% acetone, increase acetone by 10%, with triethylamine). The product eluted at 80% acetone. Collect and evaporate to dryness, gave 86.5% yield, characterized with ^{1}H- and ^{31}P-NMR.

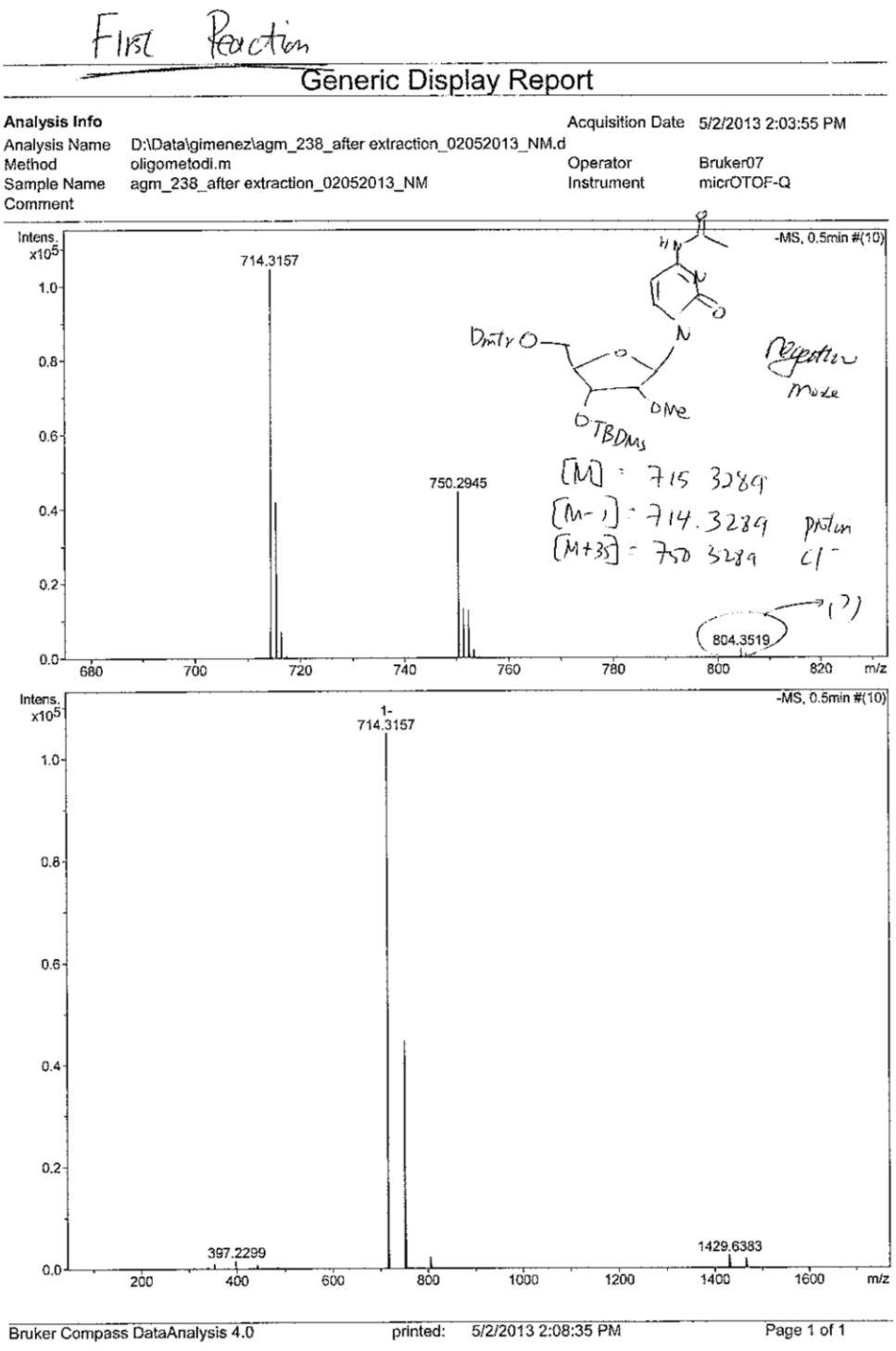


Figure D2.1 MS for the first reaction,12b

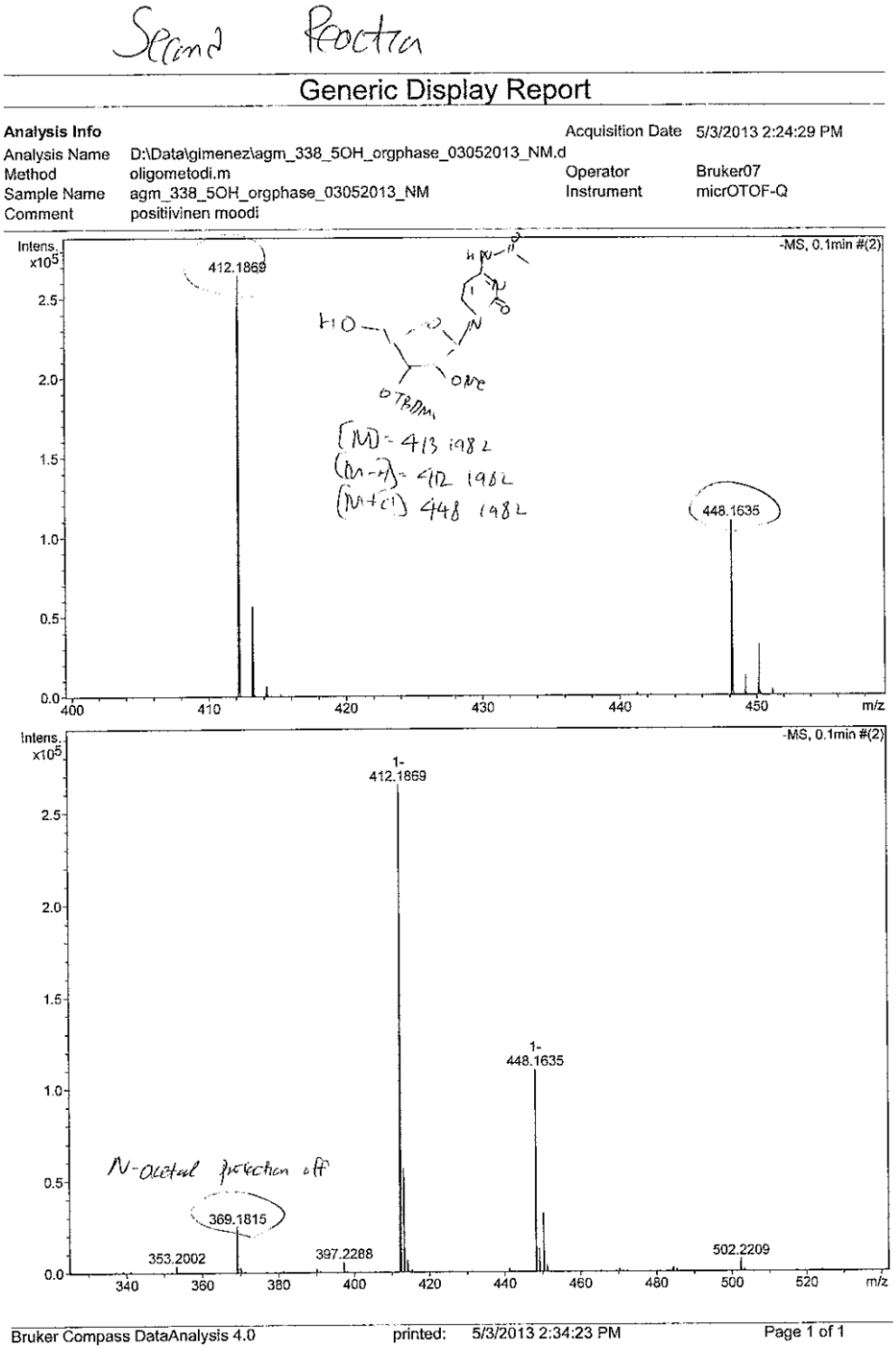


Figure D2.2 MS for the second reaction,12c

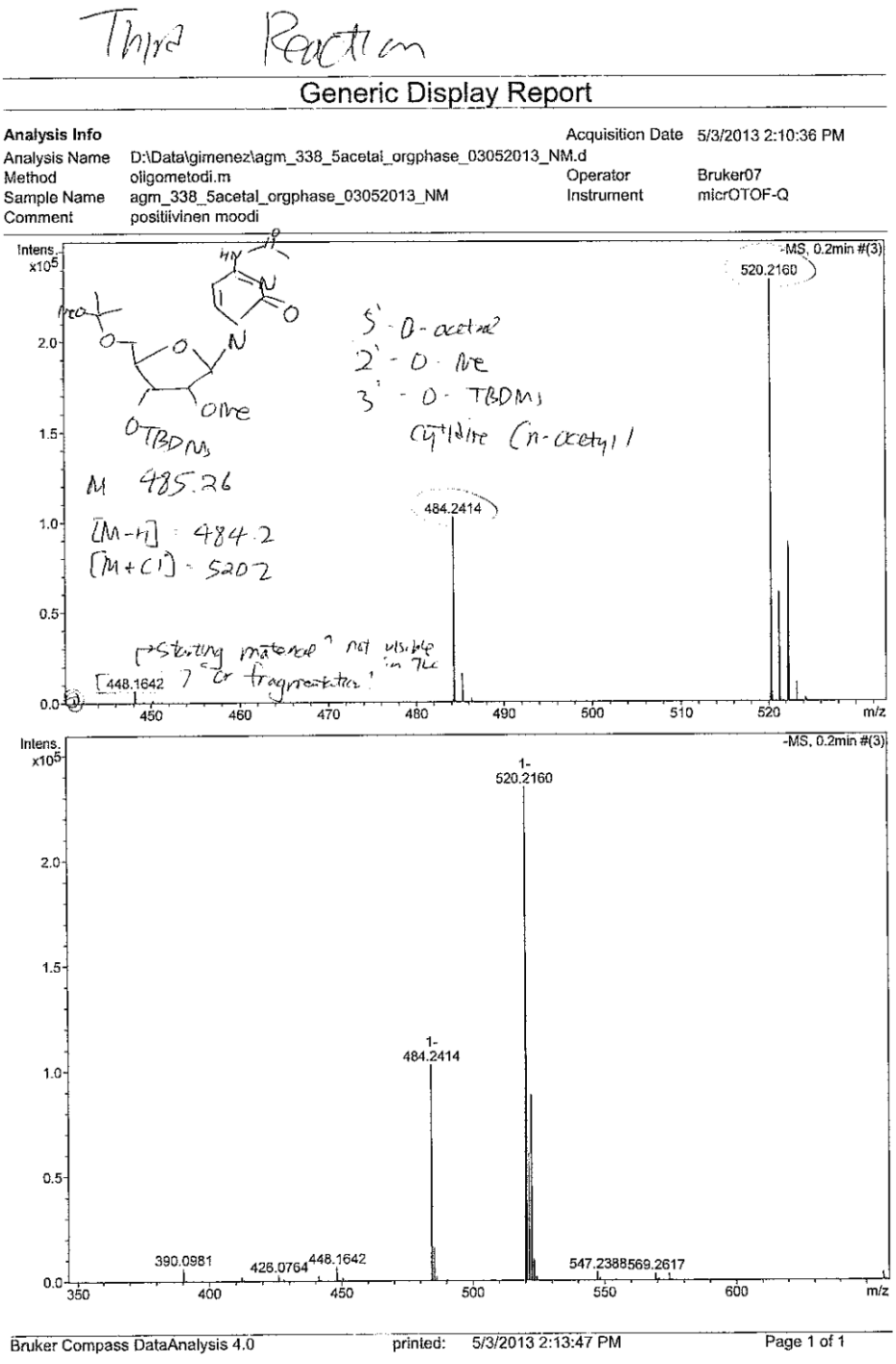


Figure D2.3 MS for the third reaction,12d

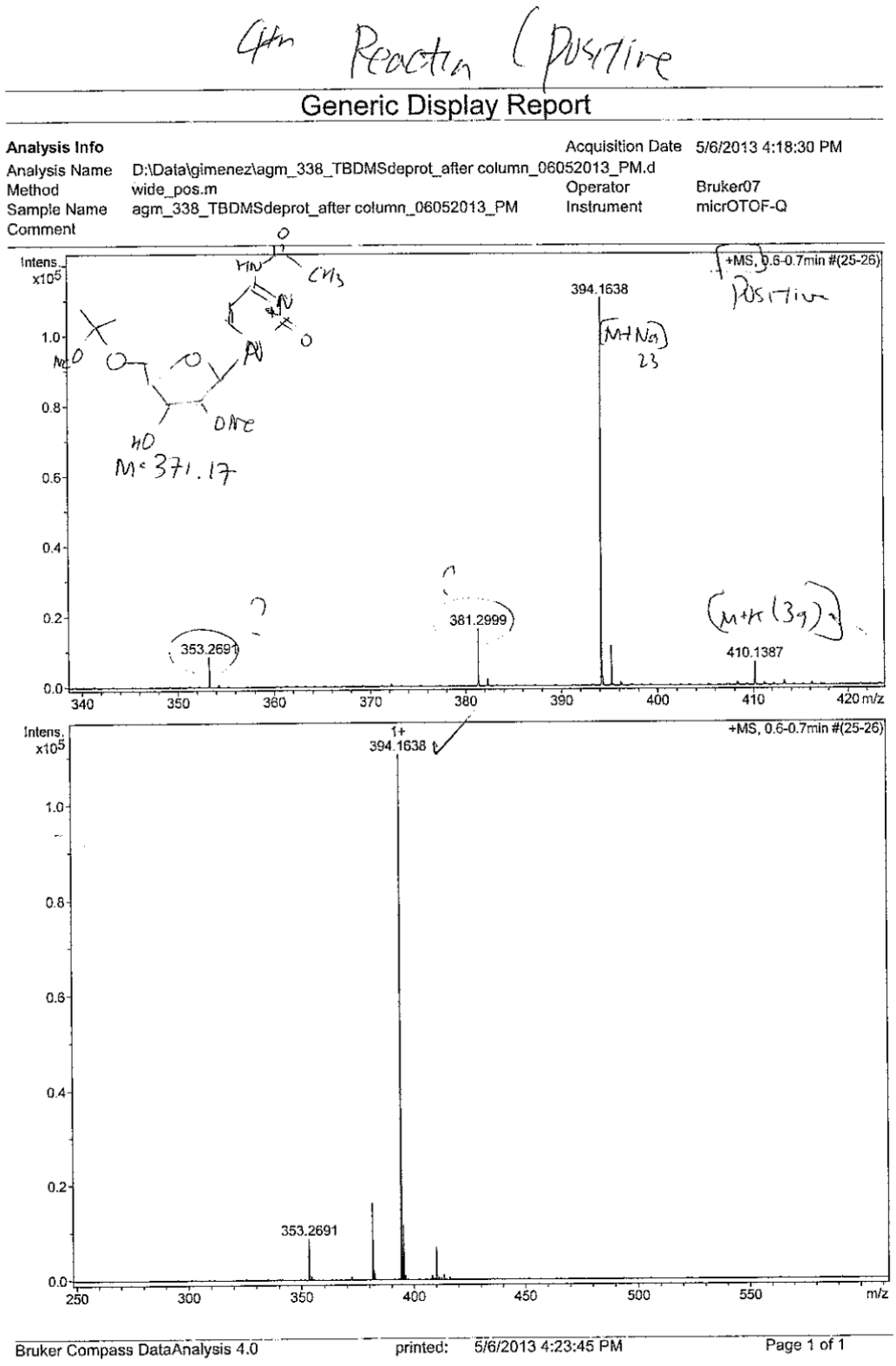


Figure D2.4 MS for the fourth reaction,12e

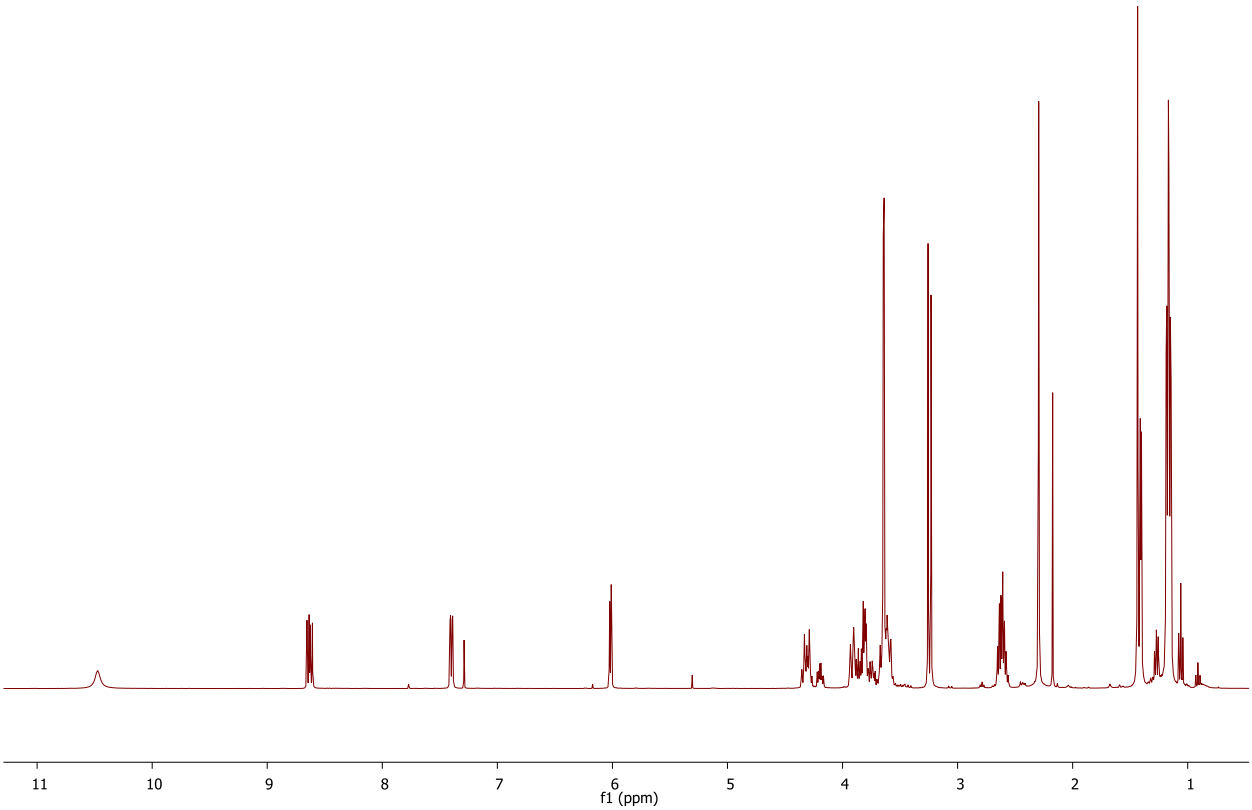


Figure D2.5 ^{1}H-NMR for the 5th reaction,12f.

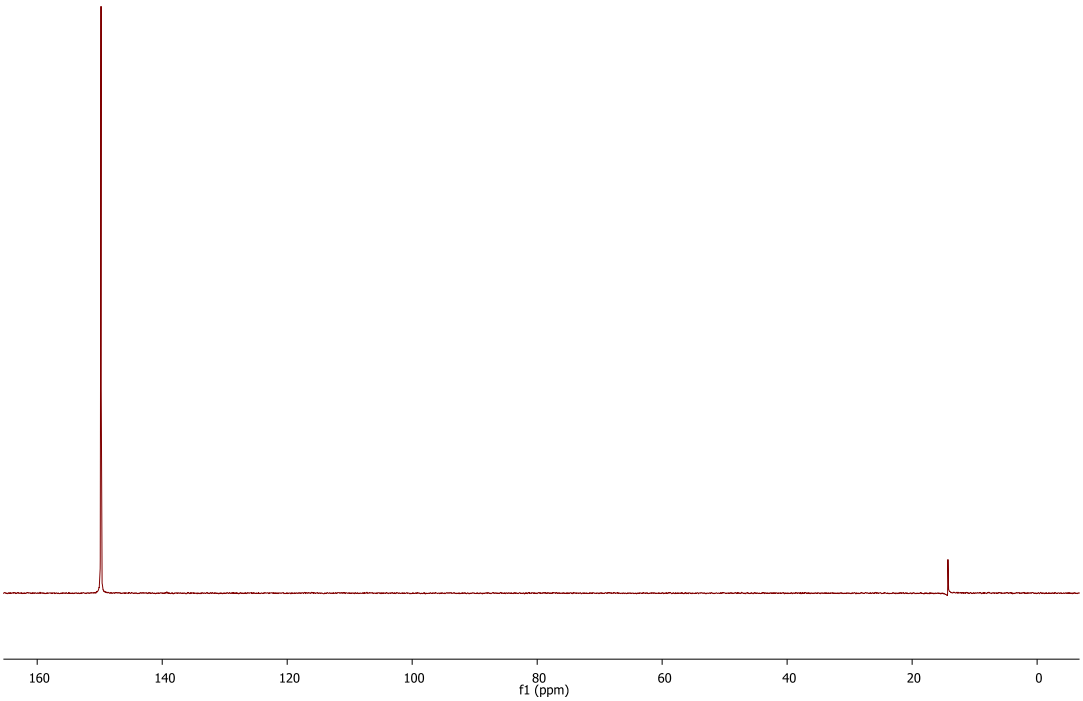
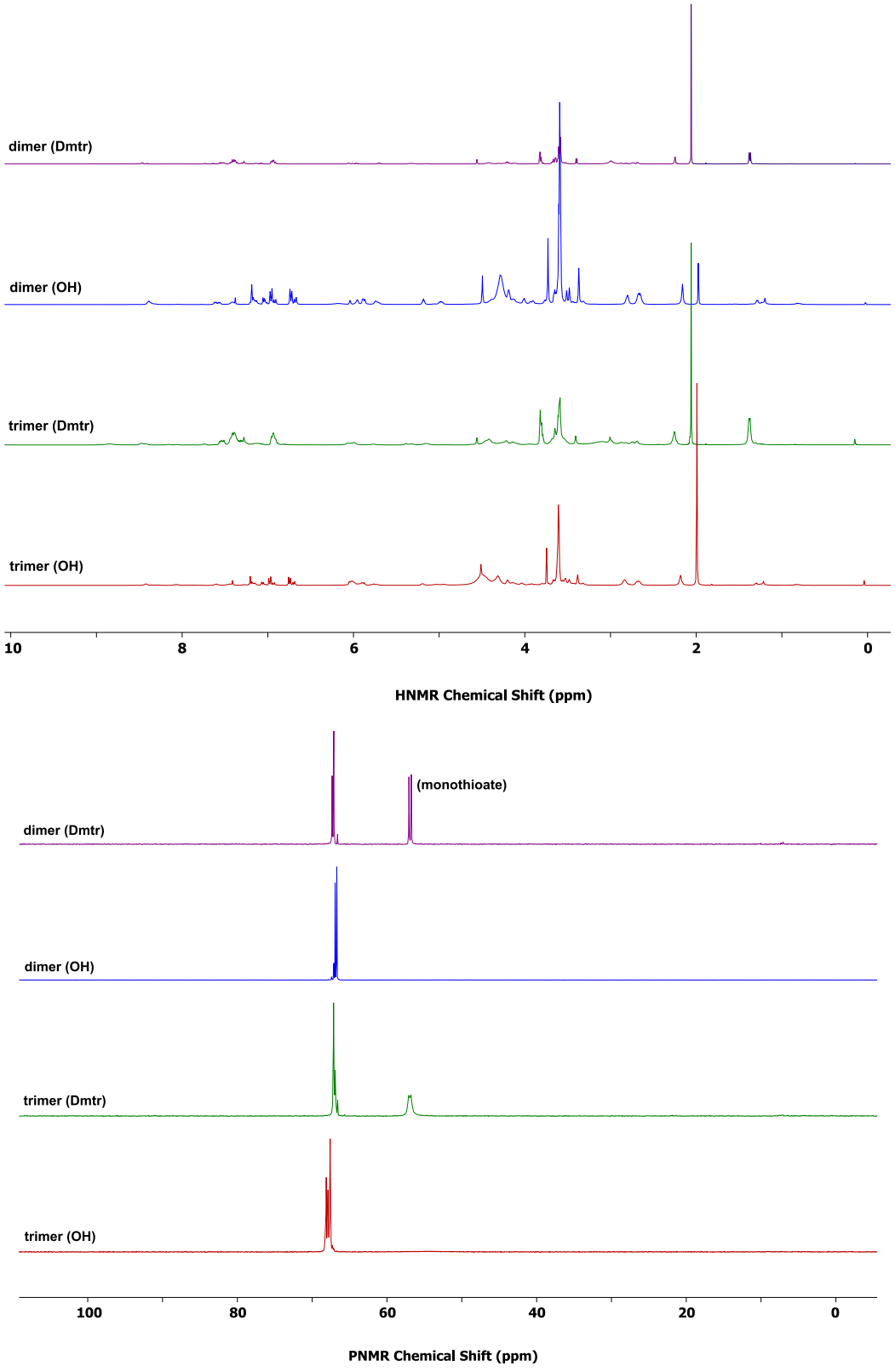
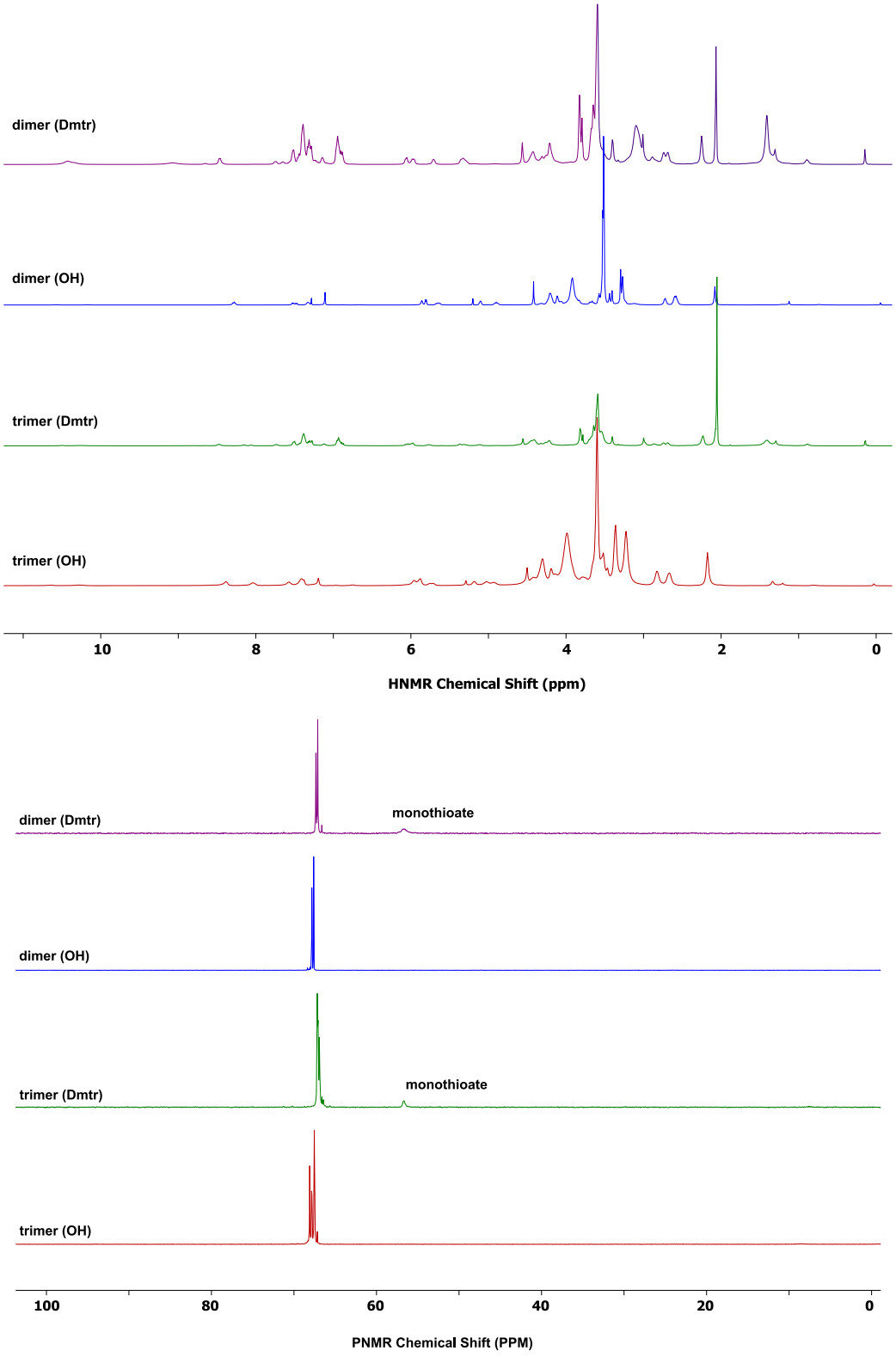


Figure D2.6 ^{31}P-NMR for the 5th reaction,12f.

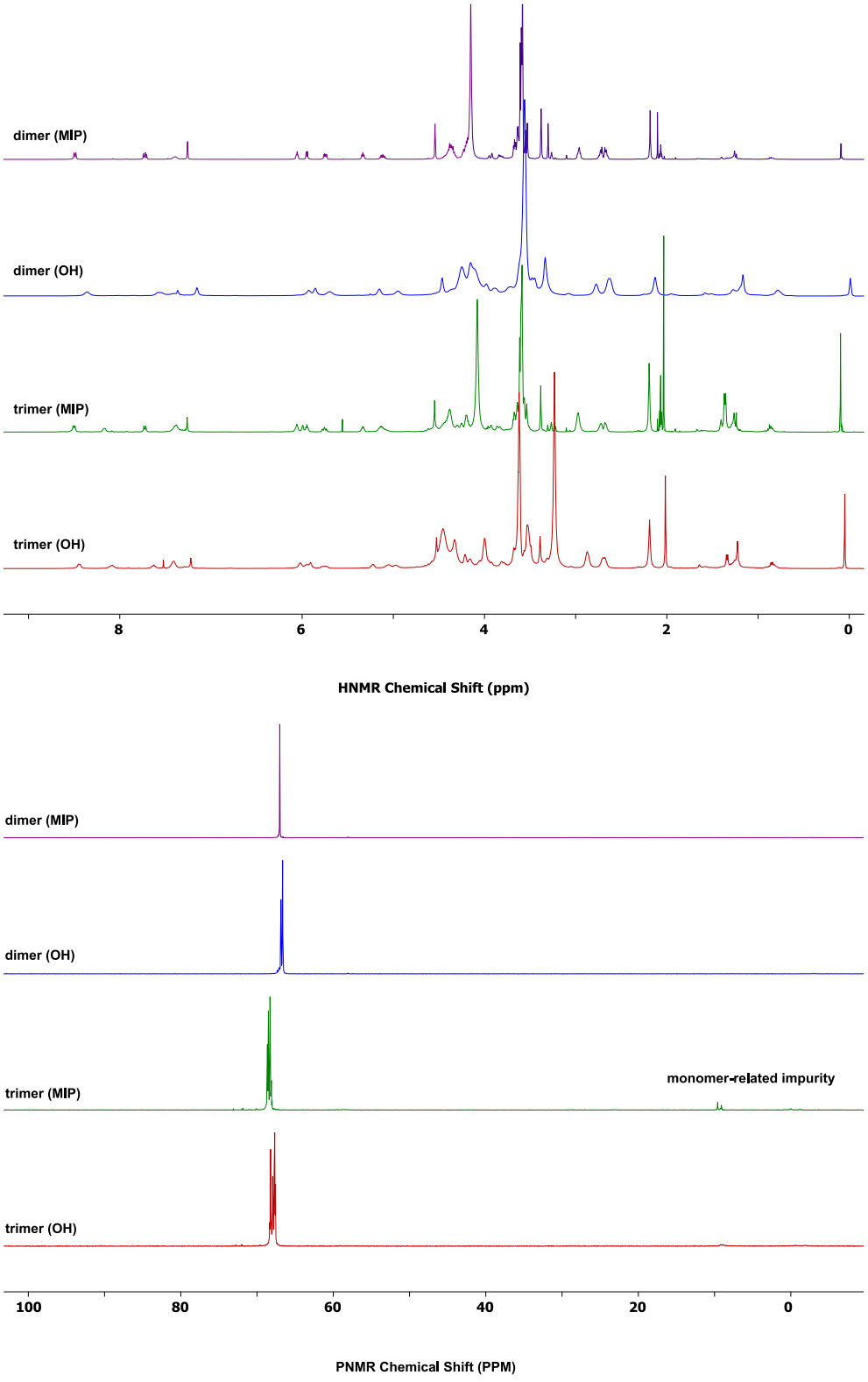
D3. NMR 3-mer prepared without HCl doping



D4. NMR 3-mer prepared after HCl doping



D5. NMR 3-mer prepared with MIP



D6. NMR 3-mer prepared with MIP and cascade

